Process-product synthesis, design and analysis through the Group Contribution (GC) approach

Alvarado-Morales, Merlin

Publication date:
2010

Document Version
Publisher's PDF, also known as Version of record

Process−Product Synthesis, Design and Analysis through a Group−Contribution (GC) Approach

Ph.D. Thesis

Merlin Alvarado−Morales

March 2010

Computer Aided Process−Product Center
Department of Chemical and Biochemical Engineering
Technical University of Denmark

Preface

This thesis is submitted as a partial fulfillment of the requirements for the PhD degree at the Technical University of Denmark ('Danmarks Tekniske Universitet'). The work has been carried out in CAPEC at the Department of Chemical and Biochemical Engineering ('Institut for Kemiteknik') from March 2007 to March 2010 under the sepervision of Prof. Rafiqul Gani, Prof. John M. Woodley and Assoc. Prof. Krist V. Gernaey. I would like to express my gratitude to Prof. Rafiqul Gani for his guidance, academic support and interest in my work. Also I am grateful to Prof. John M. Woodley and Assoc. Prof. Krist V. Gernaey for all the fruitful discussions besides the support provided during the development of this work.

I would like to thank all the personnel at CAPEC that offered their help and support whenever it was needed. I would like to thanl the co–workers at CAPEC who I had the oppurtinity to work with and have so many discussion about different topics: Hugo E. González, Elisa, Kavitha, Martina, Philip, Axel, Jakob, Kamaruddin, Rasmus, and especially to Ana Carvalho, Paloma, Oscar, and Ricardo for all the great moments and advantures that we shared together besides the work.

I want to have a special thanks to my lovely family María Luisa Morales, Benito Alvarado, Moisés Alvarado and Sonia Alvarado who supported me during the development of this project. Without your support this work would never be completed. Muchas gracias familia, los amo..!

Lyngby, March 2010
Merlin Alvarado–Morales

Abstract

This thesis describes the development and application of a framework for synthesis, design, and analysis of chemical and biochemical processes. The developed framework adresses the formulation, solution, and analysis of the synthesis/design problem in a systematic manner. Emphasis is given on the process−group contribution (*PGC*) methodology within this framework for synthesis/design, which is used to generate and test feasible design flowsheet candidates based on principles of the group−contribution approach used in chemical property estimation.

The three fundamental pillars of the *PGC* methodology are the process−groups (building blocks) representing process unit operations, connectivity rules to join the process−groups and flowsheet property models to evaluate the performance of the flowsheet structures. In order to extend the application range of the *PGC* methodology, a set of new process−groups together with their specifications have been developed. The synthesis of the chemical and biochemical processes flowsheets is performed through a reverse property approach, where the process−groups are combined to form feasible flowsheet structures having desired (targets) properties. The design of the most promising process flowsheet candidates is performed through a reverse simulation approach, where the design parameters of the unit operations in the process flowsheet are calculated from the specifications of their inlet and outlet streams inherited from the corresponding process−groups. The reverse simulation methods supporting the framework are based on the attainable region (*AR*) and driving force (*DF*) concepts, which guarantees a near optimal performance design with respect to selectivity for reactor units and with respect to energy consumption for separation schemes.

The framework for synthesis and design of chemical and biochemical processes together with the models, methods and tools is generic and can be applied to a large range of problems, either to improve an existing process flowsheet (known as a retrofit problem) or to design a new process flowsheet. The developed framework and associated computer aided methods and tools have been tested using a series of case studies and application examples.

Resume på dansk

Denne afhandling beskriver udvikling og anvendelse af et rammeværktøj for syntese, design og analyse af kemiske og biokemiske processer. Det udviklede rammeværktøj adresserer systematisk formulering, løsning og analyse af syntese/design problemet. Der er lagt vægt på proces−gruppebidragsmetodikken (process−group contribution; *PGC*) indenfor dette rammeværktøj for syntese og design, hvilket er anvendt til at generere og teste mulige procesdiagram kandidater, baseret på principperne om gruppebidrag, kendt fra kemisk egenskabsestimering.

De tre fundamentale søjler i *PGC*−metodikken er: Procesgrupperne (byggeklodser) der repræsenterer processens enhedsoperationer, kombineringsregler til at forene procesgrupper og procesdiagram-egenskabsmodeller for at evaluere diagramstrukturerne. For at udvide anvendelsen af *PGC*−metodikken, er et sæt af nye procesgrupper samt deres specifikationer udviklet. Syntese af kemiske og biokemiske procesdiagrammer er udarbejdet bagvendt, hvor procesgrupperne er kombineret til mulige kandidat processtrukturer, der opfylder ønskede egenskaber. Design af de mest lovende procesdiagram kandidater er udarbejdet ved en bagvendt simuleringsfremgangsmåde, hvor designparametrene for enhedsoperationerne i procesdiagrammet er beregnet fra specificering af deres ind og udløbsstrømme, nedarvet fra deres tilsvarende procesgrupper. Denne simuleringsmetode, der understøtter rammeværktøjet, er baseret på koncepterne om opnåelig region og drivkraft, hvilket garanterer et næsten optimalt design mht. udvælgelse af reaktorenheder og energiforbrug i separationsdelen.

Dette rammeværktøj for syntese og design af kemiske og biokemiske processer, med tilhørende modeller, metoder og andre værktøjer, er generisk og kan finde anvendelse til et stort udvalg af problemer; enten ved at forbedre eksisterende procesdiagrammer (retrofit), eller til at designe nye procesdiagrammer. Det udviklede rammeværktøj og tilhørende computerassisterede metoder og værktøjer er blevet testet gennem en serie af case studies og anvendelseseksempler.

Contents

List of Figures

List of Tables

1 Introduction

Process flowsheet synthesis and design are challenging tasks, which can generally be described as follows: given a feed (raw materials) description and product specifications, identify the process flowsheet that will allow the manufacture of the desired product matching the given specifications and constraints. In practice, process synthesis and design implies the investigation of chemical reactions needed to produce the desired product, the selection of the separation techniques needed for downstream processing, as well as taking decisions on the precise sequence of the separation unit operations. The heat/mass integration networks to be included in the flowsheet and finally the control strategy to be applied need to be considered as well. Furthermore, the synthesis and design tasks also include the design of the equipment in the process flowsheet and finally the formulation of recommendations of appropriate operating conditions for the designed equipments.

Consequently, three types of problems can be formulated in the synthesis and design of chemical and bioprocesses. First, process synthesis is the determination of the process topology, i.e., the process flowsheet structure. Second, process design is the determination of the unit sizes, the system flowrates, and the various operating parameters of the units for a given flowsheet. Third, process optimization is the determination of the best overall process flowsheet. Before the best system can be developed, a suitable measure of the performance of the system must first be established. This measure becomes the objective function for the optimization problem. These problems can either be considered sequentially or simultaneously within the process synthesis and design procedure to determine the final process flowsheet matching the given specifications and constraints.

There currently exists a large wealth of literature on systematic process synthesis and design methods for chemical processes. Excellent reviews of process synthesis are given by Nishida et al.[70], Westerberg[94], Johns[50], and Li & Kraslawski[61]. In contrast, the same abundance of literature does not exist in the bioprocess synthesis field. Bioprocess synthesis is often performed in a sequential fashion, proceeding from one unit to the next until product specifications are met, and individual units are subsequently optimized to improve plant performance. Although this approach may produce economically adequate processes, alternative designs that are currently not explored in the bioprocess synthesis procedures may be more profitable. On the other hand, process design in the bioprocess–based industries has made recourse to existing processes and has relied heavily on the use of expensive pilot–plant facilities in which to test out proposed new process sequences. This has proven to be time–consuming and not very systematic. As a consequence different types of approaches have therefore been developed trying to overcome these problems.

Therefore, in this chapter a brief review of the state of the art in the synthesis and design of chemical processes and bioprocesses is presented. Special emphasis is given to the development of methods for synthesis and design of bioprocesses. The objectives and the motivation behind this work as well as the general framework proposed are also described in this chapter.

1.1 State of the Art in Chemical and Bioprocess Synthesis and Design

In this section, different approaches to solve the synthesis and design problem, such as methods that employ heuristics or are knowledge–based, methods based on thermodynamic/physical insights, methods based on optimization techniques, and hybrid methods that combine different approaches into one method are described.

1.1.1 Heuristic or Knowledge–based Methods

The most commonly used synthesis/design approach is the heuristic approach. The purpose of heuristics is to narrow the list of possible processing steps based on general experience. There are numerous examples in the literature of the use of heuristics to solve the synthesis and design problems from the chemical industry. Particularly, heuristics dealing with synthesis of separation processes in the chemical industry are fairly well developed. A number of heuristic methods have been reported in the open literature, and a brief overview is given below.

Sirrola & Rudd[83] made an attempt to develop a systematic heuristic approach for the synthesis of multi–component separation sequences. In recent years, a significant amount of work has been carried out based on this approach. The hierarchical heuristic method is an extension of the purely heuristic approach. Seader & Westerberg[81] developed a method, which combines heuristics together with evolutionary methods for synthesizing systems of simple separation sequences. Douglas[18] proposed a hierarchical heuristic procedure for synthesizing process flowsheets where a set of heuristic rules are applied at different levels to generate the alternatives. In this approach shortcut calculations, based on economic criteria, are performed at every level of process design. The process synthesis procedure decomposes the design problem into a hierarchy of decision levels, as follows:

- Level 1: Batch *vs*. Continuous
- Level 2: Input–Output Structure of the Flowsheet
- Level 3: Recycle Structure of the Flowsheet and Reactor Considerations
- Level 4: Separation System Specification
- Level 5: Heat exchanger Network

During the design process, an increasing amount of information is available at each higher level and the particular elements of the process flowsheet start to evolve towards promising process alternatives. Similarly, Smith & Linnhoff[84] proposed an onion model for decomposing the chemical process design into several layers. The design process starts with the selection of the reactor and then moves outward by adding other layers –the separation and recycle system.

Barnicki & Fair[4,5] developed a task–oriented knowledge–based expert system for the separation synthesis problem. The design knowledge of the expert system is organized into a structured query system, the separation synthesis hierarchy (SSH). The SSH divides the overall separation synthesis problem into sub problems or "tasks", which consist of series of ordered heuristics based on pure component properties and on process characteristics. The selector module in the knowledge–based system then selects the separation techniques for each task, based on pure component properties and on process characteristics.

Chen & Fan[12] proposed a heuristic synthesis procedure with special emphasis on stream splitting, where only sharp separations are assumed. More recently, Martin *et al.*[69] presented a systematic procedure based on a philosophical approach. The methodology is based mainly on the intelligent and practical application of heuristic rules developed by experience. The holistic methodology decomposes the original problem into four simpler problems, namely: reaction, localization, separation and integration; the solution resulting by solving of each problem could modify the solution resulting from problems solved earlier or later, providing a holistic character to the methodology.

The heuristic approaches have been used in many applications, such as the synthesis of separation systems (Seader & Westerberg[81]; Nath & Motard[70]), complete process flowsheets (Siirola & Rudd[83]; Powers[76]), waste minimization schemes (Douglas[20]) and metallurgical process design (Linninger[66]). Douglas[19] illustrated, in detail, the hierarchical heuristic method using as a case study the synthesis of benzene through the hydrodealkylation of toluene (commonly known as the HDA process).

With respect to synthesis and design of bioprocesses, an enormous number of heuristics originally applied for chemical process synthesis/design have also found use in bioprocesses, namely:

1. Remove the most plentiful impurities first
2. Remove the easiest to remove impurities first
3. Make the most difficult and expensive separation last
4. Select processes that make use of the greatest differences in the properties of the product and its impurities
5. Select and sequence processes that exploit different separation driving forces

Note that these heuristics were not developed for bioprocesses. Petrides *et al.*[75] proposed a generalized block diagram for downstream bioprocessing shown in Figure 1.1. For each product category, (intracellular or extracellular) several branches exist in

the main pathway. Selection among the branches and alternative unit operations are based on the properties of the product, the properties of the impurities, and the properties of the producing microorganisms, cells or tissues. Bioprocess synthesis thus consists of sequencing steps according to the five heuristics and the structure of Figure 1.1. The majority of bioprocesses, especially those employed in the production of high–value, low–volume products are likely to operate in batch or fed-batch mode. Continuous bioseparation processes are utilized in the production of commodity biochemicals, such as organic acids and biofuels (ethanol, butanol).

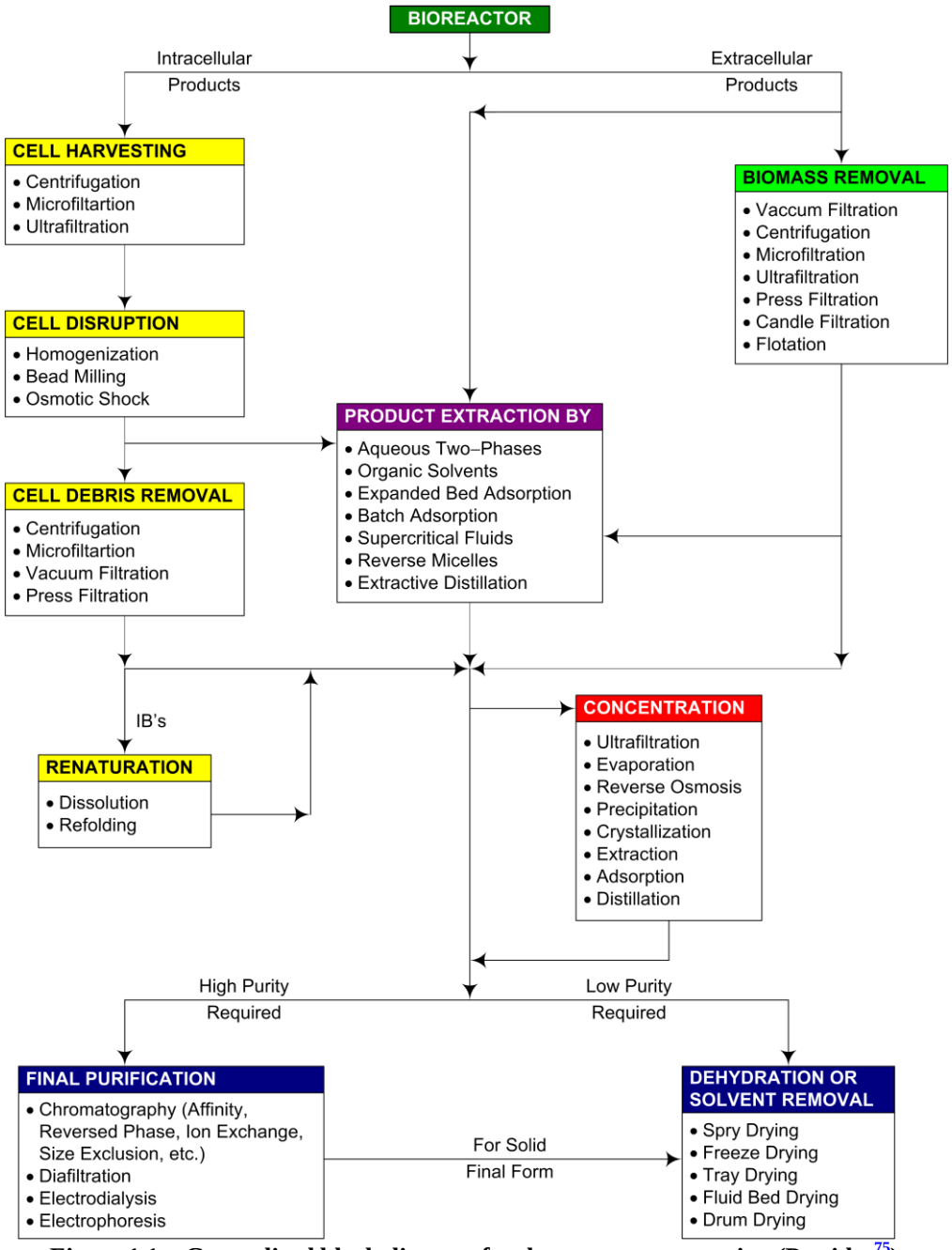

Figure 1.1 – Generalized block diagram for downstream separation (Petrides[75]).

1.1.2 Thermodynamic/physical Insight–based Methods

Thermodynamic/physical insight–based methods for synthesis and design are those that rely on physical/chemical insights to identify feasible process flowsheets, rather than employing heuristic or optimization methods. The insight–based techniques are thus relying on thermodynamic data of the mixture compounds in the synthesis problem as well as the design and analysis of feasible solutions to chemical process flowsheets.

Jaksland *et al.*[48] and Jaksland[49] proposed a methodology for design and synthesis of separation processes based on thermodynamic insights. Jaksland[48] applies thermodynamic insights combined with a set of rules related to physicochemical properties rather than heuristics for selecting and sequencing the separation techniques. This methodology is hierarchical and consists of two main levels. In the first level, differences in component properties are calculated as ratios for a wide range of properties. These ratios are used for initial screening among a large portfolio of separation techniques to identify those that are feasible. In the second level, a more detailed mixture analysis is performed for further screening. Also for separation techniques using solvents (for instance, extractive distillation where an entrainer is needed), these solvents are identified using a molecular design framework adapted from Gani *et al.*[24]. After this, in the second level suggestions for the sequencing of the separation tasks with the corresponding separation techniques, as well as determination of the conditions of operation are made. The methodology assumes that a knowledge base consisting of information on pure component properties and separation techniques is available together with methods for prediction of pure component properties (not covered by the knowledge base) and mixture properties. Therefore, the thermodynamic insight–based methods relies on estimates of the physicochemical properties of the components in the system.

Based on the definition of driving force (*DF*), as the difference in chemical/physical properties between two co–existing phases that may or may not be in equilibrium, Bek–Pedersen[6], Bek–Pedersen & Gani[7] and Gani & Bek–Pedersen[25] developed a framework for synthesis and design of separation schemes. The framework includes methods for sequencing of distillation columns and the generation of hybrid separation schemes. The *DF* approach makes use of thermodynamic insights and fundamentals of separation theory, utilizing property data to predict optimum or near optimum configurations of separation flowsheets. This approach allows identifying feasible distillation sequences as well as other separation techniques (different than distillation).

The use of physicochemical properties information for bioprocess synthesis and design is not a new concept. Leser & Asenjo[67] defined a separation coefficient which is a function of the physical properties difference between components and may be used to choose between high–resolution purification options. Lienqueo *et al.*[63] developed a

hybrid expert system which combines expert knowledge and mathematical correlations to synthesize downstream purification processes for proteins. Physicochemical data on the protein product and other proteins present (contaminants) are used to select a sequence of unit operations to achieve the desired level of purity in the system. The selection of separation processes is based on the quantitative values of the deviation of individual physicochemical properties between the protein product and the contaminating proteins (such as electrical charge as a function of pH, surface hydrophobicity, molecular weight, and affinity) and efficiency of the separation operations to exploit this difference.

1.1.3 Optimization Methods

The problem to be solved using optimization methods can be described as (Biegler *et al.*[10]):

Given a system or process, find the best solution to this process within a specified set of constraints.

To solve an optimization (synthesis/design) problem, a measure of what is the best solution is needed. Therefore, an objective function is defined for the problem, usually a mathematical expression related to the yearly cost or profit of the process. The result of an optimization problem is the optimal value for a set of (decision) variables, where some of them may be bounded to lie within a defined set of constraints. A lot of studies have been carried out on this approach, and it has been widely applied in process synthesis and design for chemical processes. Grossmann & Daichendt[32] and Grossmann[31,33] have published reviews of suitable optimization techniques for process synthesis.

Lin & Miller[64] developed a meta–heuristic optimization algorithm, namely, Tabu Search (TS), to solve a wide variety of chemical engineering optimization problems. Tabu Search (TS) is a memory–based stochastic optimization strategy that guides a neighborhood search procedure to explore the solution space in a way that facilitates escaping from local optima. TS starts from an initial randomly generated solution. Then, a set of neighbor solutions are constructed by modifying the current solution. The best one among them is selected as the new starting point, and the next iteration begins. Memory, implemented with tabu lists, is used to escape from locally optimal solutions and to prevent cycling. At each iteration, the tabu lists are updated to keep track of the search process. This memory allows the algorithm to adapt to the current status of the search, so as to ensure that the entire search space is adequately explored and to recognize when the search space has become stuck in a local region. Lin & Miller[64] highlight the approach through three chemical process examples: heat exchanger network (HEN) synthesis, pump system configuration, and the 10sp1 HEN problem.

Angira & Babu[2] developed a novel modified differential evolution (MDE) algorithm, for solving process synthesis and design problems. The principle of modified differential evolution (MDE) is the same as differential evolution (DE). The major

difference between DE and MDE is that MDE maintains only one array. The array is updated when a better solution is found. These newly found better solutions can take part in mutation and crossover operation in the current generation itself as opposed to DET (when another array is maintained and these better solutions take part in mutation and crossover operations in the next generation) Updating the single array continuously enhances the convergence speed leading to less function evaluations as compared to DE. Angira & Babu[2] illustrate the use of the MDE algorithm for solving seven test problems on process synthesis and design.

Raeesi *et al.*[78] presented a mathematical formulation of a superstructure based solution method, and then used an ant colony algorithm for solving the nonlinear combinatorial problem. Karuppiah *et al.*[54] applied heat integration and mathematical programming techniques to optimize a corn–based bioethanol process. Karuppiah *et al.*[54] first proposed a limited superstructure of alternative designs including the various process units and utility streams involved in the ethanol production process. Short–cut models for mass and energy balances for all the units in the system are used. The objective function is the minimization of the energy requirement for the overall plant. The mixed–integer non–linear programming problem is solved through two nonlinear programming subproblems. Then a heat integration study is performed on the resulting process flowsheet structure.

Recently, Li *et al.*[61] presented an environmentally conscious integrated methodology for design and optimization of chemical processes specifically for separation processes. The methodology incorporates environmental factors into the chemical process synthesis at the initial design stage. The problem formulation, considering environmental and economic factors, leads to a multi–objective mixed–integer non–linear optimization problem which is solved by means of a multi–objective evolutionary algorithm (a non–dominated sorting genetic algorithm). Li *et al.*[61] highlight the application of the methodology through two case studies, the dimethyl carbonate production process using pressure–swing distillation, and an extractive distillation process.

1.1.4 Hybrid Methods

Since application of heuristic or physical insight–based methods does not seek to obtain optimal flowsheets, while mathematical (structural optimization) techniques are limited by the availability and application range of the model and/or the superstructure, hybrid methods use the physical insights of the knowledge–based methods to narrow the search space and decompose the synthesis problem into a collection of related but smaller mathematical problems. Hybrid methods are usually implemented as step–by–step procedures in which the solution of one problem provides input information to the subsequent steps in which other smaller mathematical problems are solved. Finally, such a procedure leads to an estimate of one or more feasible process flowsheets. The final step of hybrid methods is a rigorous simulation for verification of the proposed process flowsheet.

Hostrup[41] developed a hybrid approach for the solution of process synthesis, design, and analysis problems. The hybrid approach combines thermodynamic insights with mathematical programming based synthesis algorithms and consists of three main phases:

1. Pre-analysis
2. Flowsheet and superstructure generation
3. Simulation and optimization

In this way, Hostrup[41] took advantage of optimization techniques to compare the alternative synthesis routes generated by thermodynamic insights. Some other examples of flowsheet synthesis frameworks incorporating multiple techniques are Daichendt & Grossmann[14] who combined hierarchical decomposition with mathematical programming, while Kravanja & Glavič[57] integrated pinch analysis with mathematical programming for the synthesis of heat exchangers networks (HENs).

Based on the principles of the group–contribution approach in chemical property estimation, d'Anterroches & Gani[15] and d'Anterroches[16] developed a framework for computer aided flowsheet design (CAFD). In a group–contribution approach for pure component/mixture property prediction, building blocks are molecular groups, whereas for process flowsheets synthesis these building blocks, namely *process–groups*, are unit operations. The CAFD framework is a combination of two reverse problems; the first problem involves the synthesis of process flowsheet structures similar to a reverse target property estimation approach: defining the property targets for the flowsheet structure, and then the process–groups are combined based on a set of connectivity rules generating thereby a list of feasible flowsheet structures matching the targets. The second, the reverse simulation approach, is applied to obtain the minimum set of design parameters to fully describe the process flowsheet from the process–groups in the flowsheet structure. By knowing the state variables of the inputs and outputs of a unit operation (*i.e.*, individual molar flow rates, pressure, and temperature), through the reverse simulation approach the design parameters of the corresponding unit operation are calculated as the unknown variables from the process model. d'Anterroches[16] illustrates the application of the framework with a set of case studies related to the chemical industry.

Given the particular characteristics of biological manufacturing processes such as (Zhou *et al.*[102]):

- Mixed mode batch, semi batch, continuous, and cyclic operation
- Performance affected by biological variability
- Highly interactive unit operations
- Multiple processing steps and options
- Complex feed stream physical properties

Several major obstacles arise when attempting to apply optimization methods to solve the bioprocess synthesis/design problem. For instance, unit operations commonly

used for downstream purification generally separate components non–sharply, a large selection of unit operations is available depending on the type of product (intracellular or extracellular), biological streams are highly dilute and generally contain a large number of compounds. Clearly, these characteristics lead to a large number of flowsheet structure candidates and, therefore, a corresponding large search space for the synthesis algorithm. Synthesis problems of this size are difficult to solve using numerical optimization approaches.

The use of hybrid approaches has become a more attractive strategy to solve the synthesis and design problem in bioprocesses. Steffens *et al.*[87] presented a procedure for synthesis of bioprocesses which combines the thermodynamic insights–based method developed by Jaksland *et al.*[48,49] together with discrete programming techniques to convert the MINLP synthesis problem into a discrete optimization problem. Stream characteristics and unit design parameters are discretized so that all searching is performed on discrete variables leading to a discrete optimization problem. After this, physical property information is used to screen candidate units thereby reducing the size of the synthesis problem. In this way, only unit operations which exploit large differences between components in a bioprocess stream are selected. Steffens *et al.*[87] presented two case studies to illustrate the use of the synthesis method: the generation of process flowsheet candidates for the downstream purification process for a protein secreted from *S. cerevisae* and for the purification of an animal growth hormone bovine somatotropin (BST).

Rigopoulos & Linke[79] described the application of a general synthesis framework for reaction and separation process synthesis to the activated sludge process design problem —the biochemical process most widely used for wastewater treatment. This synthesis framework consists of two basic elements: a) a general modeling framework to account for all possible design options in form of a superstructure model (includes generic synthesis units and interconnecting streams), and b) an optimization framework to systematically search the solution space defined by the superstructure in order to identify targets of maximal performance and a set of designs that exhibit near target performances.

More recently, Gao *et al.*[28] developed an agent–based system to analyze bioprocesses based on a whole process understanding and considering the interactions between process operations. They have proposed the use of an agent–based approach to provide a flexible infrastructure for the necessary integration of process models. The multi–agent system (MAS) consists of a number of agents that work together to find answers to problems that are beyond the individual capabilities or knowledge of any single agent. The MAS comprises a process knowledge base, process models, and a set of functional agents. The proposed agent–based system framework can be applied during process development or once manufacturing process has commenced. During process development, the MAS can be used to evaluate the design space for ease of process operation, and to identify the optimal level of process performance. During manufacture the MAS can be applied to identify abnormal process operation events and then to provide suggestions to cope with the deviations. In all cases, the function of the system is

to ensure an efficient manufacturing process. Gao *et al.*[28] present a typical intracellular protein production process to illustrate the application of the framework.

1.2 Concluding Remarks

In the previous section, a selection of methods reported in the literature for synthesis and design of chemical and bioprocesses has been described. These methods can in general be categorized as either heuristic or knowledge–based approaches, insight based–approaches, optimization approaches, or hybrid approaches. Some of these methods can be combined into one framework to solve the synthesis/design problem either sequentially or simultaneously. That is, a designed process flowsheet can be the result from the application of an insight based–approach and the solution, which is not necessarily optimal, can be used as a good initial estimate for the formulation of an optimization problem; or when the process–group concept is applied to process synthesis to generate all possible flowsheet structures, then those most likely to be optimal with respect to the performance criteria are selected to be further analyzed in detail using an optimization technique. The hybrid approaches, which combine different approaches into one method, concentrate the strategy on narrowing the search space in order to reduce the size of the synthesis problem and to obtain near–optimal solutions which deserve to be analyzed in more detail.

The heuristic methods are often based on a limited number of operational data, and are thus limited to only specific types of operations. If the methods are broader and several heuristics are proposed, then they might be contradictory. On the other hand, since the heuristic rules are based on observations made on existing processes, the application of heuristic methods deserves careful consideration as they may lead to the elimination of novel process flowsheets which seem to contradict prevailing experience, yet have interesting or desirable features. Insights–based methods are useful to identify feasible separation techniques needed to perform a given separation task, as they are based on properties of the mixture to be separated. Methods based on thermodynamic insights such as the driving force approach are most likely to predict near optimal solutions to the synthesis problem. Afterwards the optimization problem becomes a straightforward task to be solved. However, if experimental data of the pure compounds or mixture properties are not available in the open literature, the major drawback of these methods is that they rely on the accuracy of the models and/or methods to estimate the necessary physical properties.

Mathematical programming techniques are widely used to identify optimal solutions for the design/synthesis problem. These solutions are based on mathematical models of the unit operations as well as the mass and energy balances, and the optimality of the solutions is dependent on the solver being available and the level of accuracy in each unit operation model. In addition, a superstructure of alternative solutions needs to be generated *prior* to solving the problem, and the different alternative solutions (and combination of these) must be considered when solving the problem. In the case the

optimization problem consists of only linear equations, the resulting optimization problem is called Linear Programming (LP), and methods for solving LP problems effectively are readily available (*i.e*. the simplex method). Usually, however optimization problems for process flowsheets contain non–linear equations, thereby resulting in Non–Linear Programming (NLP). In order to solve an optimization problem of this nature certain techniques must be applied, for example reduced gradient approaches or a Successive Quadratic Programming (SQP) method (Biegler *et al.*[10]). However, the methods for solving NLP problems cannot guarantee that the solution found is globally optimal, unless the objective function and the feasible region are convex.

An important part of solving a process synthesis problem is to determine which equipment should be used in the process. If more than one flowsheet structure exists for a particular unit operation in the process, a decision as to which flowsheet structure to use must be made. Such decisions/selections among the flowsheet structures can be included in the optimization problem as a vector of integer (often Boolean) variables, thereby, implying the use of superstructures. In this case where the optimization problem consists of linear equations and discrete variables the resulting problem is a Mixed Integer Linear Programming (MILP) problem. But if the optimization problem consists of non–linear equations and discrete variables the resulting problem is called Mixed Integer Non–Linear Programming (MINLP) problem.

The development of a superstructure involved in the MINLP problem for process flowsheet synthesis, is in principle, difficult. Even for the separation synthesis part of the process flowsheet, there is a large number of process flowsheet structures to take into account. In some cases heuristic rules can often be applied to reduce the size of the related structural optimization problem. The size of the task/techniques selection and sequencing problem is determined by the number of compounds (NC) in the mixture to be separated and the number of potential separation techniques (NT) to be used in the synthesis problem. For a separation system where all components need to be separated from each other, Thompson & King[90] proposed an expression to calculate the number of possible sequences based on simple binary sharp splits:

$$NS = \frac{\left[2\ \ NC-1\ \right]!}{NC!\ \ NC-1\ !}\, NT^{NC-1} \qquad (1.1)$$

Equation (1.1) has been applied for the calculation of the number of possible sequences considering only one separation technique (NT = 1) for a different number of compounds in Table 1.1 (column 2). As can be noticed from the Table 1.1, even when only sharp splits and only one separation technique (*i.e*. simple distillation) are considered, the number of process flowsheets in the superstructure rapidly increases with the number of compounds in the mixture to be separated.

It is clear that if the superstructure is expanded further to include, for instance, non–sharp separations, multiple processing steps and options implying more than one separation technique to be used in the separation synthesis problem, then the size and complexity of the problem will become immense. In addition to that, if the process reaction is considered where for example non–linear reaction models are encountered in biocatalytic systems, the complexity of the problem will increase as well.

Table 1.1 – Number of possible sequences to separate *NC* components by *NT* potential separation techniques.

NC/*NT*	1	2	7	10
2	1	2	7	10
3	2	8	98	200
4	5	40	1715	5000
5	14	224	33614	140000
6	42	1344	705894	4.2E+006
8	429	54912	3.533E+008	4.29E+009
10	4862	2489344	1.962E+011	4.862E+012
20	1.767E+009	9.266E+014	2.014E+025	1.767E+028

Another important aspect that also needs to be taken into consideration is how rigorous the models of the individual unit operations are, as it is crucial for the solution of the optimisation problem that the models in the superstructure are consistent and correct.

Even when methods such as the Generalized Benders Decomposition (GBD) and the outer approximation methods, are available to solve this type of problems, the formulation of a superstructure model and solving the corresponding MINLP optimisation problem directly are very large tasks, both mathematically and computationally. Therefore, if the superstructure is large and detailed, it is advantageous to screen out infeasible separation techniques through either heuristics or property insights methods to decrease the size of the feasible region of the MINLP problem and exploit it so as to reduce the computational costs and increase the reliability of the solution.

1.3 Motivation and Objectives

Considering the current state of the art, it is obvious that there is a lack of methodologies to solve the synthesis and design problem in bioprocesses compared with the development in the chemical industry which has been enormous. On the one hand, heuristic methods are often based on a limited number of operational data and their application needs to be considered carefully as they may lead to the elimination of novel process flowsheets as mentioned. On the other hand, methods based on thermodynamic insights are most likely to predict near optimal solutions. Nevertheless, their major drawback is that they rely on the accuracy of the models and/or methods to estimate the necessary physical mixture/pure compound properties if they are not available in the open literature. Structural optimization frameworks have been developed for separation synthesis, and the common focus has been primarily towards distillation sequences. However, it is clear that the separation synthesis problem has a potential danger of combinatorial explosion that needs to be addressed. The common strategy to be followed is to use the existing methods and approaches to solve the synthesis problem. Nevertheless, in some cases, this strategy has not been very successful and the synthesis problem becomes of special concern when the portfolio of potential separation techniques to be used in the synthesis/design problem is large as it is the case for bioprocesses. This is often a long and cumbersome task which demands a huge computational effort.

Clearly, this is a highly undesirable situation and there is a strong need for a systematic framework for a quick and reliable selection of high−performance process configurations. Therefore, the logical pattern to be followed is the integration of different approaches and tools in a systematic synthesis and design framework to solve the synthesis and design problem. This work is focused on the development of a generic synthesis framework for chemical and biochemical processes that aims to overcome the above limitations.

By combining different approaches in a systematic manner, a framework for synthesis, design, and analysis of chemical and biochemical processes has been developed in this work. The developed framework consists of five stages: 1) available process knowledge data collection, 2) modelling and simulation, 3) analysis of important issues, 4) process synthesis and design, and 5) performance evaluation and selection. The framework exploits the advantages of some of the approaches described previously. For instance, it employs the thermodynamic insights in identifying feasible separation techniques which can be represented by a set of process−groups. Then the CAFD technique is employed through the combination of the process−groups to generate only feasible flowsheet structures. The framework is supported by a collection of computer aided methods and tools which can help to reduce time and computational effort.

Another objective of this work is to extend the range of application of the process−group concept developed by d'Anterroches[16] in order to cover various types of products and their corresponding processes, in particular the ones related to bioprocess area. Therefore, a new set of process−groups together with their contributions has been developed.

1.4 Structure of the Ph.D. Thesis

This thesis is organized as follows:

In **Chapter 2** the theoretical background of the concepts employed in this work is given. Concepts such as process–group, driving force, attainable region and reverse approach are explained in detail as these concepts are the core of the methods that support the framework.

Chapter 3 gives the full picture of the developed framework for synthesis, design and analysis of chemical processes and bioprocesses. The framework is presented in detail together with the computer–aided methods and tools supporting the framework.

Chapter 4 highlights the application of the framework through examples and cases studies of industrial interest. The framework is highlighted with three case studies, namely, bioethanol production process (downstream separation), succinic acid production process, and diethyl succinate production process.

Chapter 5 gives the conclusions and lists the main contribution of this work as well as suggestions for future directions and developments.

2 Theoretical Background

2.1 Introduction

In this chapter the fundamental background needed for the framework for design and analysis is described. First, a definition of the integrated synthesis, design, and control problem is given. Then, the concepts of driving force (*DF*), attainable region (*AR*), process–group (*PG*) and reverse simulation are described. The *DF* or *AR* concepts are at the core of the reverse simulation methods used in the framework. Finally, examples highlighting the application of these concepts are presented.

2.2 Definition of Integrated Synthesis, Design and Control Problem

Process synthesis, design, and control are three different problems that are usually solved independently. In order to solve these problems simultaneously, it is necessary to determine what is the common information (variables) involved in the three problems. Many process synthesis, design and control problems deal with process variables such as temperature (*T*), pressure (*P*) and/or composition ($\underline{x}$). These variables are usually regarded as intensive variables, which can be measured and based on these, other process variables such as enthalpies, densities, volumes, and fugacities can be estimated. These intensive variables therefore provide useful information for process synthesis, design, and control problems, but have different functions. In process synthesis, effects of intensive variables on the properties are determined in order to generate the process flowsheet/configuration. In process design, optimal values of the intensive variables are determined such that the process satisfies the specified design objectives, while in process control, the sensitivities of the intensive variables are determined in order to design the control system structure (*i.e.* determine what to control and what to manipulate). Consequently, when the process synthesis, design, and control problems involve the same set of variables, they can be integrated and solved as a common problem.

2.3 Concepts

2.3.1 Driving Force (DF)

According to Bek–Pedersen[6], the definition of the driving force (*DF*) is the difference in composition of a compound *i* in two co–existing phases that may or may not be in equilibrium. As Bek–Pedersen[6] pointed out, this difference in composition may be due to the thermodynamic equilibrium between the two phases as in the case of distillation. Nevertheless, transport mechanisms other than thermodynamic equilibrium, for instance diffusion or convection, can also promote driving forces, and therefore allow the separation to take place.

The starting point is the availability of phase composition data, and the graphical representation of the phase composition data (that is, plot of the *DF* as a function of liquid (or vapor) composition) as shown in Figure 2.1. It can be seen that *DF* is a concave function with respect to composition with a well–defined maximum. Since energy needs to be added to or removed from the system in order to create and maintain two co–existing vapor–liquid phases, the value of the *DF* is indirectly related to the energy added or removed. If the *DF* is large, less energy is involved, while if the *DF* is small more energy is involved.

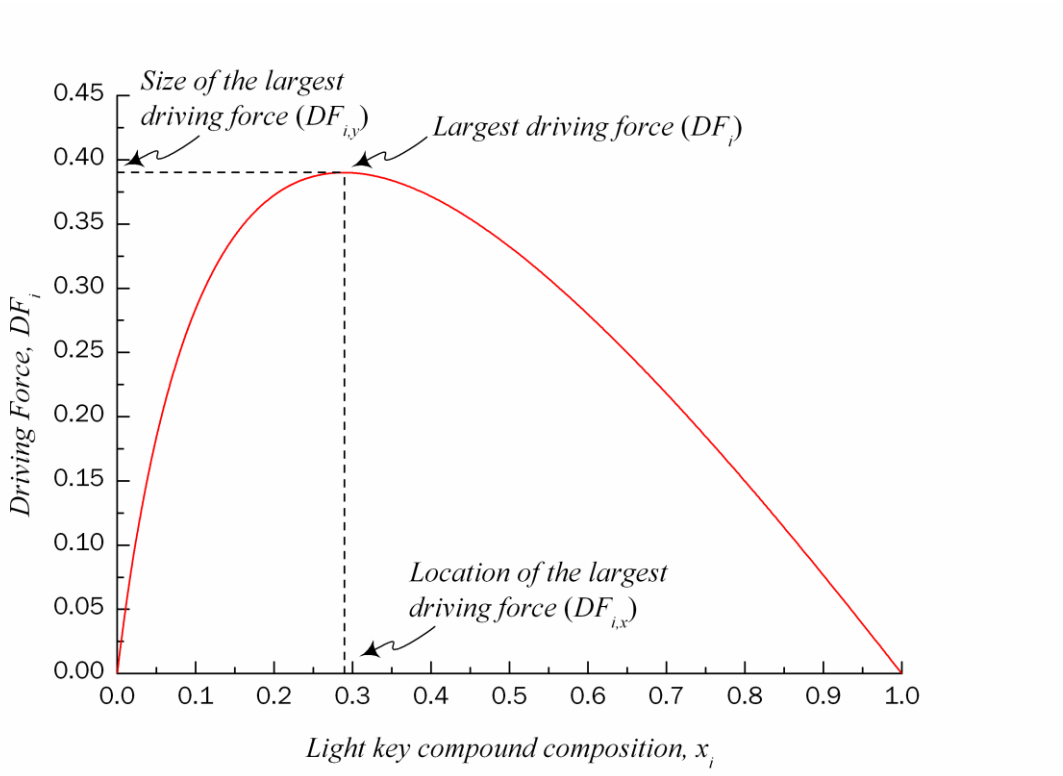

Figure 2.1 – Driving force as function of composition.

Based on this concept, Gani & Bek–Pedersen[24], Bek–Pedersen[6], and Bek–Pedersen & Gani[7] developed a method for synthesis and design of distillation based separation processes. With this concept, the size and relative location of the maximum

DF is used as a design parameter for the identification of the number of stages in a distillation column, the feed stage location, reflux ratio, etc., as illustrated in Figure 2.2. The $BD_{i,y}$ and $AD_{i,y}$ lines represent operating lines corresponding to minimum reflux, while *BD* and *AD* represent operating lines intersecting on the line $D_{i,y}$–$D_{i,x}$ for a reflux greater than the minimum. Therefore, by targeting the separation task at the largest *DF* value, an optimal (or near optimal) solution in terms of energy consumption is found. Consequently, designing any type of process based on the largest *DF* leads to a highly energy–efficient design.

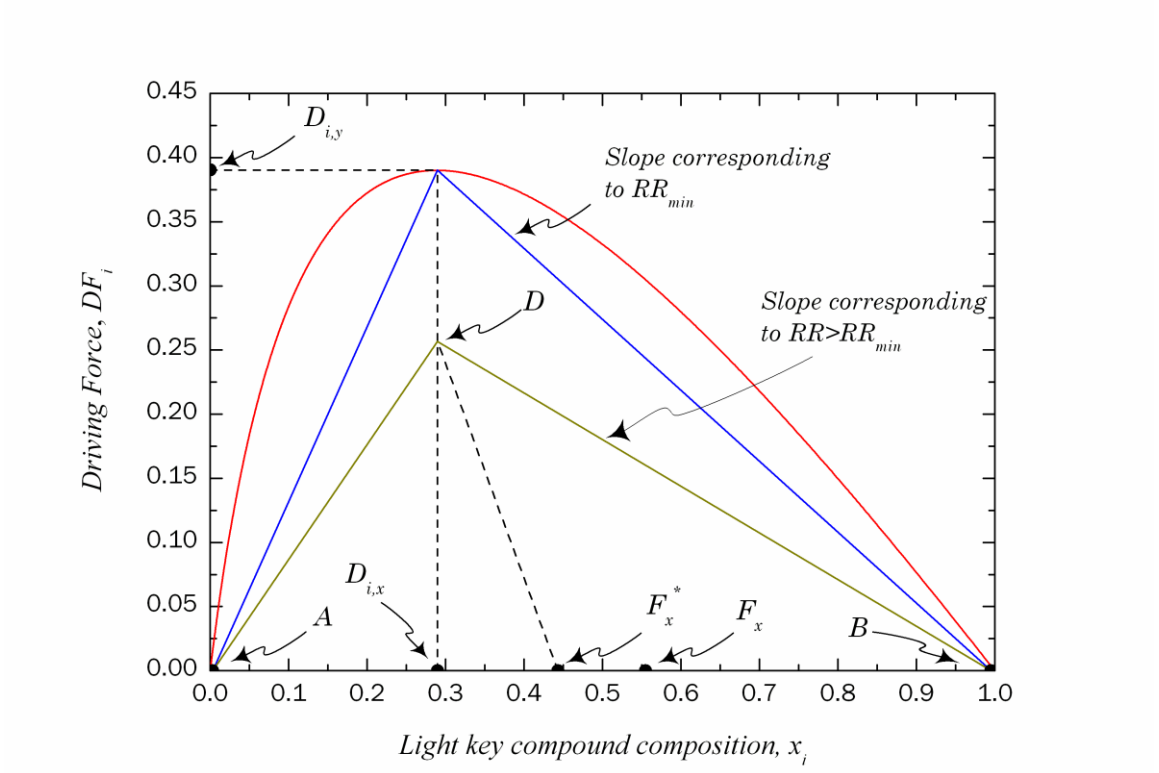

Figure 2.2 – Driving force diagram with illustrations of the distillation design parameters (Bek–Pedersen[6]).

2.3.2 Attainable Region (AR)

Horn[39] defines the attainable region (*AR*) as the region in the stoichiometric subspace that could be reached by any possible reactor system. The *AR* is the set of all possible output concentrations that can be obtained using the allowable fundamental process, subject to specified constraints, for a system with specified inputs. Fundamental processes that may be considered are physical and chemical phenomena such as mixing, reaction, separation, and heat or mass transfer. The only element required to describe the *AR* is its boundary. The objective function is usually optimized somewhere on the boundary of the *AR*, as the boundary represents extremes in operation and efficiency.

Once the *AR* has been found, the resulting boundary must be interpreted. The various surfaces that comprise the boundary represent the various processing units. The arrangement of these surfaces in the boundary determines the layout of the processing units within the process.

In Figure 2.3 the *AR* in the concentration space of compounds of *A* and *B*, has been determined for the van de Vusse[91] reaction scheme. It shows that the boundary of the *AR* is defined by the by–passed CSTR (Constant–flow Stirred Tank Reactor) followed by a PFR (Plug Flow Reactor). More details on the construction of this *AR* are provided in section 2.3.4. The important results to note are that once the boundary of the *AR* has been constructed and interpreted, the best layout and the best operating conditions with respect to the objective function can be determined. For instance, the objective function could be to maximize the production of ***B*** given the feed conditions represented by point ***O***. Cost, partial pressure, temperature, selectivity, and residence time are some other examples for possible objective functions.

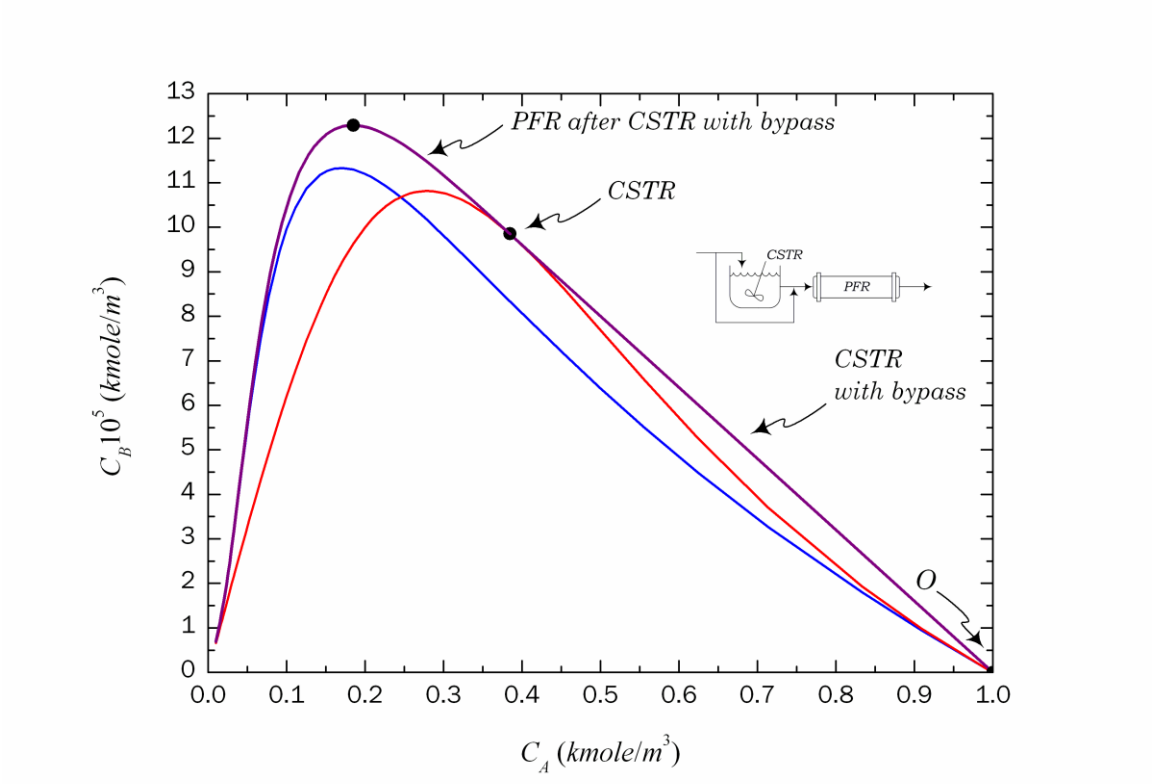

Figure 2.3 – Attainable region for the van de Vusse reaction (van de Vusse[91])

2.3.3 Process–Group (PG)

The process–group concept (d'Anterroches & Gani[14]; d'Anterroches[15]) applies the principles of the group–contribution approach from chemical property estimation to the synthesis and design of chemical processes. In a group–contribution method for pure component/mixture property prediction, the molecular identity is described by means of a set of functional groups of atoms bonded together to form a molecular structure. The process–groups represent either a unit operation (such as a reactor, a distillation column, or a flash), or a set of unit operations (such as, two distillation columns in extractive distillation, or pressure swing distillation). The bonds among the process–groups represent the streams connecting the unit operations, in an analogous way to the bonds combining (molecular) functional groups. For example, in Figure 2.4 (*a*), a simple process flowsheet composed of a distillation column, followed by an extractive distillation column to separate a binary azeotropic mixture by using ionic liquids as entrainer (with the addition of a makeup of solvent), followed by a flash drum and a stripping column to recover the solvent, could be represented with process–groups.

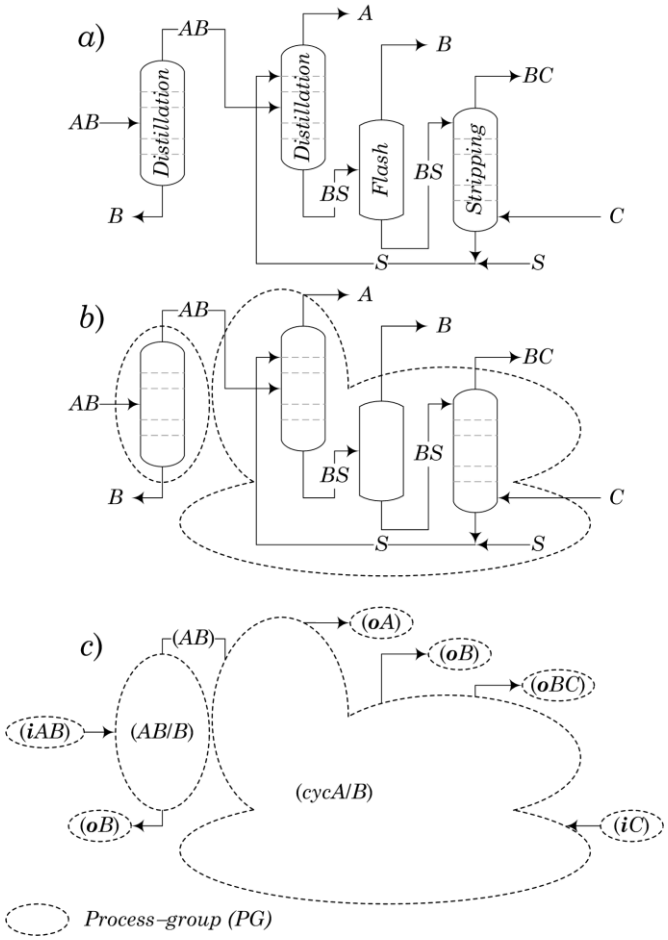

Figure 2.4 – a) Representation of a simple process flowsheet; b, c) with process groups.

Consider the process flowsheet in Figure 2.4 (*a*). The feed mixtures are represented by two process–groups; one inlet process–group (*iC*), and the inlet

process−group containing two compounds (*iAB*). The end products are represented by two outlet process−groups (also process−groups with one attachment), (*oA*), (*oB*) (a product of purity ≥ 99.5%), and one outlet process−group containing two compounds (*oBC*). The two process−groups representing a distillation (*AB*/*B*) and a solvent−based separation (*cycB/C*) have at least one inlet and one outlet stream. From the list of available process−groups a feasible flowsheet structure can be created as shown in Figure 2.4 (*b*/*c*) where a binary azeotropic mixture is separated with a downstream separation process in which the feed mixture is concentrated up to its azeotropic point and then by a special process−group, *A* and *B* are obtained as pure products (a product of purity ≥ 99.5%).

As in group contribution based molecular property prediction (where the same molecular groups may be used to represent many molecules), the process−groups are also not component dependent, but component property dependent. Therefore, the use of the same process−groups to represent different components having similar properties is also valid in the case of process flowsheets of a process. Note, however, that the inlet and outlet streams (bonds) of process−groups must maintain the list of components present in them and that the path of a component through a process−group establishes the flowsheet structure. That is, process−groups (*A/BC*) and (*B/C*) can be connected to form [−(*A/BC*)−(*B/C*)−] without knowing the identities of the components *A*, *B*, and *C*. The identities of the chemicals (components) are only needed when the properties of the flowsheet need to be calculated.

Currently, nineteen types of process−groups are available. These are listed in Table 2.1 and they represent the following unit operations: simple distillation column, solvent based azeotropic distillation using organic solvents, solvent based azeotropic distillation using ionic liquids, solvent based azeotropic distillation using hyperbranched polymers, flash separation, kinetic model based reactor, fixed conversion reactor, pressure swing distillation, polar molecular sieve−based separation, molecular sieve based separation, liquid membrane based separation, liquid adsorption based separation, gas membrane based separation, crystallization, liquid−liquid extraction using organic solvents, pervaporation, simple solid−liquid separation, absorption and ion exchange.

Table 2.1 – Available process–groups.

Process–Groups	Unit Operation	Process–group example
Simple Distillation Column	Distillation column	(*AB*/*C*), (*AB*/*BC*)
Solvent Based Azeotropic Separation	Extractive distillation	(*cycA*/*B*)
Flash Separation	Flash	(*fABC*/*BCD*)
Kinetic Model Based Reactor	CSTR, PFR, mixer, divider	(*rABC*/*nE*/*pABCD*)
Fixed Conversion Reactor	CSTR, PFR, mixer, divider	(*rABC*/*nE*/*pABCD*)
Pressure Swing Distillation	Distillation column, mixer, compressor, valve	(*swA*/*B*)
Polar Molecular Sieve Based Separation	Molecular sieve, regeneration process	(*pmsABC*/D)
Molecular Sieve Based Separation	Molecular sieve, regeneration process	(*ms*ABC/*D*)
Liquid Membrane Based Separation	Membrane	(*lmemABC*/*D*)
Liquid Adsorption Based Separation	Molecular sieve, regeneration process	(*ladsABC*/*D*)
Gas Membrane Based Separation	Membrane	(*gmemABC*/*D*)
Pervaporation Based Separation	Pervaporation	(*pervABC*/*D*)
Crystallization Based Separation	Crystallization	(*crsABC*/*D*)
Liquid–Liquid Extraction Based Separation	Extractive column	(*llABC*/***S***/***S***C/*AB*)
Simple Solid–Liquid Separation	Filter (e.g. belt press filter)	(*slAB*/*CD*)
Absorption	Absorption	(*abEAB*/e*F*/*EABF*/*EF*)
Ion Exchange Separation	Ion exchange column	(*ieABCD*/*ABC*)

Process group combination rules and feasible structure generation

Using the same approach as Computer Aided Molecular Design (Harper[35]) it is possible, through the process–group combination rules, to generate flowsheet structures, to evaluate them and to find the best process flowsheet matching the targets.

For instance, the process–group (*ABC*)(*DE*) has three attachments: one input and two outputs. The combination rules are as follows:

- Get all the process–groups matching the set of components to be processed by the process–group (*ABC*)(*DE*). There are only two combinations: 1 input process–group defined as ***i****ABCDE* or a process–group with (*ABCDE*) as output such as (***o****ABCDE*)(***o****F*) that will serve as input to the process–group (*ABC*)(*DE*).
- Get all the process–groups matching the set of componets for each output of the process–group (*ABC*)(*DE*). There are three possible combinations: 2 output process–groups defined as ***o****ABC* and ***o****DE*, 1 output process–group defined as ***o****ABC* and one process–group such as (*DE*) and which will serve as input to process–groups such as (*D*)(*E*) and one process–group defined as ***o****DE* and one process–group such as (*ABC*), and which will serve as input to process–groups such as (*AB*)(*C*) or (*A*)(*BC*).

Following these combination rules and based on the definition of each process–group in the flowsheet structure ensures that the flowsheet represents a feasible flowsheet structure.

Flowsheet property model

Similar to the situation where each molecular group in a given molecular structure provides a contribution for a given property target (such as normal boiling point, critical pressure, critical temperature, etc.) each process–group provides a contribution to the property of the flowsheet. This property can be the performance (in terms of energy consumption, operating cost, profit, etc.,) defined in such a way that once the flowsheet is described by the process–groups, the flowsheet property can be calculated by means of the corresponding flowsheet property model.

As pointed out by d'Anterroches & Gani[14], a flowsheet property is the energy consumption of the process flowsheet, which can be predicted by a process–groups based model where the process flowsheet is represented by process–groups. d'Anterroches[15], has proposed the following flowsheet property model based on the driving force concept to estimate the energy consumption for a process flowsheet involving distillation columns with one feed stream and two product streams.

$$E_x = \sum_{k=1}^{n=NG} Q_k = \sum_{k=1}^{n=NG} \frac{1+p_k}{df_{ij}^k} a_k \qquad (2.1)$$

where E_x is the energy consumption of the flowsheet (*MkJ*/*h* for *M* moles/*h* of feed), Q_k the energy consumption of each process−group, NG is the number of process −groups, df_{ij}^k represents the maximum driving force of the process group k, a_k the contribution of the process group k. Every unit operation has a position in the flowsheet where it can attain the theoretical maximum driving force. At any other position, the unit operation is able to attain a lower driving force than the maximum. The topology factor p_k takes into account this fact and it is a function of the attainable driving force.

$$p_k = \sum_{i=1}^{nt} D_i \qquad (2.2)$$

Two important facts can be drawn from this flowsheet property model:

- Based on driving force theory, it is clear that any process−group contribution method calculating the energy consumption (as flowsheet property) will be component independent if it is based on the driving force as input (known) variable, in the sense that different component binary pairs may have the same driving force.
- From the driving force diagram (see Figure 2.1), it can be observed that driving forces can be computed for any type of two−phase system as long as the composition data of the two co−existing phases are available. This is true irrespective of whether the separation process is rate−based or equilibrium−based since the driving force can be calculated from measured or estimated composition data. Therefore, modelling/design of separation processes based on vapor−liquid, liquid−liquid or solid−liquid driving forces can also be handled by the flowsheet property model in Eq. (2.1) together with the appropriate parameter a_k.

Model parameter estimation

The contributions a_k of the process−groups of the flowsheet property model in Eq. (2.1) have been regressed by means of fitting experimental data. For the purpose of this work, extractive distillation columns separating different azeotropic mixtures into different product specifications by using novel entrainers such as ionic liquids and hyperbranched polymers have been simulated through a validated rigorous distillation column model. These simulation results provide a set of *pseudo* experimental data on the feasibility of separation as well as the corresponding energy consumption. For the model

parameter regression, as the driving force and the group identities are known for each simulated task, the corresponding list of process–groups is also known. Therefore, the process–group parameter a_k can be estimated through regression by matching the *pseudo* experimental values of E_x obtained by simulation. The following procedure is proposed to obtain the E_x model parameter a_k.

Procedure to obtain the E_x model parameters

1. Define the separation task related with the process–group.
2. Construct the solvent free *DF* diagram for different solvent fractions, either from experimental data or *VLE* calculations.
3. Perform a set of simulations for different solvent free fractions to generate *pseudo* experimental data with respect to the energy consumption of the process.
4. For each solvent fraction used in step 3, obtain the maximum df_{ij}^{k} from the solvent free *DF* diagram.
5. From Eq. (2.1) obtain a_k parameters through the minimization of the energy consumption of the process as shown in the objective function given by Eq. (8.13) in the Appendix.

The detailed procedure to obtain the energy index E_x model parameters is highlighted in the Appendix (section 8.3.1.5).

2.3.4 Reverse Simulation

Using knowledge on the state variables in inputs and outputs of a unit operation (*i.e.* individual flow rates, pressure, and temperature), the reverse simulation method is the procedure by which the design parameters of the corresponding unit operation are calculated as the unknown variables from the process model. This methods is described in Figure 2.5 for a simple distillation column example.

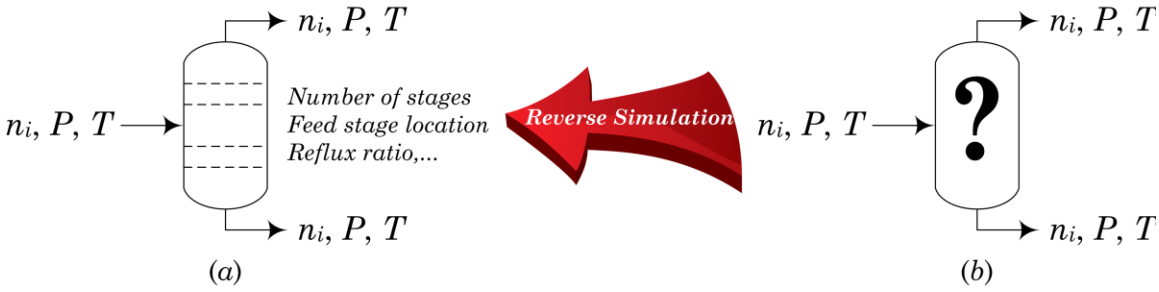

Figure 2.5 – Reverse simulation overview.

From the inlet and outlet stream definitions and the properties of the mixture in Figure 2.5(*b*), the number of stages, the feed stage location and reflux ratio of the column are back–calculated as shown in Figure 2.5(*a*). As pointed out by d'Anterroches[15], the term *reverse* is used to highlight the difference with respect to *conventional* simulation. By using conventional simulation, the design problem is solved by trial and error. Indeed, when knowing the desired targets of a given unit operation, the design parameters are modified or optimized to match the targets. In this case the targets are related to values of product purities or recoveries and/or energy consumption for a separation unit such as distillation; selectivity and/or residence time for a reaction unit. As shown in Figure 2.6, for a simple distillation column, an initial set of design parameters is assumed first, and then simulation is performed and the results are compared with the desired targets. If the difference with the targets is above the acceptable error, then another set of design parameters has to be assumed and simulation is performed again, until a satisfactory match is found. In this section, procedures to apply the reverse simulation to a simple distillation process–group as well as a kinetic model reactor process–group are presented together with their corresponding examples.

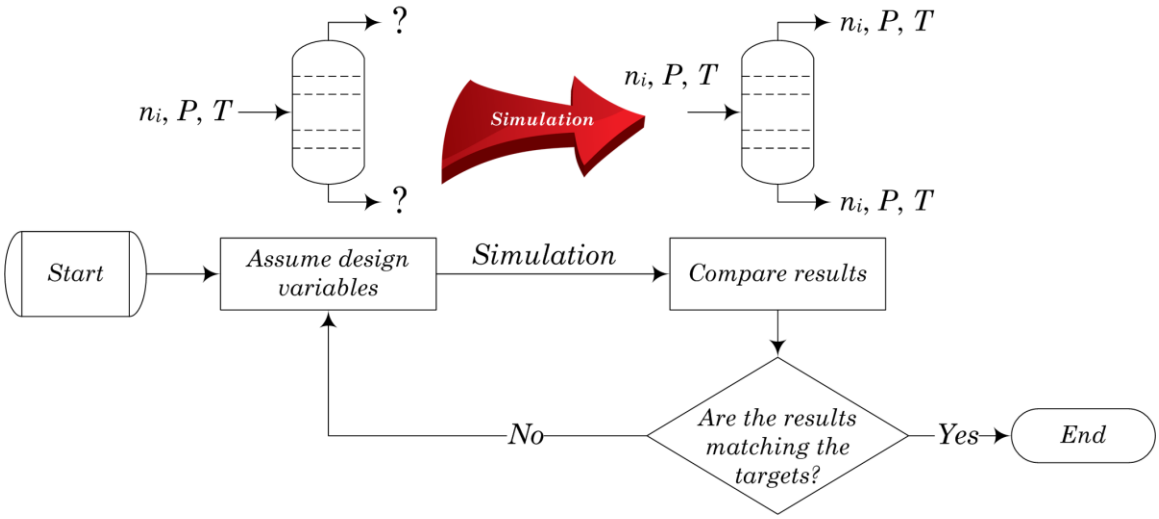

Figure 2.6 – Conventional simulation overview.

Reverse simulation procedure for the distillation process–group based on the *DF* concept

The procedure to determine the design parameters of a distillation column in the distillation process–group is as follows:

1. Given a distillation process–group with *NC* components.
2. Order the components by relative volatility and identify the key components.

3. Retrieve the maximum *DF* between the key components $F_{Di}|_{Max}$, and the composition of the light key at its maximum D_x, either from experimental data or *VLE* calculations.
4. Select the values of product purities or recoveries for the key components. If they are not given use 99.5% by default.
5. If the input composition is between the requested purities for the bottom and top products, then get the ideal number of stages N_{ideal} for the column from the table of pre–calculated values (Table 8.10) in Appendix.
6. Set the feed plate location of the column to be $N_F = 1 - D_x \ N_{ideal}$ (plate one is the top plate of the column).

Example of reverse simulation for the distillation process–group

In this section, an example of reverse simulation through the distillation process–group (*A*/*BCDE*) for the separation of a five components mixture by simple distillation is presented. The components and the inlet composition specification are given in Table 2.2. The relative volatilities have been calculated on the basis of the feed composition, assuming a system pressure of 27.22 *atm* using the Peng–Robison Equation of State with interaction parameters set to zero.

Table 2.2 – Definition of the components in the (*A/BCDE*) process–group.

Component	Flowrate (*kmole*/*h*)	Normal Boiling Point (*K*)	Relative volatility	Relative volatility between adjacent components
A – Methane	20	111.66	358.57	6.37
B – Ethane	46	184.55	56.30	3.92
C – Propane	30	231.11	14.36	3.88
D – Butane	3	272.65	3.70	3.70
E – Pentane	1	309.22	1.00	

The key components are *A* and *B*, methane and ethane, respectively. From the driving force diagram in Figure 2.7, $F_{Di}|_{Max} = 0.478$ at $D_x = 0.798$. From Table 8.10 of pre–calculated values $N_{ideal} = 10$ and $RR_{min} = 0.54$. Given D_x and N_{ideal}, the feed plate location is $N_F = 1 - D_x \ N_{ideal} = 2$. At this stage, the distillation column is fully defined for further rigorous simulation.

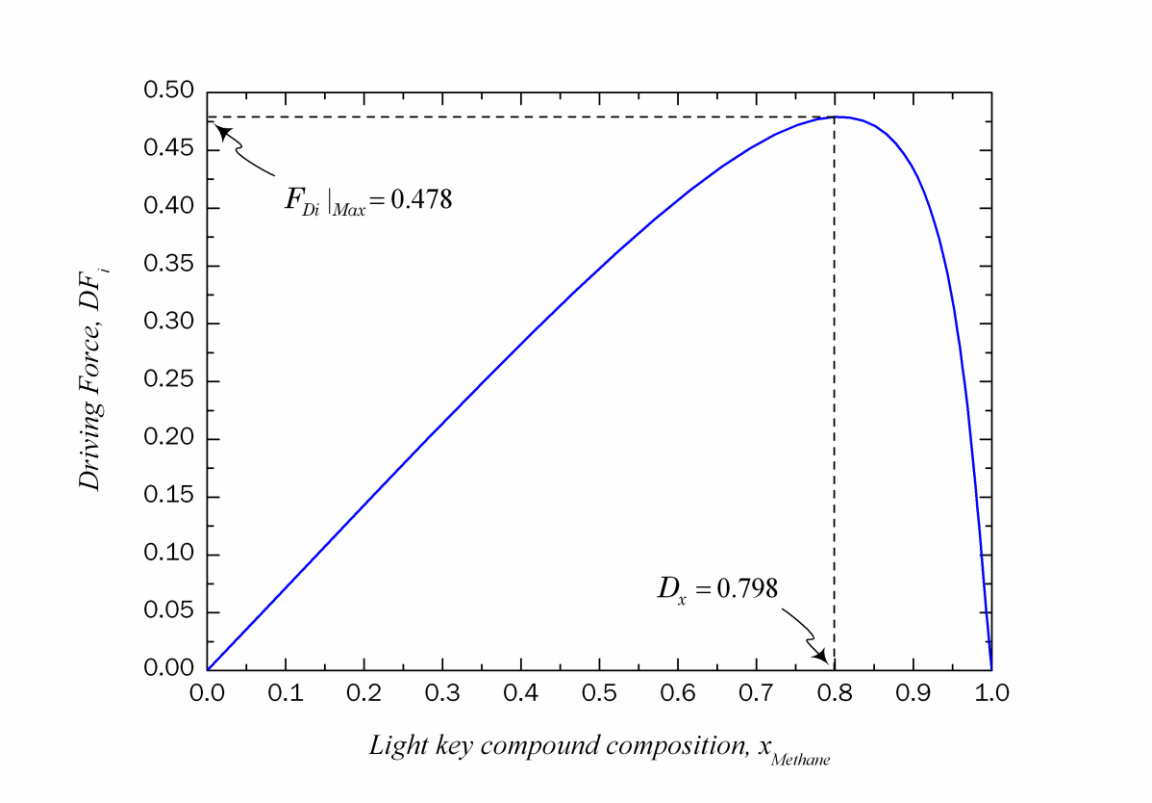

Figure 2.7 – Driving force diagram for the binary pair methane/ethane.

Reverse simulation procedure for the kinetic based reactor process–group based on the *AR* concept

The reverse simulation for the kinetic based reactor process–group is based on the *AR* concept presented in Section 2.3.2. In this section, only the attainable region analysis is applied to the kinetic model based reactor process–group. The *AR* concept provides a systematic geometric method for the synthesis of chemical reactor networks (Glasser & Hildebrandt,[28]; Hildebrandt & Glasser[37]). Once the *AR* diagram has been constructed, the idea is to use the location of the maximum value of the desired product composition as the basis for the reactor design to calculate other important variables such as residence time, temperature, and reactor volume.

The kinetic model based reactor process–group provides the following information which is necessary to proceed with the attainable region analysis.

- Nature of the components in the reactions.
- Complete definition of the reactions and their corresponding kinetic models.

The *AR* based analysis is a procedure which comprises of the following steps:selection of the fundamental processes, selection of the state variables, definition and drawing of the process vectors, constructing the *AR*, interpretation of the boundary,

and finding the optimum for the specified objective function (operating cost, selectivity, residence time).

1. *Selection of the fundamental processes*. *Fundamental processes* considered in the synthesis of a reaction system are physical and chemical phenomena such as reaction, mixing, separation, and heat and/or mass transfer.

2. *Selection of the state variables*. The state of the system is characterized by *state variables*. These describe the fundamental processes, but it may also include variables from the specified objective function.

3. *Definition and drawing of the process vectors*. *Process vectors* give the instantaneous change in the system state caused by fundamental process occurring in that unit. For example, if only a reaction process is occurring, the reaction vector $\mathbf{r} = \mathbf{r}(C_A, C_B)$ will give the instantaneous direction and magnitude of change from the current concentration position. For mixing processes this vector gives the instantaneous change from the current state of the system $\mathbf{C}$ based upon the added state $\mathbf{C^*}$ or $\boldsymbol{v}(\mathbf{C}, \mathbf{C^*}) = \mathbf{C} - \mathbf{C^*}$.

4. *Constructing the AR*. A definite methodology to find the *AR* for given fundamental processes is not available, and often a trial and error procedure is required. Nevertheless, the *AR* candidate must respect the following necessary conditions, as demonstrated by the works of Hildebrandt & Glasser[37] and Glasser & Hildebrandt[28]. It is necessary that the attainable region $\boldsymbol{A}$ with feed(s) $\boldsymbol{C}^0$ is such that:

   - (*a*) It is convex.
   - (*b*) No reaction vector on the boundary of $\boldsymbol{A}(\partial\boldsymbol{A})$ points outwards from $\boldsymbol{A}$, that is, the reaction vectors in $\partial\boldsymbol{A}$ point inward, are tangent to $\partial\boldsymbol{A}$, or are zero.
   - (*c*) No reaction vector in the complement of $\boldsymbol{A}$ can be extrapolated backwards into $\boldsymbol{A}$.
   - (*d*) No two points on a PFR in the complement of $\boldsymbol{A}$ can be extrapolated back into $\boldsymbol{A}$.

   It is important to point out that when using the *AR* technique we are interested in constructing only the boundary of *AR* (*∂AR*). Any other interior point can be achieved by mixing points from the boundary. Hildebrandt & Glasser[37] describe a general approach for constructing the *AR*. A brief description of each step is given bellow.

   - **Step 1**: Draw the PFR(s) from the feed point(s).
   - **Step 2**: Allow mixing between all the points than can be achieved by the PFR(s). This process is known as finding the convex hull of the curve(s).

- **Step 3**: Check whether any reaction vectors point out of the surface of the convex hull. If the reaction vector points outwards over certain regions, then find the CSTR(s) with feed points in the convex hull that extend the *AR* the most. If no reaction vectors point outwards, then check whether necessary conditions (*c*) and (*d*) are meet. If they are not met, extend the region using the appropriate reactor.
- **Step 4**: Find the new, enlarged convex hull. If a CSTR lies in the boundary at this stage, the reaction vectors must point out of the region, and the PFR with feed points on the CSTR will extend the region. Extend the region by finding the convex hull with these PFR´s included.
- **Step 5**: Repeat the last two steps, alternating between PFR's and CSTR's, until no reaction vectors point out over the region, and necessary conditions (*c*) and (*d*) are met.

Generally no more than four construction stages are required. The region that we construct in this way will be attainable, but as we do not have a complete sufficiency condition as yet, the region may not be the full *AR*. We do however know that this region cannot be extended by any combination of PFR's, CSTR's, recycle reactors and any differential combination of reaction and mixing.

5. *Interpretation of the boundary*. *AR* analysis will not only demonstrate that a specific output is achievable, but will also determine the process required to achieve it, such as, mixing, reaction, separation, and heat or mass transfer. The advantage of the geometric approach to finding the *AR* is that the process layout or the operating sequence can be determined directly from the geometry of the diagram. For a particular output of interest there will be a path from the input to achieve the output point. This path is interpreted in terms of the sequence of fundamental processes required to follow the path. There is usually only one path to a particular point on the *AR* boundary and an infinite number of paths to any point in the interior on the *AR* region.

6. *Finding the optimum*. The final step is to determine the optimum for the specified objective function. In most instances, the objective function will be optimized at a point in the boundary due to the the fact that the boundary points represent extremes in operation. Since the point which optimizes the objective function has already been determined and interpreted as a process specification and structure, the result is that the attainable region analysis determines the best process design (the best process layout or sequence and the best operating conditions). Also, the sensitivity of the process design to changes in the objective function can be tested. Since the region has already been constructed all that is required

is to find the point that optimizes any suitable new objective function. This point is then interpreted as the new process design.

Example of reverse simulation for the kinetic based reactor process−group

In this section an example of reverse simulation for the kinetic based reactor process−group based on the *AR* concept is presented. The following liquid phase, constant density, isothermal reaction network is used as example (van de Vusse[91]).

$$A \underset{k_2}{\overset{k_1}{\rightleftharpoons}} B \xrightarrow{k_3} C \tag{2.3}$$

$$2A \xrightarrow{k_4} D \tag{2.4}$$

The initial characteristics of the reaction network are shown in Table 2.3. The problem consists of finding the best reactor network that maximizes the amount of product *B* for a feed of pure *A*. The desired product *B* is formed from *A* via a reversible reaction from *A*, and is consumed by a consecutive irreversible reaction to *C*, and is also in competition with the by−product *D*.

Table 2.3 – Reaction network constants and feed concentrations.

Parameter	Value	Units
k_1	0.01	$1/s$
k_2	5	$1/s$
k_3	10	$1/s$
k_4	100	$m^3/kmole\,s$
Feed concentrations	**Value**	**Units**
C_A^0	1	$kmole/m^3$
$C_B^0 = C_C^0 = C_D^0$	0	$kmole/m^3$

In this particular example, as fundamental processes mixing, perfectly mixed reaction (CSTR) and reaction with no mixing (PFR) are considered. The mass balance equations for a PFR are:

$$\frac{dC_A}{d\tau} = -k_1 C_A + k_2 C_B - k_4 C_A^2 \tag{2.5}$$

$$\frac{dC_B}{d\tau} = k_1 C_A - k_2 C_B - k_3 C_B \tag{2.6}$$

$$\frac{dC_C}{d\tau} = k_3 C_B \tag{2.7}$$

$$\frac{dC_D}{d\tau} = k_4 C_A^2 \tag{2.8}$$

The mass balance equations for a CSTR are:

$$C_A - C_A^0 = \tau \ -k_1 C_A + k_2 C_B - k_4 C_A^2 \tag{2.9}$$

$$C_B - C_B^0 = \tau \ k_1 C_A - k_2 C_B - k_3 C_B \tag{2.10}$$

$$C_C - C_C^0 = \tau \ k_3 C_B \tag{2.11}$$

$$C_D - C_D^0 = \tau \ k_4 C_A^2 \tag{2.12}$$

The state variables for this example are C_A and C_B. Firstly, C_B is a state variable because it is its value that we wish to optimize. C_A is a state variable because, looking at the right hand side of Eqs. (2.5)–(2.12), the behavior of C_B is entirely dependent on the change in C_A. τ is not a state variable because it is the independent variable in the system.

Before moving further into the analysis, it is useful to determine the dependence of species concentrations as function of residence time. For a PFR, this is determined by numerically solving the mass balances in Eqs. (2.5)–(2.8), giving the concentration profiles of C_A and C_B in Figure 2.8. Similarly, the set of mass balance Eqs. (2.9)–(2.12) can be solved to give the locus for the CSTR as τ is varied, provided in Figure 2.9.

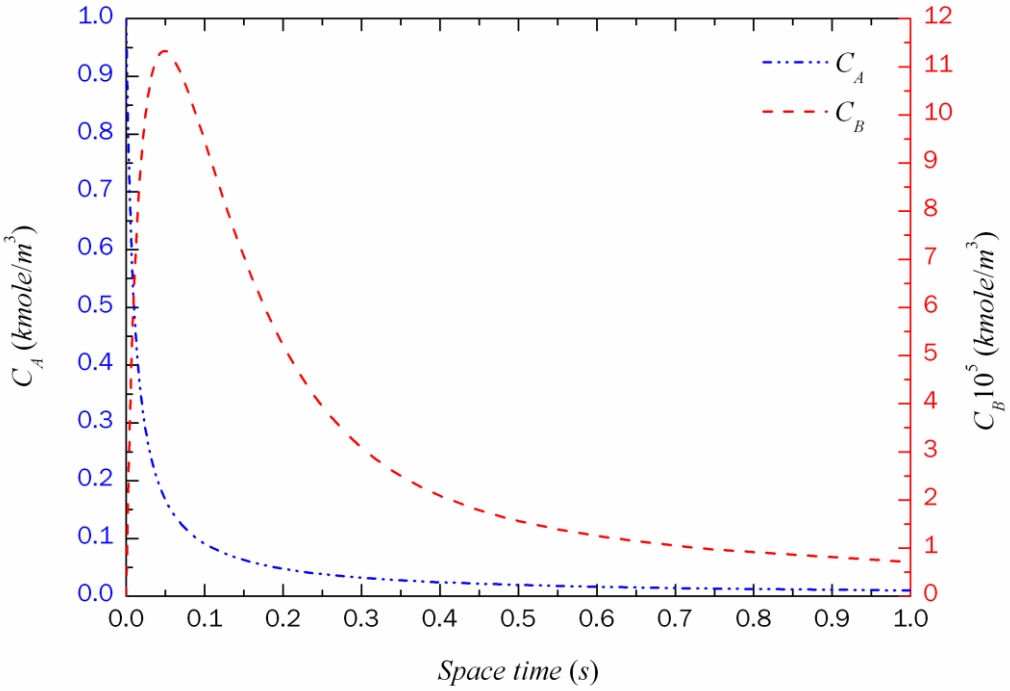

Figure 2.8 – Concentration profiles as a function of space–time for a PFR. Note that profiles for C_C and C_D are not shown.

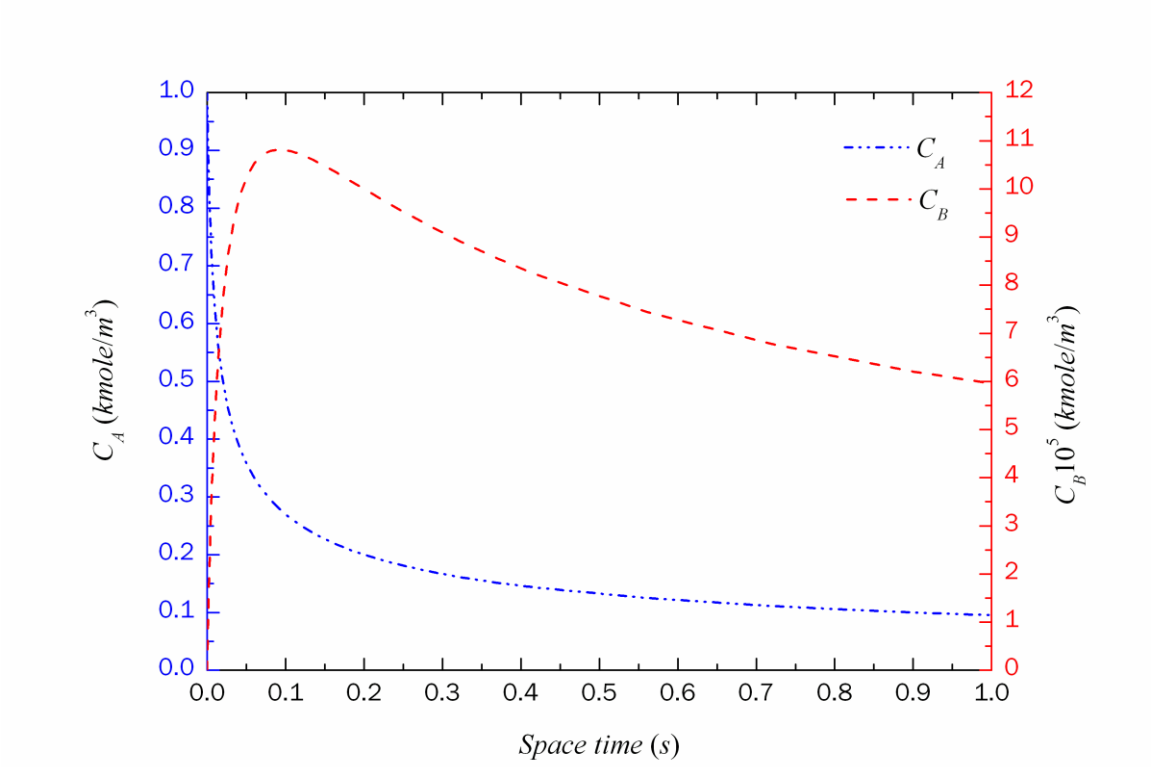

Figure 2.9 – Concentration profiles as a function of space–time for a CSTR. Note that profiles for C_C and C_D are not shown.

With this information we can plot a state–space diagram $C_B - C_A$, as shown in Figure 2.10.

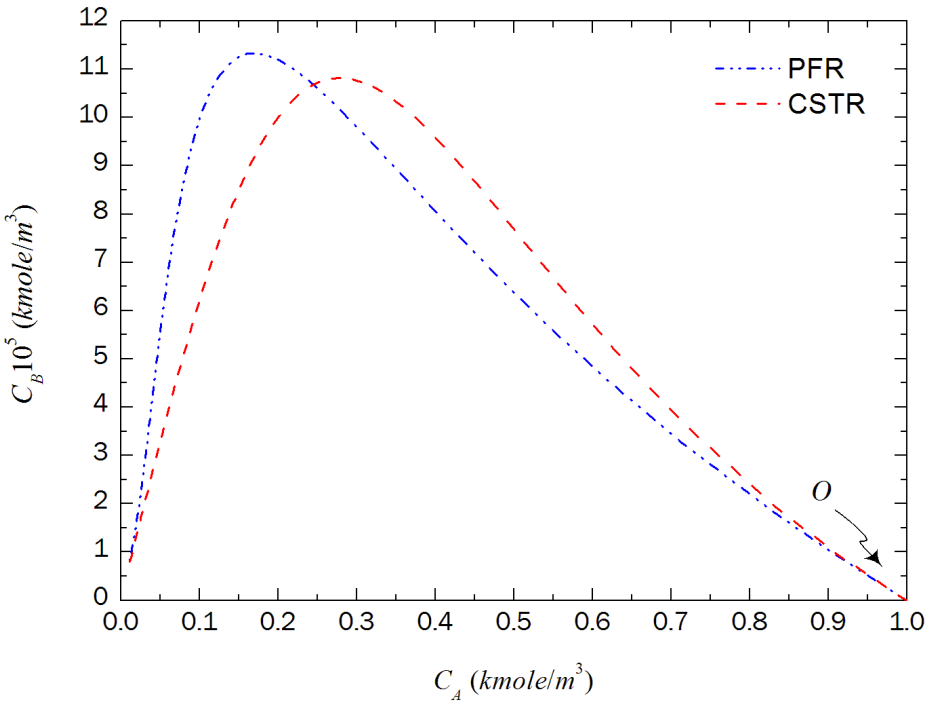

Figure 2.10 – State–space diagram. Point *O* represents the feed point.

It may be seen that a PFR gives a somewhat higher concentration of B at C_A around 0.15 ($\eta \approx 0.85$), while CSTR gives an optimum concentration of B at C_A around 0.3 ($\eta \approx 0.70$). Thus, taking into account the performance of ideal reactors it comes out that a PFR is preferred. Now the question is wether we can find a better reaction system. The construction of the *AR* can provide the answer to this question.

4. *Constructing the AR*

- **Step 1**: Draw the PFR from the feed point. Alternatively, the trajectory of the reaction in the $C_B - C_A$ space of the PFR can be drawn directly from the relation:

$$\frac{dC_B}{dC_A} = \frac{k_1 C_A - k_2 C_B - k_3 C_B}{-k_1 C_A + k_2 C_B - k_4 C_A^2} \qquad (2.13)$$

In others words, the tangent to the reaction trajectory of species B and A in PFR is given by the ratio of the corresponding rates, as shown in Figure 2.11.

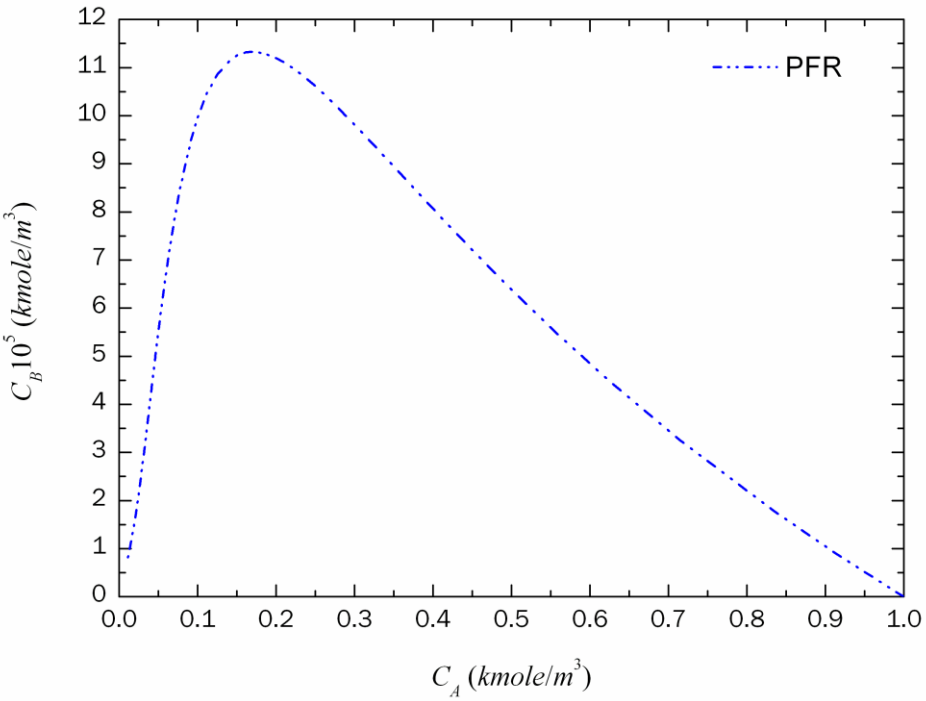

Figure 2.11 – State–space diagram for PFR.

- **Step 2**: Finding the convex hull of the curve. As the PFR region is not convex, the full correction to convexity can be obtained by building what could be called a "convex hull". This can be done graphically by means of the segment OX. It can be observed that a point on the segment OX represents a PFR with by–pass, the position depending on the fraction of feed split (see Figure 2.12).

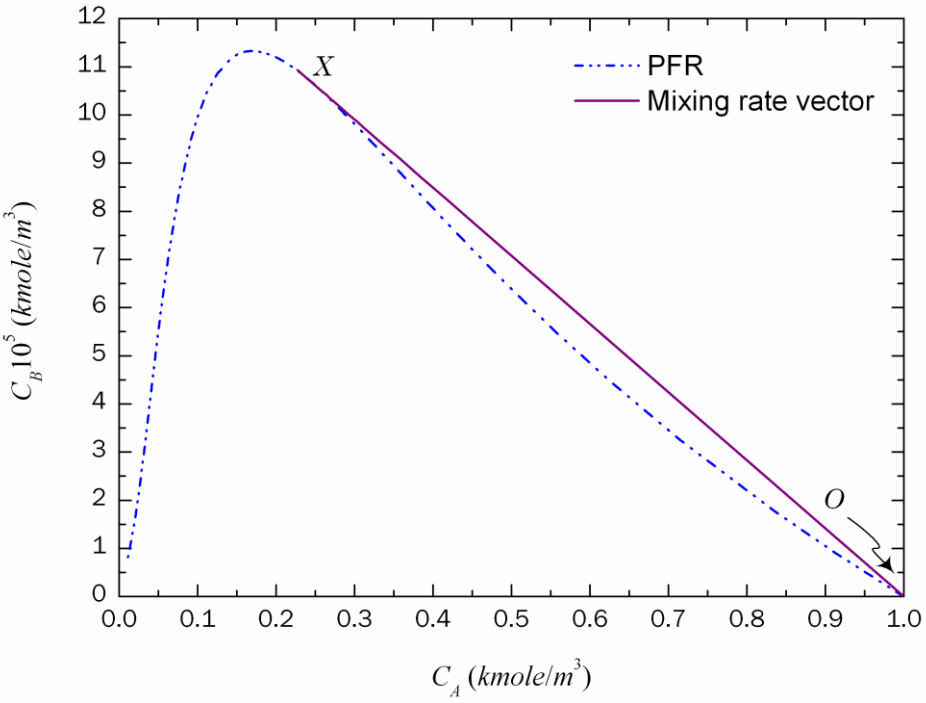

Figure 2.12 – Determination of *AR* –extension through mixing process (solid line).

Summing up, we have obtained a candidate *AR*. This obeys the first three conditions, because it contains the feed, and it is convex. The question is if it also satisfies the fourth condition? The answer is no. Indeed, we have seen that a CSTR starting from the feed gives a better selectivity than a PFR. Thus, a CSTR should be considered firstly.

- **Step 3**: Draw the CSTR from the feed point. It can be seen in Figure 2.13, when PFR and CSTR trajectories start from the same feed point, there is a large overlap in the behavior of the two reactors. However, CSTR gives a better selectivity at lower conversion, while PFR gives a higher selectivity at higher conversion. We proceed as before adding a convex hull at the right of the CSTR region, starting with the feed point. This can be done by drawing the tangent *OP*, as indicated in Figure 2.13.

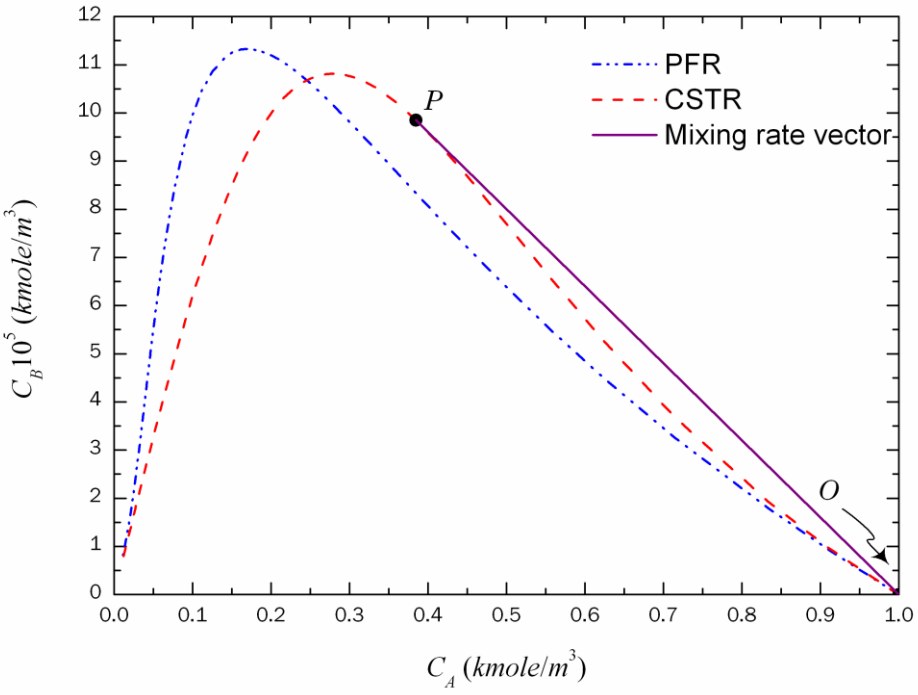

Figure 2.13 – Determination of *AR* –extension through mixing process (solid line).

In fact, the vector OP represents a CSTR, due to the relation:

$$\frac{C_B^0 - C_B}{C_A^0 - C_A} = \frac{-k_1 C_A + k_2 C_B - k_4 C_A^2}{k_1 C_A - k_2 C_B - k_3 C_B} \tag{2.14}$$

Points on the line represent a CSTR with by–pass, where the ratio of the direct feed and by–pass is found by means of the Lever Arm Rule.

Step 4: Finding the new convex hull. From Figure 2.13, it can be seen that the region at the left of the point P is not convex. We can keep on extending the region from the point P with a PFR, as indicated in Figure 2.14. The computation is performed by simply integrating the differential equations of the PFR but this time input concentrations are supplied by the exit of the CSTR. The new augmented region is convex. This time all the four conditions are fulfilled. No other mixed reactors can be found above the boundary that could give a higher amount of *B*. Therefore, the solid line corresponds to the final *AR*.

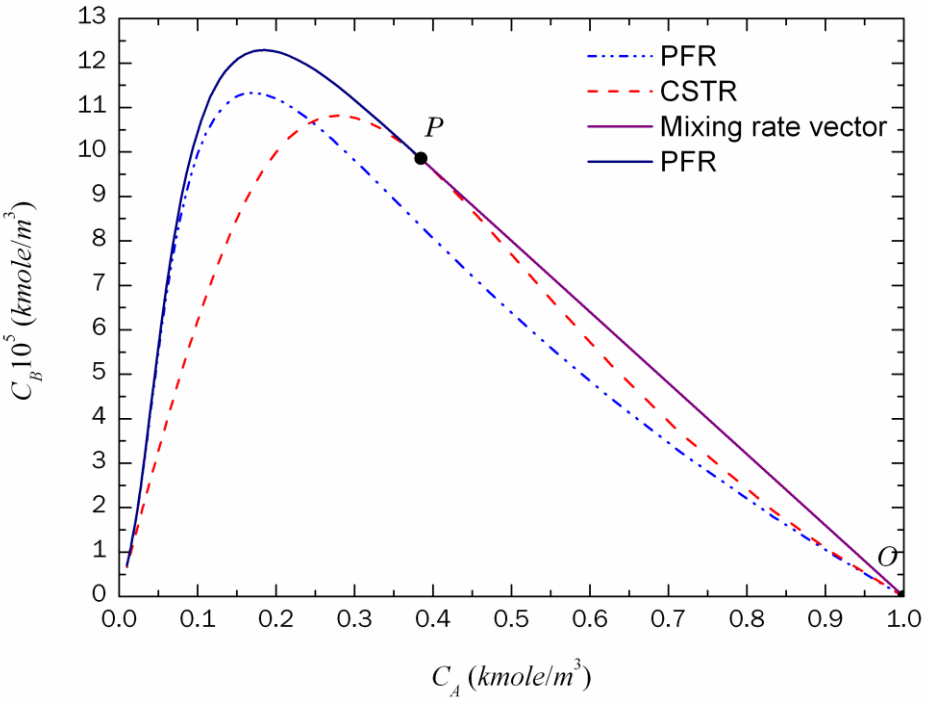

Figure 2.14 – Resulting *AR* candidate.

5. *Interpretation of the boundary*

After obtaining the *AR*, in fact by only drawing its boundary, the synthesis of the reaction network is easy. Figure 2.15 shows possible configurations. For instance, up to 60% conversion a single CSTR with by–pass gives the best selectivity. The highest selectivity of all the reaction systems is obtained with a combination CSTR–PFR. The graphical construction gives the intermediate conversion, and enables us to determine the size of the two reactors. The CSTR has to be sized to reach a conversion of 60%, followed by a PFR to complete the reaction up to 78%.

Hence the combination CSTR–PFR gives a higher yield in *B* than that could be obtained with either a single CSTR or PFR, as well as with other CSTR or PFR arrangements, in series or parallel. In general, the proposed configuration is the best combination of the all–imaginable combinations of CSTR and PFR reactors. The last result is important, and illustrates the power of the *AR* approach. Now we are sure that a better reactor configuration cannot be obtained, and the search for other systems is not necessary.

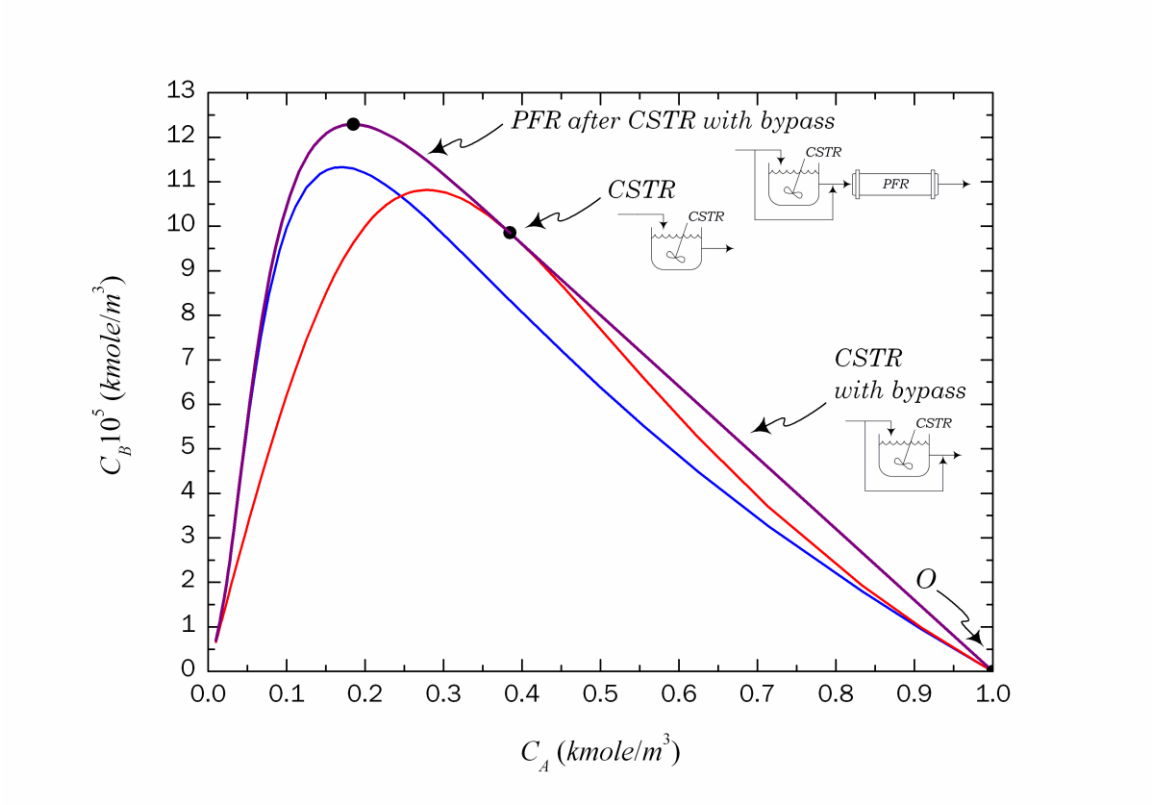

Figure 2.15 – Possible configurations for the reactive system.

6. *Finding the optimum*

The final step is to determine the optimum for the specified objective function. In this case, the objective function is to maximize the production of *B* given the feed of 1 $kmole/m^3$ of *A*. It can be seen easily from Figure 2.15 that a maximum of 1.24×10^{-4} $kmole/m^3$ of *B* can be achieved using a CSTR with effluent concentration of *A* of 0.4 $kmole/m^3$ followed by a PFR with an effluent concentration of *A* of 0.18 $kmole/m^3$. The corresponding residence time of the CSTR and the FPR are 0.037 *s* and 0.031 *s* respectively.

2.4 Discussion

In this chapter, driving force (*DF*), attainable region (*AR*), process-group (*PG*), and reverse simulation concepts have been described. The idea behind of the reverse simulation concept is that the solution (target) for a given design problem is known in advance. As in a reverse simulation method the entire space of feasible solutions to the design problem is determined *a priori*. Therefore, it is immediately known if the solution (our target) exists or not, and if it exists, if it is also feasible or not. In this way the conventional procedure of trial an error is avoided. Nevertheless, the reverse simulation

method does not guarantee that the design will be the final optimal design, but it does guarantee that the design will match the constraints and will be a feasible design. With regard to the *PG* concept, the range of application relies on having a set of process−groups representing all types of unit operations as well as suitable property models for each type of unit operation. One important feature of the *PG* concept itself is that the *PG´*s are not component dependent, but component property dependent. Therefore, the ability to use the same *PG* with different components having similar properties is exploited such as it is in a group contribution based molecular property prediction method. By means of the CAMD techniques, but using *PG´*s like building blocks to generate flowsheet structures, the entire solution space is determined. Afterwards, the solution space is reduced through screening with performance criteria, and only the most promising flowsheet structures according to the performance criteria can be selected to be analyzed in more detail.

3 Framework for Design and Analysis

3.1 Introduction

In this chapter, first the proposed framework for design and analysis of chemical and biochemical processes is presented together with its workflow and the various tools used in the different calculation stages. Each stage is described in detail pointing out the main goals to be achieved at each calculation stage of the framework. Second, since one of the supporting methodologies at stage four of the framework is the process–group contribution methodology (*PGC*) which in turn is supported by various computer–aided tools and methods It is also presented in detail together with its workflow. Third, a description of ICAS (Gani *et al.*[23]; Gani[26]), the Integrated Computer Aided System developed at CAPEC (Computer Aided Process Engineering Center) is also given. This software package integrates the methods and tools used in the framework to assist the user in the resolution of product/process engineering problems. A list of the tools used at different stages of the framework is given together with a brief description of them.

3.2 Overview of the Framework

The proposed framework for design and analysis of chemical and biochemical processes consists of five stages, and its workflow together with the supporting tools and methods at each stage is outlined in Figure 3.1. Stage 1 involves a pre–analysis of the product qualities and its characteristics which will define the process needs. The objective of this stage is to establish a base case design to manufacture the product. In stage 2, the objective is to evaluate the base case design and generate information for further analysis. This additional information is generated by performing mass and energy balances on known production process steps through process simulation. The information generated in stage 2 is analyzed in stage 3 to identify bottlenecks and/or critical points where the base case design can be improved. Based on the identification of these bottlenecks, targets for further improvements are defined. It is worth pointing out that the starting point is a reference (or known) design of a process. In stage 4 design candidates are generated that match the targets defined in stage 3. Finally, in stage 5, the most promising design candidates are verified through rigorous simulation and the most promising one is selected based on suitable performance criteria. The performance criteria chosen depends on the goal of the synthesis/design problem to be solved. In the following sections each one of the five stages of the framework is described in detail.

3.2.1 Stage 1 –Available Process Knowledge Data Collection

As the starting point is a base case design, in general, the minimum amount of knowledge needed for the production route should be the data needed to perform the modelling and simulation in stage 2. Some of the data, if not available from literature or from experiments, could be generated via predictive software. For example, the properties of identified chemicals, and conversions of reactants/substrates (if the corresponding kinetic models are available) could be predicted. These data are important because they affect the energy and water demand for the process operations. Therefore, the availability of accurate values for properties such as heats of reaction, vapor pressures, heats of vaporization, heat of formation to mention some, for example, are extremely important.

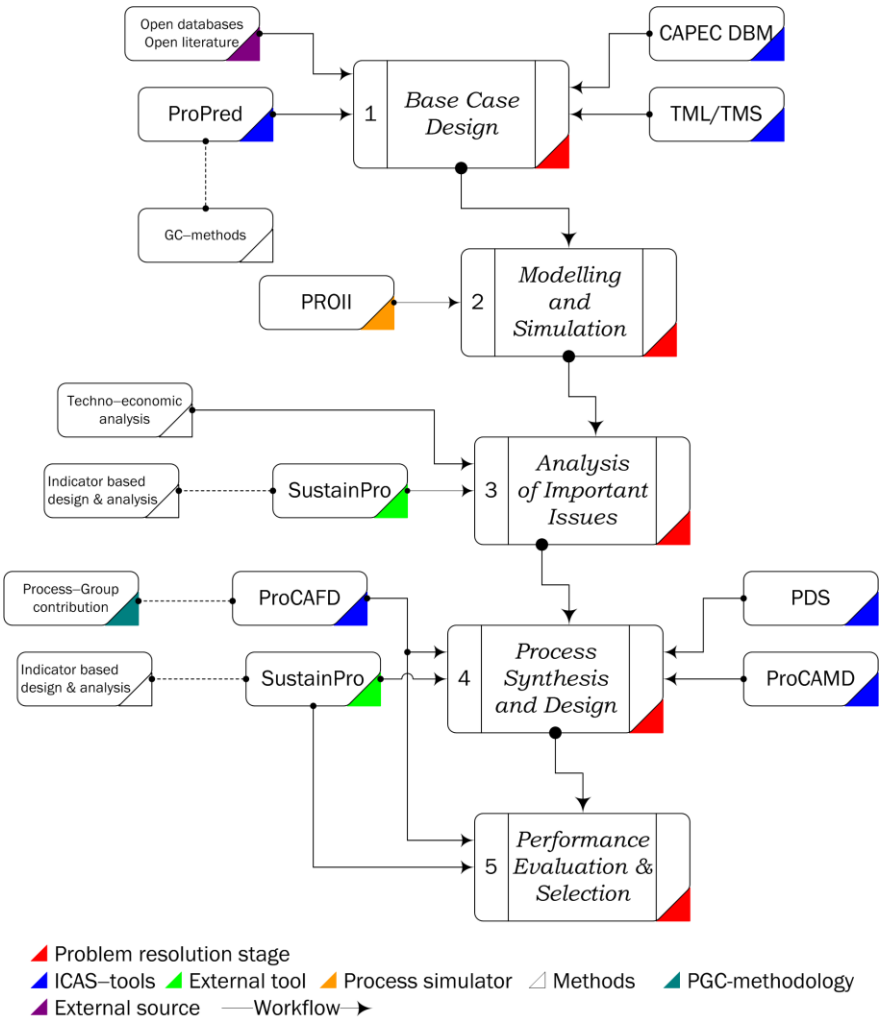

Figure 3.1 – Workflow diagram of the framework for design and analysis.

3.2.2 Stage 2 –Modelling and Simulation

Analysis of any process requires data. In this case, the necessary data are related to the production steps of each operation. These data could be available in the form of measured plant data. However, not all necessary data are usually available, especially not in the process design phase, and even if they do, a check of the data for consistency is typically necessary. Another option for generating data is to perform mass and energy balances on the known production steps. This can be easily done through process simulation if all necessary models are available in the selected process simulator. In this thesis, we are only dealing with steady state/analysis and therefore, the necessary modelling/simulation tools correspond to steady state simulation. Several options for modelling and simulation exist and for reasons of availability and ease of use, the PROII® simulator supported by ICAS–tools (Gani *et al.*[23]; Gani[26]) has been used for process simulation. PROII® (PROII[77]) is a steady state simulator, while ICAS–tools (Gani *et al.*[23]; Gani[26]) is a collection of tools for property prediction (ProPred, for prediction of missing pure component properties), modelling (MoT, to generate missing models) thermodynamic property model analysis (TML, for property model analysis and parameter estimation) and design (PDS, for design of separation processes based on *DF*). More details on the ICAS–tools (Gani *et al.*[23]; Gani[26]) are provided in Section 3.4.

3.2.3 Stage 3–Analysis of Important Issues

Based on the generated data, the objective here is to establish the process points where improvements can be made, without trade–off or compromise. The improvements can be related to reduction of waste, cost, energy consumption, and/or environmental impact. If the goal is to generate a more sustainable process, the method used is the indicator based design and analysis of Carvalho *et al.*[11]. The corresponding computational tool is SustainPro, which is able to generate, screen, and then identify sustainable alternatives in any chemical process by locating the operational, environmental, economic, and safety related bottlenecks inherent in the process. If the goal is to improve the performance of a process flowsheet in terms of its operational cost and/or energy consumption, a techno–economic analysis is performed to identify those process areas with a high potential for improvement.

3.2.4 Stage 4–Process Synthesis and Design

Once the targets have been defined, the objective of stage 4 is to generate design candidates matching these targets. The focus in this stage is to improve the performance of a process flowsheet in terms of its energy consumption and/or sustainability. For the synthesis and design of more efficient processes in terms of energy consumption the process–group contribution (*PGC*) methodology to generate design candidates is used. Full description of the *PGC* methodology is provided in Section 3.3 along with its workflow.

3.2.5 Stage 5 –Performance Evaluation and Selection

The most promising design candidates are identified based on suitable performance criteria. The performance criteria chosen depend on the final goal of the design problem to be solved. If the performance criteria is the energy consumption of a process flowsheet, the *PGC* methodology is used to perform the evaluation with the corresponding flowsheet property model. For the identification of sustainable design candidates, the sustainability metrics defined by the Institution of Chemical Engineers by Azapagic[3] can be used.

3.3 PGC Methodology Overview

The *PGC* methodology relies entirely on the process–group concept presented in Chapter 2. Based on the *PG* concept d'Anterroches[15,16] proposed the *PGC* methodology which consists of the following steps: (1) synthesis problem definition, (2) synthesis problem analysis, (3) process–group selection, (4) generation of flowsheet candidates, (5) ranking/selection of flowsheet candidates, (6) reverse simulation, (7) final verification. In the following sections a detailed description of the *PGC* methodology is provided together with the different methods and tools supporting the methodology.

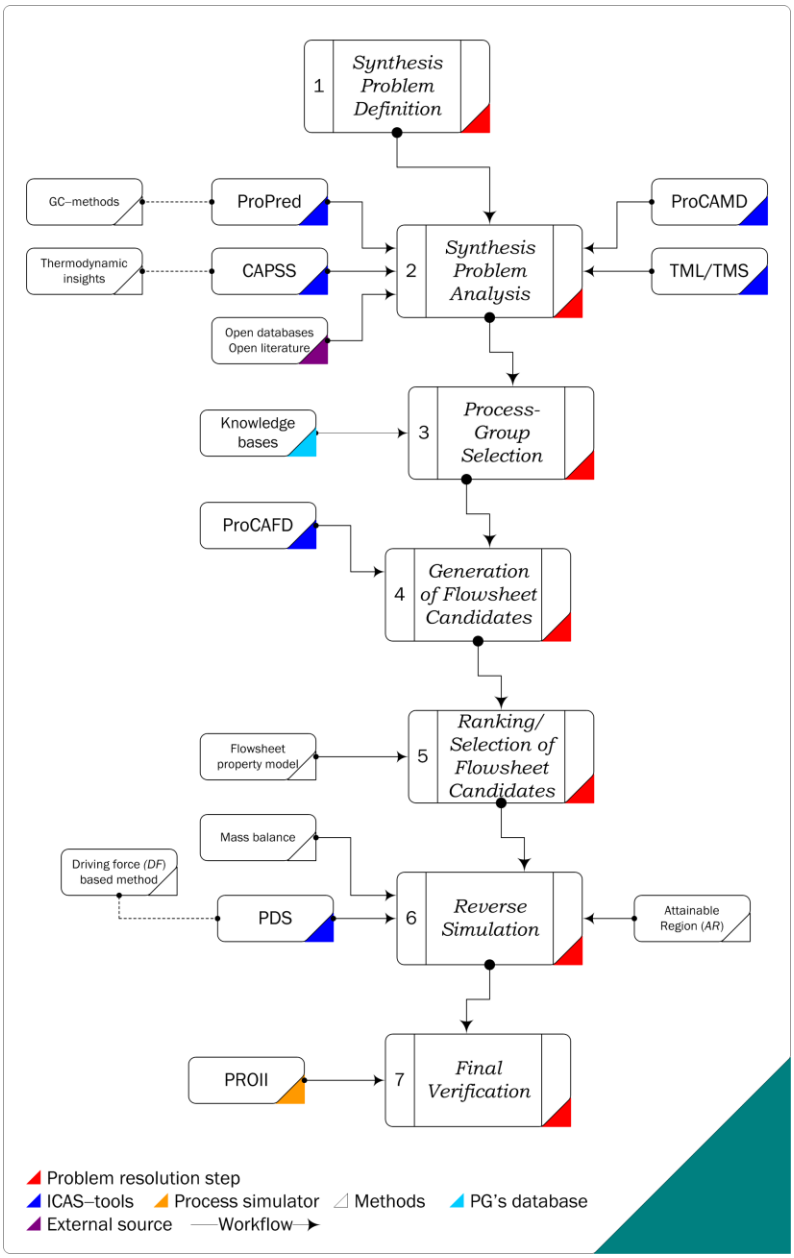

Figure 3.2 – Workflow diagram of the *PGC* methodology.

3.3.1 Step 1 –Synthesis Problem Definition

This step involves two tasks as objectives: i) the definition of the structural constraints, which are related to the definition of the raw materials (inputs) and desired products (outputs) of the process flowsheet and ii) the selection of the flowsheet property model. As inputs and outputs are represented by input and output process–groups, respectively, then the remaining task is to determine the correct sequence of unit process

operations represented by process−groups that will manufacture the desired product matching the flowsheet property target as well as the product purity.

3.3.2 Step 2−Synthesis Problem Analysis

The objective here is to generate information for the subsequent steps. This step involves two tasks: i) reaction analysis and ii) pure component/mixture property analysis. i) The reaction analysis is performed with the objective of identifying the reaction tasks needed to produce the desired product. Then, a database search is performed to find the chemical reaction or set of chemical reactions yielding the desired product. ii) The pure component/mixture property analysis is performed by means of the thermodynamic insights based method developed by Jaksland *et al.*[48] and Jaksland[49]. This method is based on the principle that the differences (or property ratios) in the values of properties among the components of the mixture to be separated can be exploited by the corresponding separation technique. Therefore, the pure component/mixture property analysis is performed with the objective of retrieving information related to the feasible separation technique to be used in the synthesis problem.

3.3.3 Step 3−Process−Group Selection

The selection of the process−groups is based on analysis of the synthesis problem. It is worth pointing out that according to the process−group concept (see Chapter 2, Section 2.3.3), a process−group is component property dependent. It means that a given process−group can be used for different sets of components as long as the properties are matched. The procedure to follow is to retrieve the process−groups from the *PG*'s database (Table 2.1) which match with the separation techniques identified in the previous step. This step involves two tasks: i) selection and initialization of reaction process−groups and ii) selection and initialization of separation process−groups. The initialization of a process−group is obtained through a procedure where a process−group is associated with a given set of components.

i). Selection and initialization of reaction process−groups: From the synthesis problem analysis, the complete list of reactions, kinetic model parameters or conversion rates are available. For each reaction (or set of reactions) if the kinetic model parameters are available, a kinetic model based reactor process−group is selected; otherwise a fixed conversion based reactor process−group is selected. As the corresponding reaction process−groups are selected, they are initialized with the components involved in the chemical reaction (or set of reactions).

ii). Selection and initialization of separation process−groups: The separation process−groups are selected based on the identified separation techniques during the synthesis problem analysis. For each feasible separation technique

identified in the synthesis problem analysis, the corresponding process−group is selected. The selected process−group can be initialized with different sets of components, if each set is matching the property dependence of the process−group.

Consider a mixture of five components labeled as *A*, *B*, *C*, *D*, and *E* in the synthesis problem. Based on their vapor pressure and boiling point ratios, a feasible separation task is identified between components *B* and *C*. The corresponding separation technique associated to this set of properties is flash separation and the process−group representing this separation technique is the flash separation process−group. Therefore, the flash process−group can be initialized with four different sets of components as shown in Table 3.1. This is based on the assumption of an ideal system, where no binary azeotropes exist, and assuming that the components are ordered according to decreasing relative volatility.

Table 3.1 – Initialization of a flash process−group with a 5 components synthesis problem.

Components in the synthesis problem	*A*, *B*, *C*, *D*, *E*			
Separation task	*B*/*C*			
Property dependence	Vapor pressure, boiling point			
Separation technique	Flash separation between *B* and *C*			
	5	4	3	2
Matching set of components	(*ABCDE*)	(*ABCD*) (*BCDE*)	(*ABC*) (*BCD*)	(*BC*)
Initialized process−groups	(*fAB*/*CDE*)	(*fAB*/*CD*) (*fB*/*CDE*)	(*fAB*/*C*) (*fB*/*CD*)	(*fB*/*C*)

After initialization, each separation process−group is ready to be used in the generation of flowsheet structures. All the initialized flash separation process−groups are grouped in the pool of process−groups used during the synthesis of the flowsheet structures.

3.3.4 Step 4–Generation of Flowsheet Candidates

The objective in step four is to combine the process−groups selected in step three according to a set of connectivity rules and specifications proposed by d'Anterroches & Gani[15] and d'Anterroches[16] to generate flowsheet structures. Each process−group has outlet specifications, which are guaranteed to be met if the connectivity rules of the process−group are satisfied. The output specifications are based on mass balance rules. For instance, consider the case of the separation of a mixture of three components labeled *A*, *B*, and C into three pure products using only one separation technique, in this case simple distillation. This leads to two possible configurations, which are represented through simple distillation process−groups, as shown in Figure 3.3. The feed mixture is

represented by an inlet process–group ***i****ABC* (groups with one attachment). The end–products (groups with a single attachment) are outlet process–groups, such as, ***o****A*, ***o****B*, ***o****C* (a pure product with at least 99.5% purity) or ***o****AB*, ***o****BC* (a mixture product). An intermediate product (groups with two or more attachments) is defined as a product resulting from one unit operation such as (*AB*) or (*BC*) which in turn serves as an inlet stream for a subsequent unit operation, such as (*A*/*B*) or (*B*/*C*), respectively (see Figure 3.3).

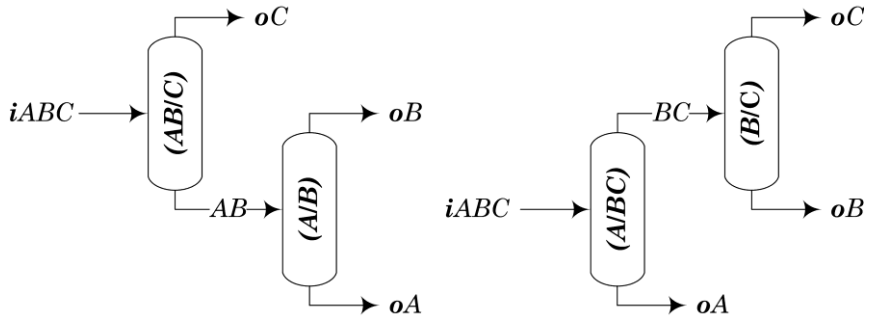

Figure 3.3 – Process–group flowsheet representation of two configurations in the separation of a three–component mixture into three pure streams.

The process–groups guarantee the recovery of the components in their outlets during the generation of the flowsheet structures. For instance, the process–group (*A*/*B*) can be connected to the output of process–group (*AB*/*C*) independently of the composition of the mixture of *A*, *B*, and *C* entering the (*AB*/*C*) process–group. In this case, the outputs of the process–group (*AB*/*C*) are ensured to be on the one hand a mixture of *A* and *B*, and, on the other hand, a stream with a high purity and recovery of component *C*. Summarizing, a process–group is flexible in its inputs and strict in its outputs. Based on this analysis, the connectivity rules and specifications for the simple distillation process–group are as follow:

- The simple distillation process–group consists of one inlet and two outlet process–groups.
- The inlet connection process–group must contain the exact same components as the ones set during the initialization procedure.
- The two outlet connection process–groups are ensured to have at least 99.5% purity in pure streams and above 99.5% recovery of key components if mixtures. The outlet pressure for both outlets is set to the process–group operational pressure and the temperature is set to the bubble point of the mixtures. The assumption is made that there is no pressure drop in the column.

As mentioned above, each process–group has its connectivity rules as well as outlet specifications, which can be found in d'Anterroches[16]. For the new set of

process–groups developed in this thesis, the complete details are presented in the Appendix.

3.3.5 Step 5–Ranking/Selection of Flowsheet Candidates

The generated flowsheet structure candidates are tested with respect to their target property values chosen in step one, using the corresponding flowsheet property model. Currently, there are available property models to assess the performance in terms of energy consumption for distillation process–groups, flash process–groups, solvent based distillation process–groups using three types of entrainers (organic solvents, ionic liquids, and hyperbranched polymers) and pressure swing distillation. The flowsheet property model for these process–groups is based on the *DF* theory presented in Section 2.3.1 of Chapter 2.

3.3.6 Step 6–Reverse Simulation

The reverse simulation step involves two tasks: i) the resolution of the mass balance through each process–group in a process flowsheet and ii) the calculation of the flowsheet design parameters of the process unit operations through reverse simulation in the flowsheet structure.

The mass balance is performed through each process–group present in the generated flowsheet option. The operating conditions such as pressure and temperature of the outlet streams are given by the process–group definition. For instance, in the case of distillation process–groups, recovery of the components lighter than the light key is equal to 100% in the overhead product and the recovery of the components heavier than the heavy key is equal to 100% in the bottom product. The recovery of the key components is greater than or equal to 99.5%. The resolution of the mass balance can be performed by means of any commercial simulator.

The reverse simulation procedure for separation process–groups (such as distillation, extractive distillation, flash) is based on the *DF* concept and it has been described in Section 2.3.4 of Chapter two. The kinetics based reactor process–group employs the identified highest point in the *AR* diagram and using this point (reactant–product concentration) as the reference, calculates all other reactor design parameters as has been described in Section 2.3.4 of Chapter two.

3.3.7 Step 7–Final Verification

At this step of the methodology, all the necessary information to perform the final verification through rigorous simulation is available. The use of rigorous simulators like PROII® (PROII[77]) to further refine the most promising process flowsheet and to perform optimization of the design parameters is used in this step.

3.4 Computer Aided–Tools in the Framework

3.4.1 ICAS–Integrated Computer Aided System

In the proposed framework various computer–aided tools are used, which are part of the Integrated Computer Aided System (ICAS) (Gani *et al.*[23]; Gani[26]). ICAS is a package of programs and tools communicating with each other to assist an engineer in the resolution of product/process engineering problems. A list of tools used at different stages of the framework is given in Table 3.2.

Table 3.2 – List of computer– aided tools supporting the framework.

Supporting tool	Purpose	Stage
ICAS–CAPEC DBM	Retrieval of pure component and mixture properties.	1
ICAS–ProPred	Prediction of pure component properties based on *GC* methods.	1
PROII®	Process simulation and optimization.	2, 4, 5
SustainPro	Process analysis (identification of bottlenecks).	3,4
ICAS–TML	*VLE*, *LLE* calculations. Estimation of thermodynamic model parameters.	1, 4
ICAS–utility toolbox	*VLE*, *LLE* and *SLE* diagrams. Separation efficiency diagrams (*DF* diagrams).	1, 4
SMSWin	*VLE*, *LLE* and *SLE* calculations.	1, 4
ICAS–ProCAFD	Computer–aided tool for process synthesis and design.	4
ICAS–ProCAMD	Computer–aided tool for molecular and mixture design; used for solvent design.	4
ICAS–PDS	Design and synthesis of distillation based separation schemes.	4

3.4.1.1 ICAS–CAPEC Database Manager (DMB)

The framework for design and analysis requires information related to the physicochemical properties of the compounds for a given synthesis/design problem. Therefore, use of a database for properties of chemicals is essential. The CAPEC database includes collected and screened experimental data of pure component properties for approximately 13200 pure compounds, mixture data and solubility data from the open

literature. A very important feature of the CAPEC database manager is that it allows to the user to add new compounds together with their property data in user defined databases. Unless otherwise stated, all properties of compounds used in this thesis were retrieved from the CAPEC database.

3.4.1.2 ICAS–ProPred: Property Prediction Toolbox

When the properties of specific compounds either do not exist in the CAPEC database or experimental data are not available in the open literature, a computational tool for the prediction of pure component properties is required. Before moving forward, it is necessary to predict the properties of these compounds before they can be added to the database and be used in the solution of a given problem. ICAS–ProPred is a tool integrated into ICAS directly for property prediction of pure component properties. ICAS–ProPred is an interactive program, where the user can draw a molecule in a graphical interface by connecting fragments of molecules such as CH_2, CH_3, OH, etc, into feasible molecules. Currently the software can predict properties using four methods – Marrero & Gani[68], Constantinou & Gani[13], Joback & Reid[50], and Wilson & Jasperson[97]. CI–MG and Van Krevelen group contribution methods (Satyanarayana & Gani[80]) are used for polymer property prediction. ICAS–ProPred was used in this work to calculate properties of the compounds when they could not be found in the available databases and other sources did not contain the needed property value.

3.4.1.3 ICAS–TML: Thermodynamic Model Library

ICAS–TML is used for three purposes. Firstly, it was used for advising which thermodynamic model should be used in process simulations for given composition ranges of compounds present in the mixture and the condition ranges (*e.g.* range of temperature and pressure). This implementation is based on the methodology presented by Gani & O'Connell[22]. Secondly, with ICAS–TML it is possible to obtain mixture properties like bubble and dew points, *PT*–flash (multi–phase), etc. Last but not least, when the selected thermodynamic model exhibits unsatisfactory deviations from experimental data, it is possible to "fine–tune" the thermodynamic model parameters with ICAS–TML. In this thesis ICAS–TML has been used for two purposes: for the selection of the thermodynamic model and for estimation of the parameters of the selected thermodynamic models based on available experimental data.

3.4.1.4 ICAS–PDS: Process Design Studio

The Process Design Studio (PDS) is used in this thesis to design the distillation columns. An important feature of this tool is the analysis of the feasibility of achieving a specified distillate or bottom product composition from a specific feed, by manipulating the reflux ratio. In the distillation design part of PDS, given the identity of the mixture

compounds, the thermodynamic model, the desired product compositions and reflux, the program returns the number of stages and the feed stage location. Moreover, ICAS–PDS can also be used to compute binary and ternary azeotropes, phase diagrams, distillation boundaries, and residue curve maps. In this way, it can be used for preliminary analysis of a mixture to be separated by distillation. In this thesis, ICAS–PDS has been used for design verification of separation processes.

3.4.1.5 ICAS–ProCAMD: Computer Aided Molecular Design

ICAS–ProCAMD is based on the multi–level computer–aided molecular design technique developed by Harper & Gani[37]. It can be used for various types of molecular as well as the mixture design problems. Each problem can defined in terms of six main categories, represented by a page in the problem setup menu. The six categories are: (1) general problem control, (2) non temperature dependent properties, (3) temperature dependent properties, (4) mixture properties, (5) azeotrope/miscibility calculations and (6) biodegradation calculations. The generated molecules can be listed and ordered according to different target (desired) properties, and are highlighted if they are present in the CAPEC database. In this thesis ICAS–ProCAMD has been used only when selection or replacement of solvent was required in stage four of the framework.

3.4.1.6 ICAS–ProCAFD: Computer Aided Flowsheet Design

ICAS–ProCAFD is the computational implementation of the computer–aided flowsheet design framework (CAFD) developed by d'Anterroches and Gani[15]. In the same way that ProCAMD is used to design molecules by combining molecular groups, ProCAFD generates flowsheet structures by means of the combination of *PG's* for a given problem specification (*e.g.* defined in terms of available raw materials and desired products). The generated flowsheet structures are then ranked based on performance criteria. Finally, the user chooses the most promising one for further analysis. It is applicable to a wide range of problems as long as the process–groups as well as the flowsheet property model needed to represent and assess the flowsheet structures respectively are available. In this thesis ProCAFD is used to generate flowsheet structures in stage four of the framework.

3.4.2 SustainPro

SustainPro is an EXCEL–based software developed by Carvalho *et al.*[11], which is able to generate, screen, and then identify sustainable alternatives in any chemical process by locating the operational, environmental, economic, and safety bottlenecks inherent in the process. The input data needed to use SustainPro are the reference (base case design) design/operational data of the process (mass–flows, energy–flows and costs). The data from PROII (PROII[77]) steady state simulations are exported to an excel

sheet. This excel sheet is then imported to SustainPro. In addition, the user needs to provide data for the calculation of safety indices, such as flammability, explosiveness, and toxicity limits of all the compounds involved in the process. SustainPro first performs a flowsheet decomposition based on identification of component mass and energy "paths" (open− and closed− paths). It then calculates a set of mass and energy *indicators* (Carvalho *et al.*[11]) that trace the paths of the component "mass−flows" and "energy−flows" as they enter and leave the process (they may also be generated or consumed within the process). Following this, the SustainPro software identifies the critical points –the ones that allow the best improvements in the process –through sensitivity analysis. In this way the target indicators are selected and local sensitivity analysis is subsequently performed to determine the design and the operational parameters that influence the targets.

3.5 Discussion

A systematic methodology for synthesis/design and analysis supported by computer aided methods and tools can help to reduce time and man−power resources. In this chapter, a framework for synthesis and analysis of chemical and biochemical processes together with the computer aided methods and tools have been presented. Within this framework, emphasis is given to the *PGC* methodology, which is used to generate and test feasible design candidates based on the principle of the group−contribution approach used in chemical property estimation. As pointed out by d'Anterroches[15] the three fundamental pillars of the *PGC* methodology are the process−groups (building blocks), connectivity rules to join the process−groups and flowsheet property models to evaluate the performance of the flowsheet structures. Therefore, through the addition of new process−groups the application range of the *PGC* methodology can be further extended. With respect to the *PGC* methodology, some aspects deserve the following remarks:

- The flowsheet property model is truly predictive and component independent, this means that different component binary pairs may have the same *DF*.

- The combination of the process−groups to form flowsheet structures does not depend on the resolution of the mass and energy balances among the process−groups, since the connectivity rules and specifications for each process−group are *a priori* defined. This means that after the generation of flowsheet structures, for the one which is most likely with respect to the performance criteria, the mass balance needs to be solved only once before going further to the reverse simulation step.

- Finally, as the reverse simulation methods supporting the framework are based on the *AR* and *DF* concepts (see Chapter 2, Section 2.3), this guarantees a near optimal (if it is not the optimal performance) performance of the design

with respect to selectivity for reactor units and with respect to energy consumption for separation schemes.

The framework and the models, methods and tools are generic and they can be applied either to improve an existing process flowsheet (retrofit problem) or to find a completely new entire process flowsheet, as will be illustrated in the following Chapter.

4 Case Studies

4.1 Introduction

In this chapter, the application of the framework for design and analysis is illustrated considering a process for the production of bioethanol from lignocellulosic biomass. In particular, the design–analysis of the downstream separation by means of the application of the *PGC* methodology is highlighted. Furthermore, in order to offset the inherent cost of processing biological materials to produce ethanol, the possibility of producing co–products from glucose is considered. Consequently, succinic acid (SA) production from glucose fermentation is considered as a second case study. Here, the design and analysis of the succinic acid downstream separation is illustrated through the *PGC* methodology. Finally, through the integration of bioethanol and succinic acid production processes, the production of a third chemical, diethyl succinate, has also been identified. The analysis and design of the diethyl succinate production process is illustrated through the *PGC* methodology.

4.2 Bioethanol Production Process

The production route for a bioethanol process has been selected, due to current interest in the use of renewable sources to produce important chemicals (the biorefinery concept). Furthermore, biofuels have become a priority to reduce the dependence on fossil fuels. Although the production of bioethanol has increased all over the world in the last few years through expansion of existing plants and construction of new facilities, the economic competitiveness of bioethanol as a liquid fuel strongly depends on the energy resources used during its production. This implies the need to determine the optimal values for the operating conditions and other operation/equipment related variables for the synthesized process flowsheet –which will be highlighted through the framework for design and analysis (to be referred to as the framework in this Chapter) presented in Chapter 3.

4.2.1 Stage 1 –Base Case Design

The starting point of the framework is to establish a base case design. The base case design is based on a bioethanol production process from lignocellulosic biomass which has been documented by the National Renewable Energy Laboratory (NREL). (Wooley *et al.*[98]). The main processing steps are illustrated in Figure 4.1 and a description of each process area is given below.

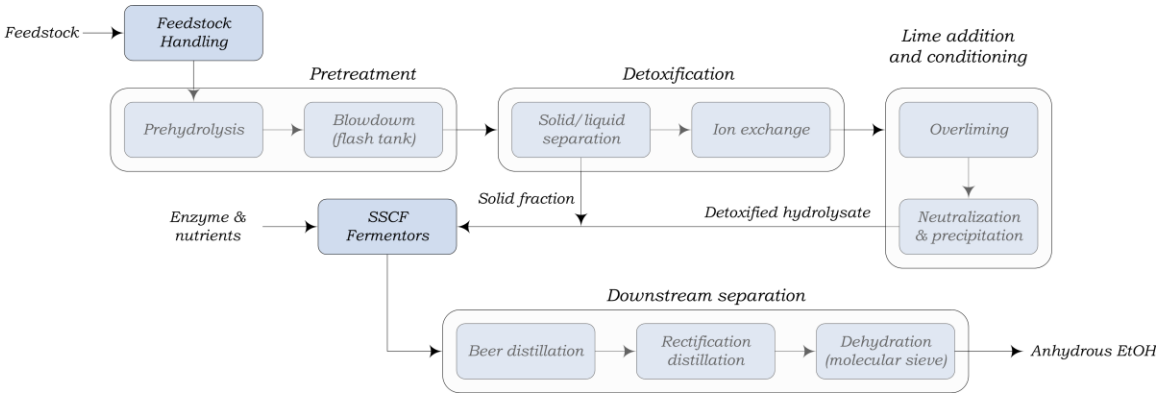

Figure 4.1 – Base case: bioethanol production process flowsheet from lignocellulosic biomass (Wooley *et al.*[98]).

Feedstock handling: The feedstock, in this case hardwood chips, is delivered to the feed handling process area for storage and size reduction. Table 4.1 lists the feedstock composition used in this case study, taken from Wooley *et al.*[98].

Table 4.1 – Feedstock composition.

Component	%Dry Basis
Cellulose	42.67
Hemicellulose	19.05
Arabinan	0.79
Mannan	3.93
Galactan	0.24
Acetate	4.64
Lignin	27.68
Moisture	47.90

Pre–treatment: The purpose of the pre–treatment of lignocellulosic materials is to make the cellulose feedstock more digestible by enzymes. The surrounding hemicellulose and/or lignin are removed and the cellulose microfiber is modified. The heart of the pre–treatment process area is the pre–treatment reactor, which converts most of the hemicellulose portion of the feedstock to soluble sugars— primarily xylose, mannose, arabinose and galactose —by hydrolysis using dilute sulfuric acid and elevated temperature. The milled wood chips are heated to about 100 °C using low-pressure steam. Then, steam and sulphuric acid are added to the mixture into the pre-treatment reactor. The pre–treatment reactor temperature is 190 °C, while the pressure is 12.2 atm. The concentration of sulphuric acid is 0.5% (weight), while the solids concentration in the outlet stream of the pre–treatment reactor is 22% (weight). Hydrolysis under these conditions also solubilizes some of the lignin in the feedstock. In addition, acetic acid is released from hemicellulose hydrolysis. Degradation products of pentose sugars (primarily furfural) and hexose sugars (primarily hydroxymethylfurfural) are also formed. Following the pre–treatment reactor, the hydrolysate —consisting of a mixture of liquid and solid particles —is flash cooled. This operation vaporizes a large amount of water, a

portion of acetic acid, and much of the furfural and hydroxymethylfurfural. Removing these heterocyclic aldehydes is beneficial, as they can be toxic to the microorganisms in the downstream fermentation. The main reactions that occur in the pre−treatment reactor are listed in Table 8.4 in the Appendix.

Detoxification, lime addition, and conditioning: In addition to flash removal of the aldehydes, the unreacted solid phase is separated from the liquid hydrolysate. The latter contains sulfuric acid and other inhibitors in addition to the hemicellulose sugars. Before fermentation, detoxification of the liquid hydrolysate is required to remove the inhibitors formed during the pre−treatment of biomass. Ion exchange is used to remove acetic acid and sulfuric acid that will be toxic to the microorganisms in the fermentation. After ion exchange the pH is raised to 10 (by adding lime) and held at this value for a period of time. Neutralisation and precipitation of gypsum follow the overliming step. The gypsum is removed via filtration and the hydrolysate is finally mixed again with the solid fraction (from the solid−liquid detoxification separation unit) before being sent to the SSCF process area. The main reactions that occur in the ion exchange and overliming processes respectively are listed in Table 8.5 in Appendix.

Simultaneous Saccharification and Co−Fermentation (SSCF): Following the lime addition, a small portion of the detoxified slurry is diverted to the SSCF seed process area for microorganisms production (*Zymomonas mobilis*) while the bulk of the material is sent to the simultaneous saccharification and co−fermentation (SSCF) process area. Two different operations are performed in this process area— saccharification (hydrolysis) of the remaining cellulose to glucose using cellulase enzymes, and fermentation of the resulting glucose and other sugars to ethanol. The enzyme used in the saccharification is assumed to be purchased from an enzyme manufacturer. For the fermentation, the recombinant *Zymomonas mobilis* bacterium is used, which will ferment both glucose and xylose to ethanol. A seed inoculum, nutrients, enzyme, and the detoxified slurry are added to a train of continuous fermentors. The resulting ethanol broth is collected and sent to the product recovery process area. The reactions and conversions used in the production SSCF fermentor are given in Tables 8.6 and 8.7 in Appendix. Saccharification or hydrolysis reactions are listed in Table 8.6; fermentation reactions are listed in Table 8.7. In the model, these reactions are performed in series, meaning that any product of the hydrolysis reactions can be consumed as a reactant in the fermentation reactions. In addition to saccharification and fermentation reactions, loss to other products occurs (see Table 8.9 in Appendix). This is modeled as a side stream by passing the SSCF reactor, where the side stream reacts to lactic acid. A total of 7% of the sugars available for fermentation are considered lost in this way.

Downstream separation and recovery: After the SSCF process area, distillation and molecular sieve adsorption are used to recover the ethanol from the fermentor effluent and produce nearly 100 % pure ethanol. Distillation is accomplished in two distillation columns. The first column (beer distillation column) removes the dissolved CO_2 and most of the water, and the second distillation column (rectification) concentrates the ethanol to near azeotropic composition. Subsequently, the residual water from the nearly azeotropic mixture is removed by vapor phase molecular sieve adsorption.

With respect to the type of compounds found in the bioethanol production process, we distinguish two main classes of compounds:

1). Compounds that are involved in vapor–liquid equilibria, for example ethanol and CO_2.
2). Compounds that are only present as insoluble solids and therefore their effect on vapor–liquid equilibria may be ignored, for example cellulose and $CaSO_4$.

Table 8.1 in the Appendix gives the minimum physical properties required by PROII® (PROII[77]) for simulation of the base case design (see stage 2 in Section 4.2.2 below). Note however, that many of the compounds used here will not be involved in vapor–liquid equilibria, as they stay in the liquid phase under the operating conditions undergone during the bioethanol production process (for example glucose, xylose, etc.). However, because of PROII® (PROII[77]) software requirements, vapor properties will be needed anyhow. These will be estimated (see stage 2), but in practice, as long as the vapor pressure is low enough, these compounds never actually show up in the vapor phase, and the liquid properties of interest are calculated correctly. Table 8.2 in the Appendix gives an overview of the compounds used in the simulation.

4.2.2 Stage 2–Generate Data for Analysis

The overall process flowsheet was simulated using the PROII® (PROII[77]) simulator. Part of the physical property data for simulation was obtained from Wooley *et al.*[98] and others were estimated using the method of Marrero & Gani[68] for pure component property estimation. The feedstock composition and operating conditions were taken from Wooley *et al.*[98] and Hamelinck *et al.*[35]. The information about the main process conditions used in the simulation is given in Alvarado–Morales *et al.*[1]. The description of the chemical and biochemical reactions taking part during the process and incorporated into the simulation model can be found in Wooley *et al.*[98] and it is also provided in Tables 8.4–8.8 in the Appendix for completeness. Each part of the process (feedstock handling, pre–treatment, detoxification, lime addition, SSCF, and ethanol recovery/purification) has been analyzed in detail together with a breakdown of the operating and capital costs of the different parts of the bioethanol production process. Once the operational and equipment costs were determined, the manufacturing cost of the bioethanol production process was calculated.

4.2.3 Stage 3–Analysis of Important Issues

First, process economy and process points where the base case design can be improved were analyzed. Then, targets for improvement have been defined.

Economic analysis

A plant producing 52.7 *Mgal*/*yr* of anhydrous ethanol and operating 8406 hours per year has been used as a base case. The feedstock rate is taken to be 159116 *kg*/*h*. The total annual manufacturing cost was found to be 2.36 *USD*/*gal* of anhydrous ethanol and includes the costs for process equipment, for steam and cooling water and other miscellaneous costs. The miscellaneous costs include feedstock, electricity, process water, general and administrative expenses, employee salaries, chemicals, enzyme, and maintenance. The physical sizing of equipment as well as the cost estimation for most of the equipment was done following the method given by Biegler *et al.*[10]. Table 8 shows the raw material and utility prices. The results are summarized in Table 4.2, and Figure 4.2 shows the manufacturing cost and the total equipment cost breakdowns. The raw material and utility prices are provided in Table 8.3 in the Appendix. The process flowsheet and the corresponding stream summary obtained through simulation can be found in Alvarado–Morales *et al.*[1].

Table 4.2 – Main characteristic of the base case design (anhydrous ethanol).

Item	Value	Units
Ethanol production	52.7	*Mgal/year*
Purity	99.95	% *wt*
Operating hours	8406	*h/year*
Enzyme cost	1.5	*USD/kg*
Total equipment cost	49.05	*MUSD*
Total manufacturing cost	124.62	*MUSD/year*
Total manufacturing cost	2.36	*USD/gal*
Sell price[43]	2.96	*USD/gal*
Profit	0.60	*USD/gal*

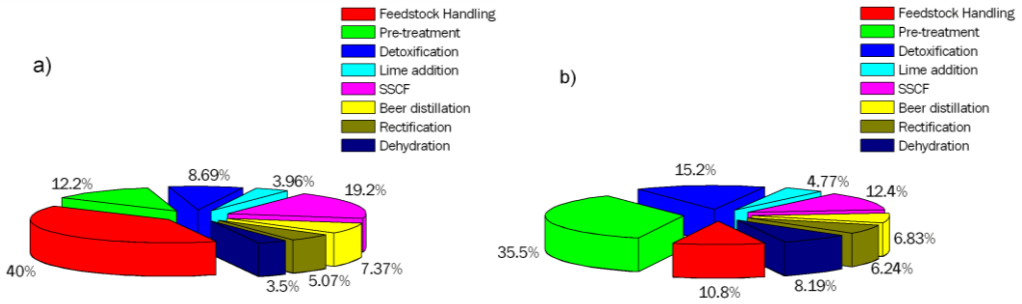

Figure 4.2 – (a) Total manufacturing cost and (b) Total equipment cost breakdowns.

Cost of near–azeotropic ethanol

Near–azeotropic ethanol is an intermediate product (81 *% wt*) in the dehydration of ethanol. It is obtained from the second distillation column (rectification column) which concentrates the ethanol to a near azeotropic composition. To determine the cost of the intermediate near–azeotropic ethanol stream, the dehydration process area was removed from the lignocellulose–to–ethanol process model and economics. Mass and energy

balances, capital and operating costs were determined for the near–azeotropic ethanol production process. The results are summarized in Table 4.3 and Figure 4.3 shows the breakdowns of the total manufacturing cost and the total equipment cost.

Table 4.3 – Main characteristic of the base case design (near–azeotropic ethanol).

Item	Value	Units
Ethanol production	52.7	*Mgal/year*
Purity	81	*% wt*
Operating hours	8406	*h/year*
Enzyme cost	1.5	*USD/kg*
Total equipment cost	45.03	*MUSD*
Total manufacturing cost	120.25	*MUSD/year*
Total manufacturing cost	2.28	*USD/gal*
Sell price[10]	2.50	*USD/gal*
Profit	0.22	*USD/gal*

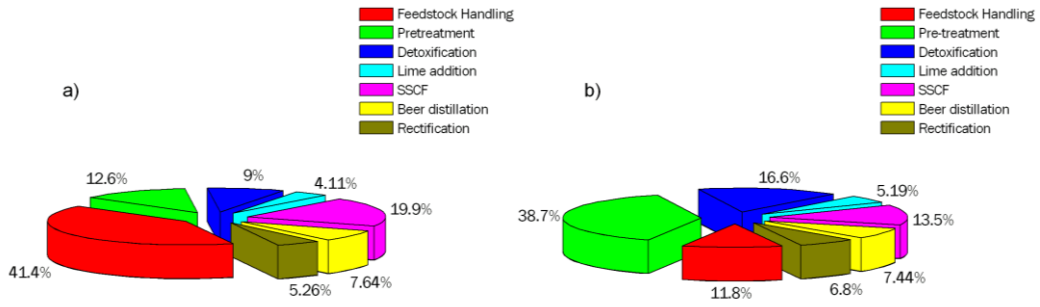

Figure 4.3 – (a) Total manufacturing cost and (b) Total equipment cost breakdowns.

Cost of non–azeotropic ethanol

Non–azeotropic ethanol is an intermediate product (44.5 *% wt*) in the dehydration of ethanol. It is obtained from the first distillation column (beer distillation column) which removes the dissolved CO_2 and most of the water. To determine the cost of the intermediate non–azeotropic ethanol stream, the following process areas were removed from the lignocellulose–to–ethanol process model and economics: dehydration and rectification. Mass and energy balances, and capital and operating costs were determined for the non–azeotropic ethanol production process. The main results are summarized in Table 4.4, and Figure 4.4 shows the breakdowns of the total manufacturing cost and the total equipment cost.

Table 4.4 – Main characteristic of the base case design (non–azeotropic ethanol).

Item	Value	Units
Ethanol production	52.7	*Mgal/year*
Purity	44.84	*% wt*
Operating hours	8406	*h/year*
Enzyme cost	1.5	*USD/kg*
Total equipment cost	42.00	*MUSD*
Total manufacturing cost	113.93	*MUSD/year*
Total manufacturing cost	2.16	*USD/gal*
Sell price		*USD/gal*
Profit		*USD/gal*

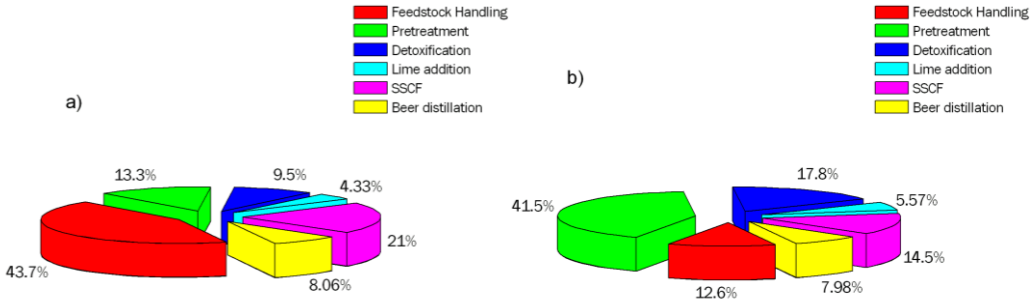

Figure 4.4 – (a) Total manufacturing cost and (b) Total equipment cost breakdowns.

Cost of dilute ethanol

Dilute ethanol is an intermediate product (5–10 % *wt*) in the dehydration of ethanol and it is obtained from the fermentor effluent. In order to determine the cost of the intermediate dilute ethanol stream, the following process areas were removed from the lignocellulose–to–ethanol process model and economics: dehydration, rectification and beer distillation. Mass and energy balances, and capital and operating costs were determined for the dilute ethanol production process. The results are summarized in Table 4.5 and Figure 4.5 shows the breakdowns of the total manufacturing cost and the total equipment cost.

Table 4.5 – Main characteristic of the base case design (dilute ethanol).

Item	Value	Unit
Ethanol production	52.7	*Mgal/year*
Purity	5–10	*% wt*
Operating hours	8406	*h/year*
Enzyme cost	1.5	*USD/kg*
Total equipment cost	38.62	*MUSD*
Total manufacturing cost	104.75	*MUSD/year*
Total manufacturing cost	1.98	*USD/gal*
Sell price		*USD/gal*
Profit		*USD/gal*

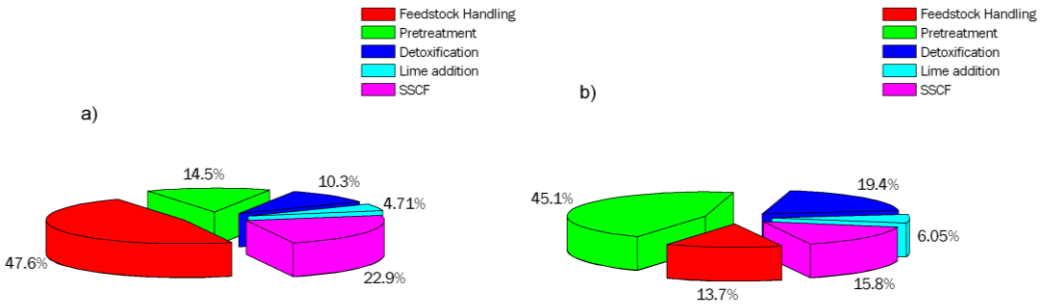

Figure 4.5 – (a) Total manufacturing cost and (b) Total equipment cost breakdowns.

Indicator based analysis of process flowsheet

SustainPro software has been applied to the base case design. For the process flowsheet and the results of the mass and energy balances, SustainPro calculated 3437 open–path (OP) indicators. Since the process flowsheet does not have any recycle streams, there are no closed–path (CP) indicators. Table 4.6 lists the indicators for the OPs with the highest (absolute) indicator values.

Define targets

Analyzing the indicators from Table 4.6, it can be concluded that there is a large waste of the raw material and utilities. For example, the MVA (material value added) indicator corresponding to OP 576 indicates that raw material in the form of lignin is being wasted (due to the MVA indicator has a large negative value). For OP 1807, the EWC (energy and waste cost) is 8084 while TVA (total value added) is –8192. This indicates that water in this stream uses a lot of energy (positive EWC) and it is losing its value (negative TVA) as it enters and leaves the process. The sensitivity analysis step performed by SustainPro then determined that the OP 1807 has the highest potential to result in an improvement in terms of TVA (water use) and EWC (energy cost due to use of water).

Table 4.6 – List of the most sensitive indicators for the open–paths (OP´s).

Path	MVA	Prob.	Path	EWC	Prob.	Path	TVA	Prob.
OP 3347 Enzyme–41–51	–6660.6	High	OP 1854 H_2O–41–51	9341.5	High	OP 1854 H_2O–41–51	–9466.4	High
OP 3204 CSL–41–51	–2763.9	High	OP 1838 H_2O–17–51	8564.0	High	OP 1838 H_2O–17–51	–8677.6	High
OP 2339 $C_2H_7NO_2$ P R2-21	–2471.6	Low	OP 1807 H_2O–14–51	8084.3	High	OP 1807 H_2O–14–51	–8191.6	High
OP 576 Lignin 1–51	–2146.0	High	OP 1823 H_2O–14–51	4964.9	High	OP 3347 Enzyme–41–51	–6664.4	High
OP 2321 $H_8N_2O_4S$ P R2–21	–1161.4	Low	OP 1583 H_2O–1–51	3849.7	High	OP 1823 H_2O–14–51	–5030.8	High
OP 3395 $CaSO_4$ P R3–33	–694.2	Low	OP 1711 H_2O–5–51	2366.3	High	OP 1583 H_2O–1–51	–3897.9	High
OP 3334 Enzyme–14–51	–661.2	High	OP 1599 H_2O–1–51	2364.3	High	OP 3204 CSL–41–51	–3102.4	High
OP 2285 NH_3–18–21	–625.5	High	OP 1775 H_2O–7–51	2240.9	High	OP 2339 $C_2H_7NO_2$ P R2-21	–2471.6	Low
OP 23 Cellulose–1–51	–606.9	High	OP 1727 H_2O–5–51	1453.2	High	OP 1711 H_2O–5–51	–2395.8	High
OP 31 Cellulose–1–36	–563.2	High	OP 1791 H_2O–7–51	1376.2	High	OP 1599 H_2O–1–51	–2393.8	High

4.2.4 Stage 4 –Process Synthesis and Design

Two options have been considered: a reduction of water consumption (in order to reduce the open−path MVA values) and alternatives for downstream separation (in order to improve process energy and operating cost, without increasing the environmental impact).

Removal of water

The first attempt to generate alternatives was to identify possibilities of reducing the TVA indicator in OP 1807 by reducing the amount of water leaving the system (that is, minimizing the fresh water requirements with respect to OP 1807). An obvious solution for reduction of fresh water is by treating the water and recycling it after the beer distillation. After adding this recycle and water recovery step, and recalculating the indicators, SustainPro confirms that the TVA indicator for water has indeed been improved, thereby improving the sustainability metrics related to waste. Table 4.7 lists the new values of the OPs for the MVA, TVA, and EWC indicators. Note that because the amount of water needed for pretreatment, detoxification and SSCF operations has not been reduced, the EWC indicator has also not been reduced. This indicates that process improvement with respect to reduction of water will not reduce the energy consumption of the process. Therefore, the subsequent life cycle assessment categories primarily based on energy usage do not show significant improvement. The above alternative has been confirmed through water−pinch analysis by Alvarado−Morales *et al.*[1].

Table 4.7 – New values of the indicators for the new process flowsheet design (with recycle).

Path	MVA	Prob.	Path	EWC	Prob.	Path	TVA	Prob.
OP 1297–new H_2O–61–58	–6.1	High	OP 1297 H_2O–61–58	288.5	High	OP 1297 H_2O–61–58	–294.6	High
OP 1807-base H_2O–14–51	–107.2	High	OP 1807 H_2O–14–51	8084.3	High	OP 1807 H_2O–14–51	–8191.6	High

Downstream separation

As described in the base case design, the product from the fermentation stage in the bioethanol production process from lignocellulosic biomass is a mixture of ethanol, cell mass, and water. To obtain anhydrous ethanol, the first step is to recover ethanol from the product stream of the fermentor. The product from the beer distillation (37 *wt. %*) is then concentrated to obtain anhydrous ethanol (more than or equal to 99.5 *wt. %*). The downstream separation is therefore defined as the separation task related to obtaining anhydrous ethanol from an ethanol/water mixture. In the following section, the synthesis, design, and analysis of the downstream separation is highlighted through the application of the *PGC* methodology.

4.2.5 PGC Methodology Application

4.2.5.1 Step 1 –Synthesis Problem Definition

Given the product stream, which is a multi−component mixture from the SSCF bioreactor in the bioethanol process from lignocellulosic biomass as raw material, determine a physically feasible process flowsheet that satisfies the product specifications, as well as estimates for the corresponding conditions of operation. The mixture information requires the identities of the components to be separated, their composition, and the temperatureand pressure of the mixture (if available). The product specification is the minimum acceptable product purity, for example, ≥ 99.5 *wt.%*. The flowsheet specification is the energy consumption of the process and the design objective (target) is to minimize this value. The component flowrates in the effluent stream are given in Table 4.8. The structural parameters of the synthesis problem that are fixed at this point are: 1 input *PG* initialized with the mixture given in Table 4.8 and 1 output *PG* initialized with the desired product ethanol.

Table 4.8 – Effluent stream of the SSCF bioreactor (Alvarado−Morales *et al.*[1]).

Label	Components	Feed flowrates (*kmole/h*)
A	Oxygen	0.0490
B	Carbon dioxide	254.5673
C	Ethanol	447.0319
D	Water	17218.7289
E	CSL	87.2908
F	Acetic acid	18.2114
G	Furfural	1.5536
H	Lactic acid	14.8641
I	HMF	0.7697
J	Glycerol	0.1526
K	Succinic acid	0.4242
L	SS (soluble solids)	41.9499
M	IS (insoluble solids)	294.9542

4.2.5.2 Step 2 –Synthesis Problem Analysis

In order to reduce the complexity of the synthesis problem without affecting the final flowsheet structure, the following assumptions have been made based on a pure component property analysis of the components found in the mixture. Firstly, all sugars present in the effluent stream (such as glucose, xylose, cellobiose, arabinose, mannose, and galactose) have been lumped into a single pseudo−component, namely, soluble solids (SS). Similarly, the solids present in the mixture (cellulose, hemicellulose, arabinan, mannan, galactan, lignin, cellulose, biomass, and *Zymomonas mobilis*) have been lumped

into a single pseudo–component, namely, insoluble solids (IS). Based on the pure component property analysis, insoluble solids can be removed from the mixture leaving the fermentor using centrifugation, and then further filtration would be used to remove any trace solid residues. On the other hand, for compounds such as glucose, and xylose, as depicted in Figure 4.6 their vapor pressure is sufficiently low such that it is reasonable to assume that these compounds will not go to the vapor phase product in, for instance, flash/evaporation operation. Considering that the physical properties of glucose and xylose are representative of the soluble solids pseudo–component, the same conclusion can be drawn for the other six and five carbon sugars in the mixture, respectively.

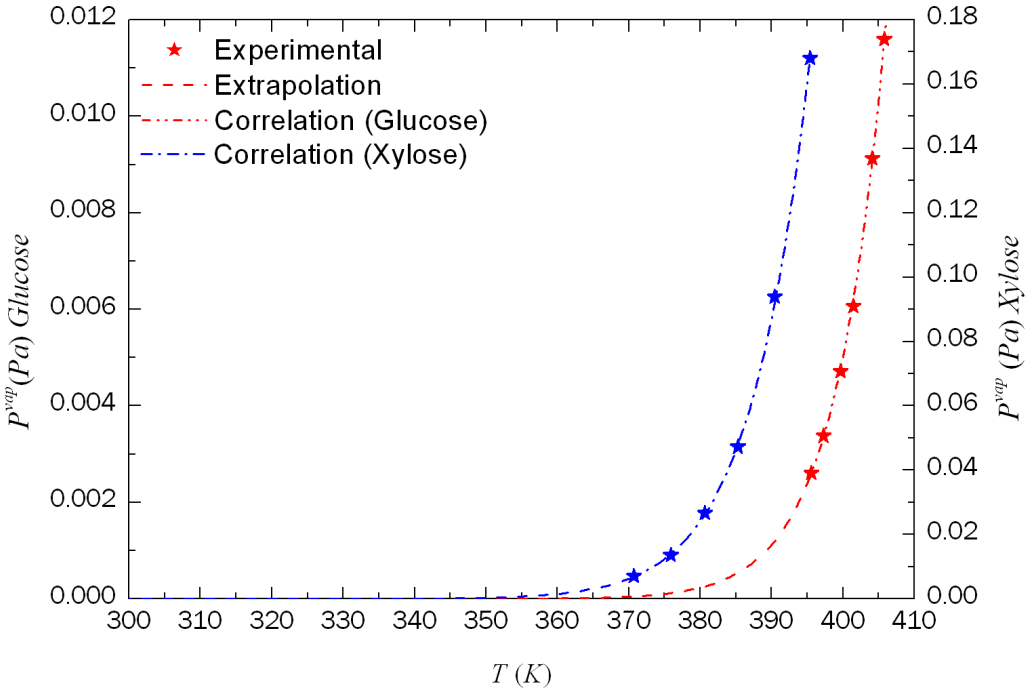

Figure 4.6 – Vapor pressures of glucose and xylose (Oja & Suuberg[72]).

After this analysis, the feasible process separation techniques are identified by means of the thermodynamic insights based method (Jaksland[48,49]). For the mixture to be separated the first separation task is identified as the split between carbon dioxide(*B*)/ethanol(*C*) due to the large adjacent normal vapor pressure difference between both components and the corresponding separation technique associated with this property is flash operation (see Table 4.9).

Table 4.9 – Pure component property ratios along with the separation techniques.

Property	Split	Ratio	Separation technique (Jaksland[48,49])
T_b	Ethanol/CO_2	1.8053(>1.40)	*Distillation* *Flash operation*
δ	Furfural/Succinic acid	1.6349	*Molecular sieve adsorption* *Pervaporation*
R_g	Ethanol/CO_2	2.1721(>1.03)	*Liquid membrane*
V_M	Acetic acid/CO_2	1.5461(>1.08)	*Liquid membrane* *Pervaporation*
SP	Furfural/CO_2	1.6211(>1.28)	*Absorption* *Liquid membranes* *Pervaporation*
WDV	Ethanol/CO_2	1.6213	*Molecular sieve adsorption* *Gas separation membrane*
VP	CO_2/Ethanol	813.3347(>15)	*Distillation* *Flash operation*

Further analysis of the mixture reveals the existence of three binary azeotropes, which are listed in Table 4.10.

Water can be separated from the other components using flash/evaporation as well, except for the binary pairs listed in Table 4.10 which form azeotropes.

Table 4.10 – Composition of the azeotropes in the process at 1 *atm*.

Binary pair	$T(K)$	x_1
Water(1)/Ethanol(2)	352.50	0.1372
Water(1)/Acetic acid(2)	371.97	0.8384
Water(1)/Furfural(2)	371.14	0.8940

Figure 4.7 shows the *VLE* temperature–composition phase diagrams for the binary systems listed in Table 4.10. From Figure 4.7, it can be seen that two of the three binary azeotropes have a close boiling region.

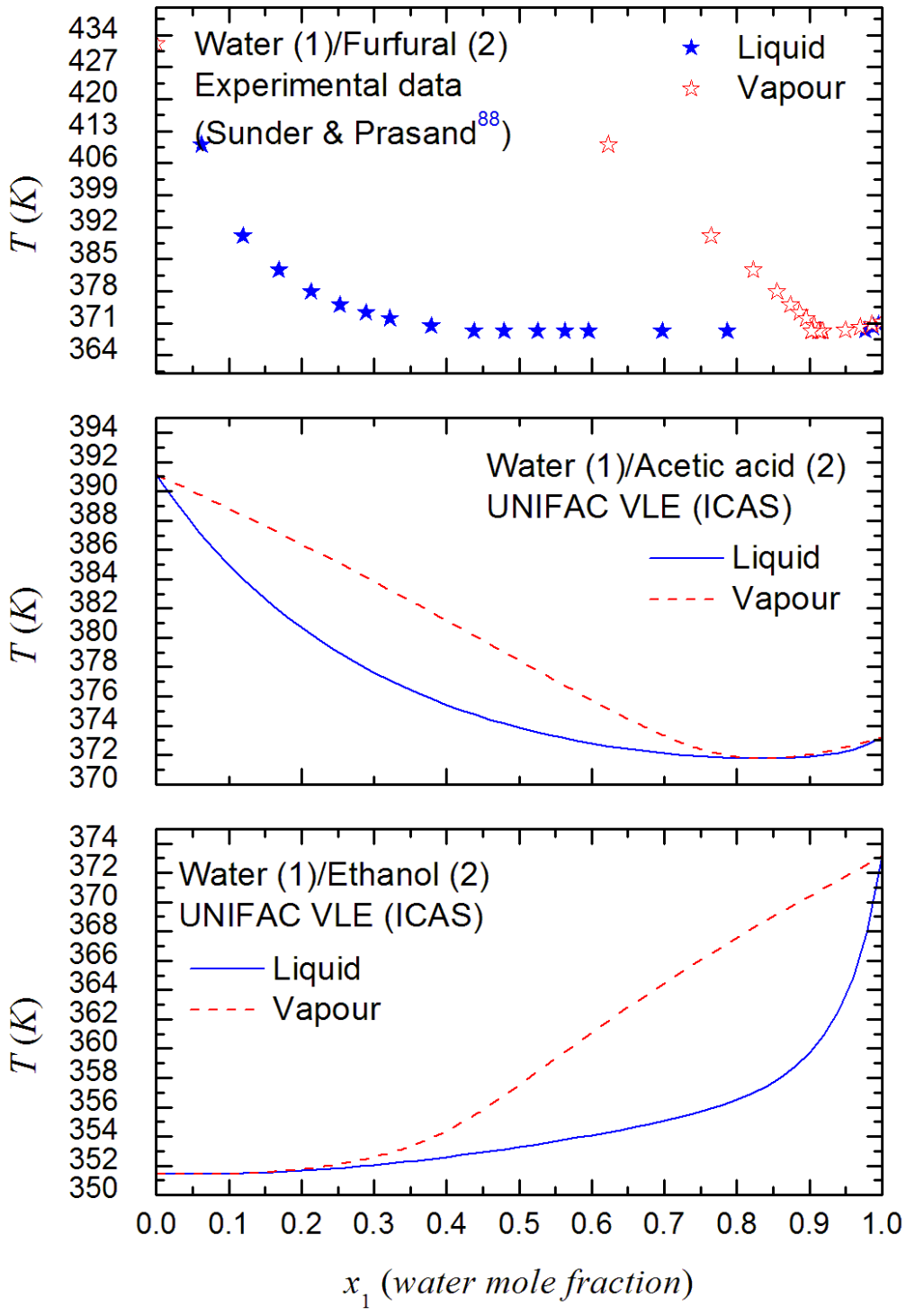

Figure 4.7 – *VLE* temperature–composition phase diagrams for water/ethanol, water/acetic acid and water/furfural.

As pointed out by Jaksland *et al.*[48], large differences in structural properties that describe the size and shape of molecules (such as kinetic diameter, Van der Waals volume, molecular diameter, radius of gyration) are a requirement for separation techniques such as gas separation membranes, liquid membranes, and molecular sieve adsorption. In the same way, large differences in physical properties (such as melting point, heat of fusion, boiling point, vapor pressure, solubility parameter) are associated with separation techniques such as crystallization, distillation, flash, and extractive distillation. Based on the pure component property ratios, a separation task is identified as a split between water(*C*)/ethanol(*D*) due to the large adjacent radius of gyration between both components and *liquid membrane* being the corresponding separation technique. A separation task is identified as split between water(*C*)/ethanol(*D*) due to the large adjacent molar volume values and the separation technique is *pervaporation*. Due to the large adjacent Van der Waals volume values, therefore, *molecular sieve adsorption* and *gas separation membrane* are also suitable separation techniques to separate ethanol from water. *Extractive distillation* has been also identified as a potential separation technique since the separability can be influenced by the effect of adding a mass separating agent (*MSA*) on vapor–liquid equilibria (*VLE*). The blue solid line (1) in Figure 4.8 shows the *DF* diagram for the binary pair water/ethanol incorporating the remaining components as fixed components. Similarly, the red dash (2) and black dotted (3) lines represent the *DF* diagrams for the binary pairs water/acetic acid and water/furfural, respectively.

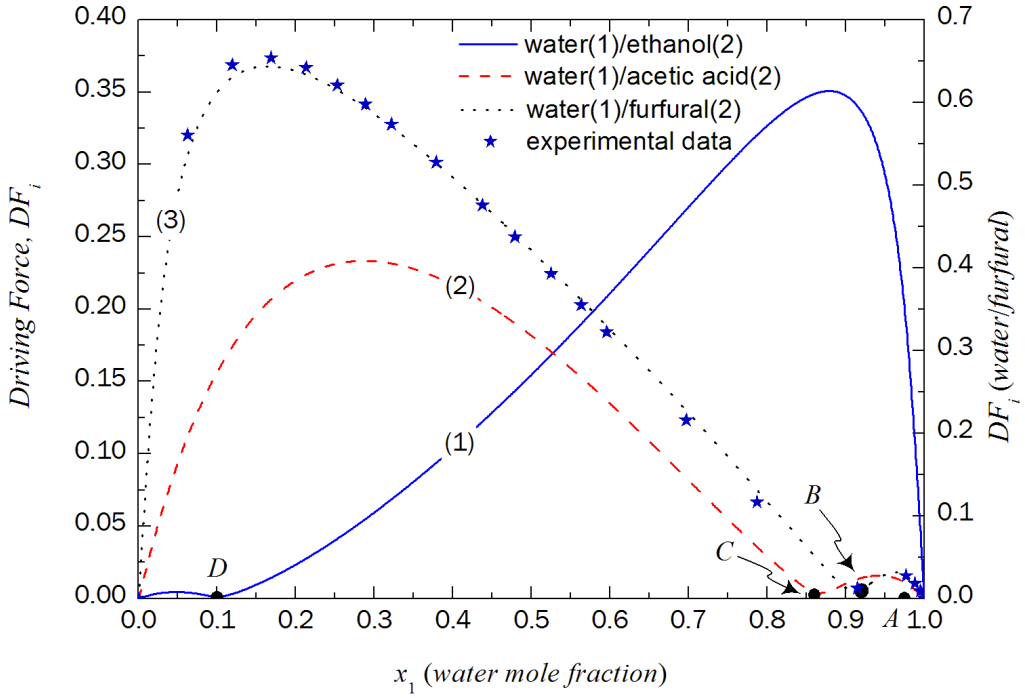

Figure 4.8 – *DF* diagrams for water/ethanol, water/acetic acid and water/furfural.

In the high concentration region with respect to water, point *A* represents the feed composition. As observed in Figure 4.8, it is not possible to obtain pure ethanol directly in one–step by ordinary distillation due to, firstly, the presence of the water/furfural azeotrope (point *B*), and secondly due to the water/ethanol azeotrope (point *D*). In accordance with the *DF* theory presented in Chapter two, when the *DF* decreases the separation becomes difficult, and the separation becomes infeasible when *DF* approaches zero, which is the case at points *B*, *C*, and *D*. Based on this analysis, the use of a hybrid process to recover ethanol becomes a feasible separation scheme. As we are dealing with a highly dilute system and due to the presence of binary azeotropes, the mixture can be concentrated to its azeotropic composition with respect to point *B* by *distillation* or *flash operation*. Then, the resulting mixture (point *B*) can be concentrated to approach its azeotropic composition with respect to point *D* by ordinary distillation, and afterwards pure ethanol can be obtained by one of the above–mentioned separation techniques.

4.2.5.3 Step 3 –Process–Group Selection

Based on the analysis performed in step 2, we have potentially seven different separation techniques to be used in the synthesis problem. Since each *PG* represents a separation technique, the objective is to match the *PG* against the separation techniques identified in the previous step. Due to the large difference in normal vapor pressure values between carbon dioxide (*B*) and ethanol (*C*), the separation technique matching this task is flash separation and the corresponding *PG* matching this separation technique is a flash separation *PG*. Then, a flash separation *PG* is selected from the *PG* database (Table 2.1), and initialized with the mixture in the synthesis problem as shown in Table 4.11.

Table 4.11 – Selection and initialization of a flash separation process–group.

Components in the synthesis problem	*A, B, C, D, E, F, G, H, I, J, K, L*
Separation task	*B*/*C*
Property dependence	Vapor pressure, boiling point
Separation technique	Flash separation between *B* and *C*
Matching set of components	12 (*ABCDEFGHIJKL*) 11 (*ABCDEFGHIJK*) (*BCDEFGHIJKL*) 10 (*ABCDEFGHIJ*) (*BCDEFGHIJK*) 9 (*ABCDEFGHI*) (*BCDEFGHIJ*) 8 (*ABCDEFGH*) (*BCDEFGHI*) 7 (*ABCDEFG*) (*BCDEFGH*) 6 (*ABCDEF*) (*BCDEFG*) 5 (*ABCDE*) (*BCDEF*) 4 (*ABCD*) (*BCDE*) 3 (*ABC*) (*BCD*) 2 (*BC*)
Selected *PG*	12 (*fAB*/*CDEFGHIJKL*) 11 (*fAB*/*CDEFGHIJK*) (*fB*/*CDEFGHIJKL*) 10 (*fAB*/*CDEFGHIJ*) (*fB*/*CDEFGHIJK*) 9 (*fAB*/*CDEFGHI*) (*fB*/*CDEFGHIJ*) 8 (*fAB*/*CDEFGH*) (*fB*/*CDEFGHI*) 7 (*fAB*/*CDEFG*) (*fB*/*CDEFGH*) 6 (*fAB*/*CDEF*) (*fB*/*CDEFG*) 5 (*fAB*/*CDE*) (*fB*/*CDEF*) 4 (*fAB*/*CD*) (*fB*/*CDE*) 3 (*fAB*/*C*) (*fB*/*CD*) 2 (*fB*/*C*)

As shown in Table 4.11 the flash separation *PG* is initialized with 20 different sets of components. As mentioned, this is based on the assumption of an ideal system, where no binary azeotropes exist between the key components and the components are

ordered according to decreasing normal vapor pressures. The same procedure is applied for the selection and initialization of the other *PGs* group matching the separation task with their corresponding separation techniques identified in step 2. Table 4.12 lists the final selection of the *PGs* to be used in the generation of flowsheet structures.

Table 4.12 – Final selection of the *PG*'s in the synthesis problem.

Separation technique	*Process–groups*	
Flash separation	12	(*fAB*/*CDEFGHIJKL*)
	11	(*fAB*/*CDEFGHIJK*) (*fB*/*CDEFGHIJKL*)
	10	(*fAB*/*CDEFGHIJ*) (*fB*/*CDEFGHIJK*)
	9	(*fAB*/*CDEFGHI*) (*fB*/*CDEFGHIJ*)
	8	(*fAB*/*CDEFGH*) (*fB*/*CDEFGHI*)
	7	(*fAB*/*CDEFG*) (*fB*/*CDEFGH*)
	6	(*fAB*/*CDEF*) (*fB*/*CDEFG*)
	5	(*fAB*/*CDE*) (*fB*/*CDEF*)
	4	(*fAB*/*CD*) (*fB*/*CDE*)
	3	(*fAB*/*C*) (*fB*/*CD*)
	2	(*fB*/*C*)
Distillation	10	(*CD/DEFGHIJKL*)
	9	(*CD/DEFGHIJK*)
	8	(*CD/DEFGHIJ*)
	7	(*CD/DEFGHI*)
	6	(*CD/DEFGH*)
	5	(*CD/DEFG*)
	4	(*CD/DEF*)
	3	(*CD/DE*)
Liquid membrane	2	(*lmemC*/*D*)
Molecular sieve	2	(*msC*/*D*)
Gas membrane	2	(*gmemC*/*D*)
Pervaporation	2	(*pervC*/*D*)
Solvent based azeotropic	2	(*cycC*/*D*)

4.2.5.4 Step 4 –Generation of Flowsheet Candidates

By combining the *PGs* listed in Table 4.12, 640 flowsheet structures have been analyzed. Out of these 640 flowsheet structures, 85 are feasible flowsheet structures satisfying the connectivity rules, and out of these, 5 flowsheet structures are of the interest to be analyzed in detail, as they are most likely the best with respect to minimum energy consumption. Table 4.13 provides the list of these flowsheet structures by means of the **SFILES** notation (d'Anterroches[15,16]) together with their corresponding energy consumption index. The flowsheet property model described in chapter 2, section 2.3.3 has been used to estimate *Ex*, and the parameters have been taken from d'Anterroches[15,16]. It should be noted that the flowsheet structures have the same energy

consumption index. This is explained by the fact that the energy index is only calculated for the ordinary distillation process–groups, while the other *PGs* do not contribute to the energy consumption.

Table 4.13 – Flowsheet structures of interest in the synthesis problem.

	Alternative **SFILES** string	*Ex* (*MkJ/h/kmole*)
1	(iABCDEFGHIJKLM)(slABCDFEGHIJKL/M) **[**(fAB/CDFEGHIJKL)**[**(CD/DFEGHIJKL)[(oDFEGHIJKL)](lmemC/D) [(oC)](oD)**]**(oAB)**]**(oM)	0.172289
2	(iABCDEFGHIJKLM)(slABCDFEGHIJKL/M) **[**(fAB/CDFEGHIJKL)**[**(CD/DFEGHIJKL)[(oDFEGHIJKL)](msC/D) [(oC)](oD)**]**(oAB)**]**(oM)	0.172289
3	(iABCDEFGHIJKLM)(slABCDFEGHIJKL/M) **[**(fAB/CDFEGHIJKL)**[**(CD/DFEGHIJKL)[(oDFEGHIJKL)](gmemC/D) [(oC)](oD)**]**(oAB)**]**(oM)	0.172289
4	(iABCDEFGHIJKLM)(slABCDFEGHIJKL/M) **[**(fAB/CDFEGHIJKL)**[**(CD/DFEGHIJKL)[(oDFEGHIJKL)](pervC/D) [(oC)](oD)**]**(oAB)**]**(oM)	0.172289
5	(iABCDEFGHIJKLM)(slABCDFEGHIJKL/M) **[**(fAB/CDFEGHIJKL)**[**(CD/DFEGHIJKL)[(oDFEGHIJKL)](cycC/D) [(oC)](oD)**]**(oAB)**]**(oM)	0.172289

Figure 4.9 depicts the flowsheet structure which makes use of extractive distillation to obtain ethanol with the desired purity. This flowsheet structure is chosen for further analysis. There are three options to initialize the solvent based azeotropic separation *PG*, by means of organic solvents (*OS*), ionic liquids (*IL*) or hyperbranched polymers (*HyPol*).

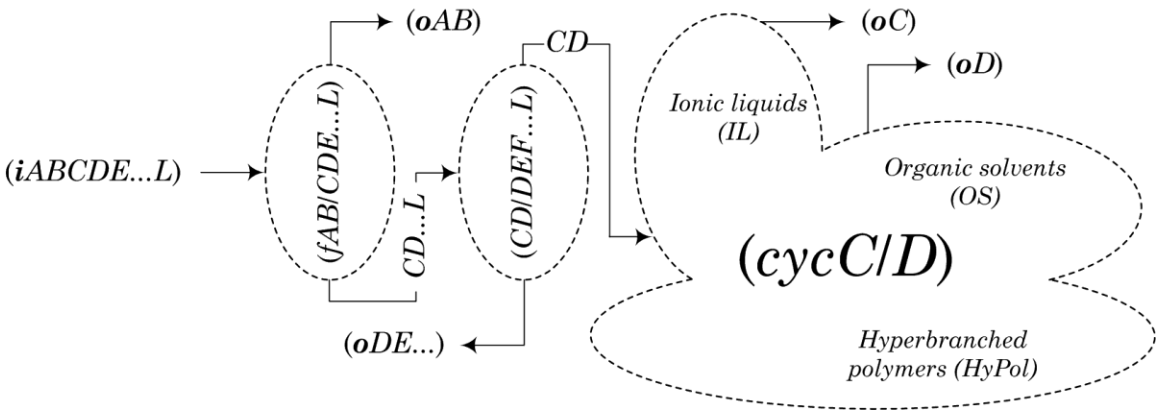

Figure 4.9 – Process–group representation of the downstream separation for bioethanol process.

Note that the solvent identity is not known at this point and it is also not necessary to know it. In the case of *OS*, a CAMD (Computer Aided Molecular Design) problem is formulated where the target to be matched could either be the solvent free *DF* or the solvent fraction, but not both. For *OS* a target solvent free *DF* equal to 0.48 is selected (Alvarado–Morales *et al.*[1]). The ProCAMD tool (Harper & Gani[37]) from the ICAS

software has been used to find potential solvent candidates. With respect to *IL* and *HyPol* the potential candidates were found through a search in the open literature and databases (Seiler *et al.*[82]; Jork *et al.*[52]; Wang *et al.*[94], Solvent Innovation[45], and ilthermo[42]). Table 4.14 lists the solvent candidates.

Table 4.14 – Potential solvent candidates.

Candidate	Solvent
	Organic solvents (*OS*)
1	Glycerol
2	Ethylene glycol
3	Triethylene glycol
4	Dipropylene glycol
5	1,2–Propylene glycol
6	1,3–Propylene glycol
7	Diethylene glycol
	Ionic liquids (*IL*)
8	$[EMIM]^+[BF_4]^-$
9	$[BMIM]^+[Cl]^-$
10	$[EMIM]^+[EtSO_4]^-$
11	$[EMIM]^+[DMP]^-$
	Hyperbranched polymers (*HyPol*)
12	Polyglycerol

Note that each solvent candidate represents a process flowsheet, meaning that there will be as many different process flowsheets as potential solvent candidates can be used to initialize the solvent based azeotropic separation *PG* in the process flowsheet in Figure 4.9. Consequently, the performance of each process flowsheet can be evaluated by means of the solvent performance.

4.2.5.5 Step 5 –Ranking/Selection of Flowsheet Candidates

As mentioned above, the performance of the downstream separation process flowsheet can be evaluated through the solvent performance. This is done through the flowsheet property model together with the corresponding parameters (depending on the nature of the solvent). A detailed description is given in the Appendix on how to initialize the solvent based azeotropic separation *PG* and how to use the property model together with the parameters to predict the energy consumption index. Table 4.15 shows the energy consumption index E_x performance for each solvent candidate.

Table 4.15 – Performance evaluation results for the potential solvent candidates.

Solvent candidate	$x_{solvent}$	DF_i	*Predict energy* (*Ex*) (*MkJ/h/kmole*)	*Energy demand*, Seiler *et al.*[82] (*MkJ/h/kmole*)
1 – Glycerol	0.63	0.48	0.0322	
2 – Ethylene glycol (EG)	0.52	0.48	0.0317	0.0335
3 – Triethylene glycol	0.63	0.25	0.0618	
4 – Dipropylene glycol	0.63	0.17	0.0909	
5 – 1,2–Propylene glycol	0.63	0.12	0.1288	
6 – 1,3–Propylene glycol	0.63	0.12	0.1288	
7 – Diethylene glycol	0.63	0.22	0.0702	
8 – $[EMIM]^+[BF_4]^-$	0.375	0.35	0.0352	0.0333
9 – $[EMIM]^+[BF_4]^-$	0.45	0.37	0.0299	
10 – $[BMIM]^+[Cl]^-$	0.30	0.37	0.0402	
11 – $[BMIM]^+[Cl]^-$	0.45	0.42	0.0260	
12 – $[EMIM]^+[EtSO_4]^-$	0.40	0.31	0.0386	
13 – $[EMIM]^+[DMP]^-$	0.40	0.38	0.0318	
14 – $[EMIM]^+[DMP]^-$	0.45	0.37	0.0296	
15 – Polyglycerol	0.035	0.36	0.0762	0.0650
16 – Polyglycerol	0.070	0.38		0.0530

Among many other organic solvents, ethylene glycol and glycerol have been identified as matching the target *DF*. Ethylene glycol has been selected because it is a known solvent for extraction of ethanol, while glycerol is a by–product from glucose fermentation. Figures 4.10 and 4.11 plot the *DF* as a function of solvent amount, for ethylene glycol and glycerol, respectively. They confirm that the *DF* target of 0.48 can be attained with an ethylene glycol fraction of 0.42 and with a glycerol fraction of 0.63.

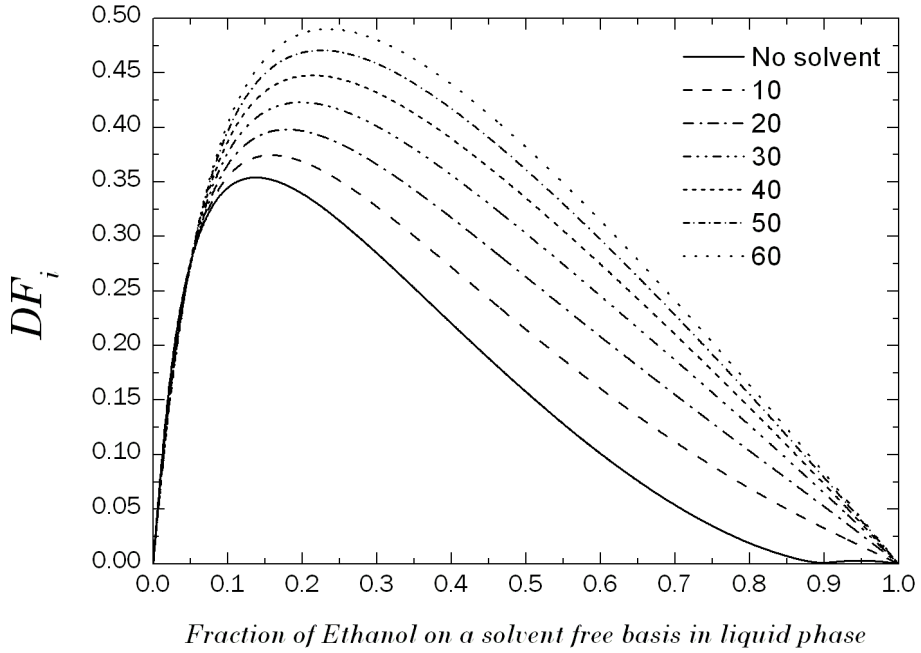

Figure 4.10 – Solvent free *DF* diagram for ethanol/water mixture separation with ethylene glycol (EG).

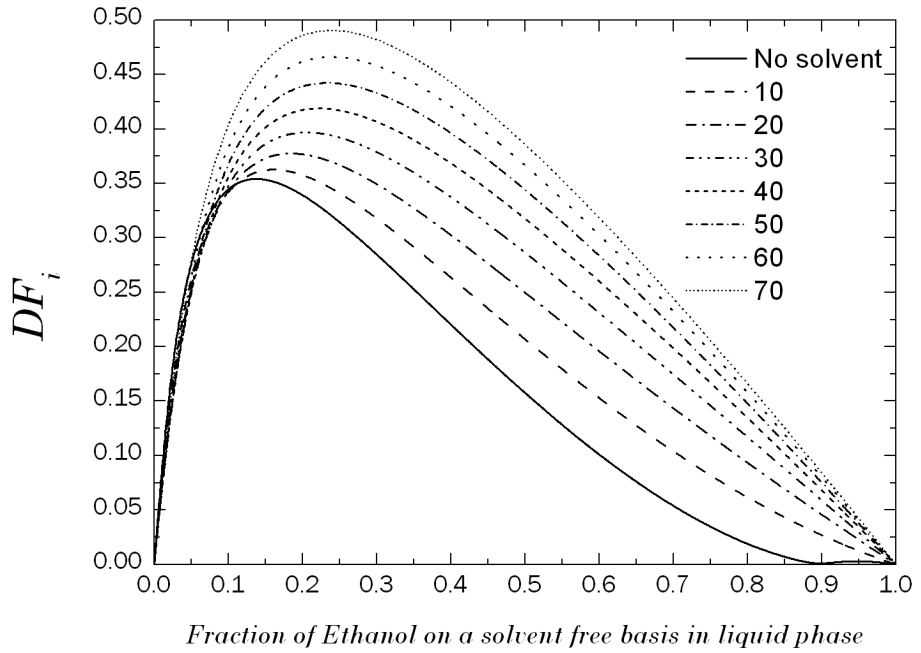

Figure 4.11 – Solvent free *DF* diagram for ethanol/water mixture separation with glycerol.

The results from Table 4.15 show that two of the solvents reported by Seiler *et al.*[82] have been independently found in this work, solvent candidates 2 and 8. In the case of candidate 2 for *OS*, candidate 8 for *IL*, and candidate 15 for *HyPol* the energy consumption index predicted by the flowsheet property model is almost similar compared to the ones reported by Seiler *et al.*[82]. On the other hand, compared to candidate 8, through the flowsheet property model, a slightly better option (candidate 9) has been found. This is explained by the fact that the candidate 9 makes use of a higher *DF* than candidate 8, representing in principle a reduction of the enrgy consumption index by 10.2 %.

Experimental evidence has demonstrated that one of the potential *IL* candidates to be used as the entrainer in extractive distillation to break the ethanol/water azeotrope is $[BMIM]^+[Cl]^-$ (Jork *et al.*[52]). Using the optimal *DF* based design target of 0.37 —which corresponds to an $[EMIM]^+[BF_4]^-$ fraction of 0.45 (see Table 4.15, candidate 9) —from the *DF* diagram in Figure 4.12, it can be observed that the fraction of $[BMIM]^+[Cl]^-$ needed to reach the target *DF* of 0.37 is 0.30 and the corresponding energy consumption for the extraction process is found to be 0.0402 *MkJ/h/kmole* of feed.

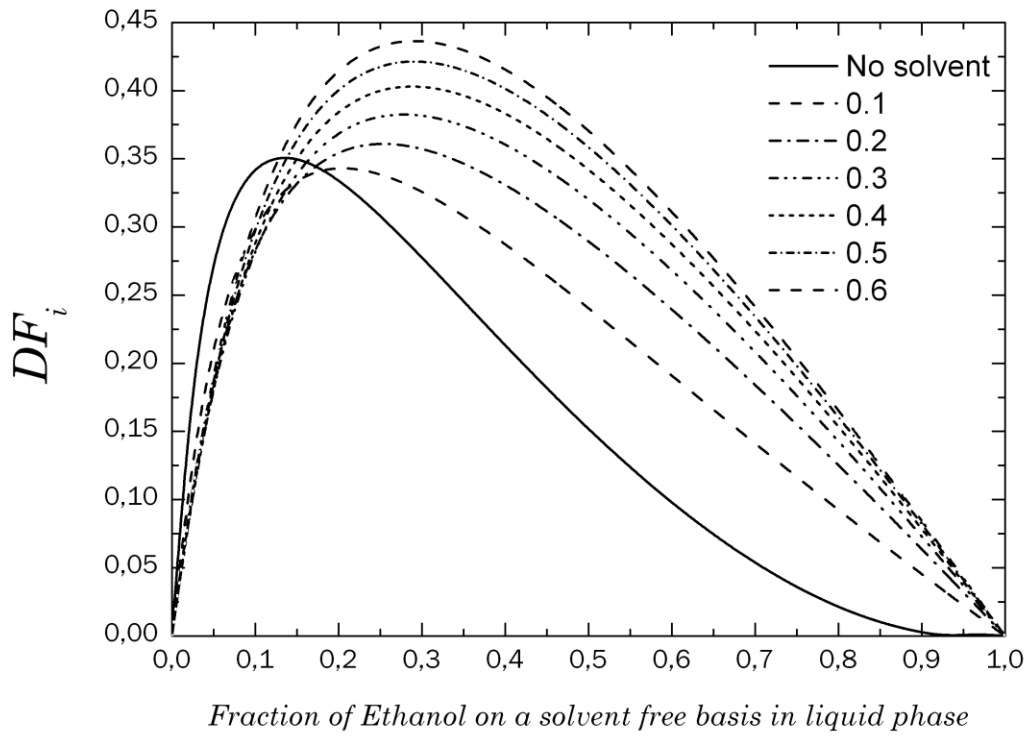

Figure 4.12 – Solvent free *DF* diagram for ethanol/water mixture separation with ionic liquid ($[BMIM]^+[Cl]^-$).

Now, if a target *DF* of 0.42 is selected, from Figure 4.12 it can be seen that the fraction of solvent needed to match this target is found to be 0.45 with a corresponding energy requirement of 0.026 *MkJ*/*h*/*kmole* of feed, thereby achieving a reduction in terms of energy consumption compared to $[EMIM]^+[BF_4]^-$ as the entrainer. Nevertheless, it should be noted also that according to Seiler *et al.*[82], *ILs* containing fluorinated anions such as $[BF_4]^-$ and $[PF_6]^-$ are expensive and show insufficient stability to hydrolysis for long–term applications. Because of the hydrolysis, they form small amounts of HF, which is corrosive and toxic. For applications of these *IL*, industrial requirements such as the environmentally acceptable disposal of halogen compounds in considerable quantities also have to be taken into consideration.

According to Wang *et al.*[94], among various *ILs* reported in literature, the ones with alkyl–substituted imidazolium cation and dialkylphosphates (such as $[EMIM]^+[DMP]^-$) are worth further investigation because of their good stability and hydrophilicity, less toxicity and corrosiveness and more importantly their ease of production and lower cost for industrial applications. From the *DF* diagram (Figure 4.13) it can be seen that the fraction of $[EMIM]^+[DMP]^-$ needed to reach the target *DF* of 0.37 is 0.45 and the corresponding energy consumption for the extraction process is found to be 0.0296 *MkJ*/*h*/*kmole* of feed.

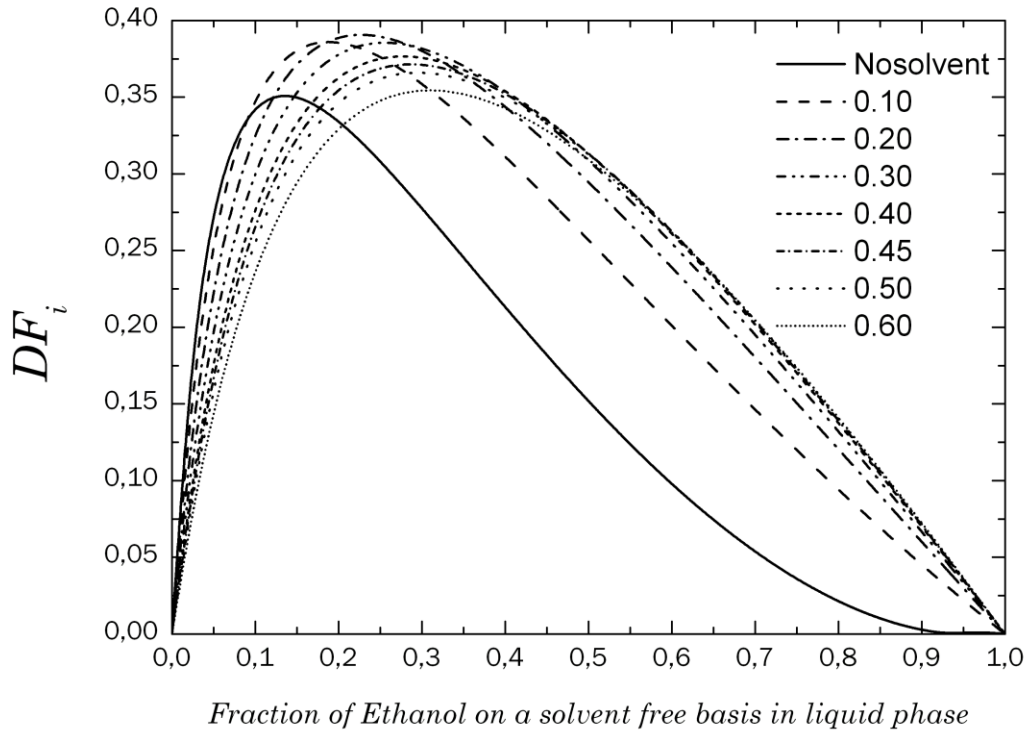

Figure 4.13 – Solvent free *DF* diagram for ethanol/water mixture separation with ionic liquid ($[EMIM]^+[DMP]^-$).

Among the generated (feasible) design candidates, the best candidate in terms of energy consumption is predicted by the flowsheet property model and corresponds to candidate 11 which makes use of $[BMIM]^+[Cl]^-$ with a fraction of 0.45. This candidate represents in terms of energy consumption a reduction of 21.9 % in comparison to candidate 8. However, because of environmental issues, it would not be practical to implement this option. In this case, candidate 14 would be the most promising option to be considered. Table 4.16 lists the solvent candidates in increasing order according to their predicted energy consumption, and the most likely candidates with respect to the performance criteria are highlighted. Systems using the highlighted solvent candidates are chosen for further investigation via reverse simulation of the process flowsheet structures.

Table 4.16 – Ranking of the solvent candidates.

Rank	Solvent candidate	$x_{solvent}$	DF_i	*Predicted energy, Ex* (*MkJ/h/kmole*)
1	$[BMIM]^+[Cl]^-$	0.45	0.42	0.0260
2	$[EMIM]^+[DMP]^-$	0.45	0.37	0.0296
3	$[EMIM]^+[BF_4]^-$	0.45	0.37	0.0299
4	Ethylene glycol (EG)	0.52	0.48	0.0317
5	$[EMIM]^+[DMP]^-$	0.40	0.38	0.0318
6	Glycerol	0.63	0.48	0.0322
7	$[EMIM]^+[BF_4]^-$	0.375	0.35	0.0352
8	$[EMIM]^+[EtSO_4]^-$	0.40	0.31	0.0386
9	$[BMIM]^+[Cl]^-$	0.30	0.37	0.0402
10	Triethylene glycol	0.63	0.25	0.0618
11	Diethylene glycol	0.63	0.22	0.0702
12	Polyglycerol	0.035	0.36	0.0762
13	Dipropylene glycol	0.63	0.17	0.0909
14	1,2–Propylene glycol	0.63	0.12	0.1288
15	1,3–Propylene glycol	0.63	0.12	0.1288

4.2.5.6 Step 6 –Reverse Simulation

Reverse simulation is performed for the process flowsheet (design) candidates with the best performance with respect to energy consumption. As mentioned in the previous step, the performance of the entire process flowsheet can be evaluated through the solvent performance. As solvent candidates highlighted in Table 4.16 are most likely design candidates with respect to the performance criteria, they are chosen for reverse simulation. As the first task of this step is the resolution of the mass balance, the topology of the entire process flowsheet needs to be defined.

As the type and thereby the identity of the solvents are known, the topology of the process flowsheet in Figure 4.14 with respect to the solvent based azeotropic separation process–group is as follows:

If an organic solvent (*OS*) is used as entrainer, Figure 4.14 depicts the process flowsheet.

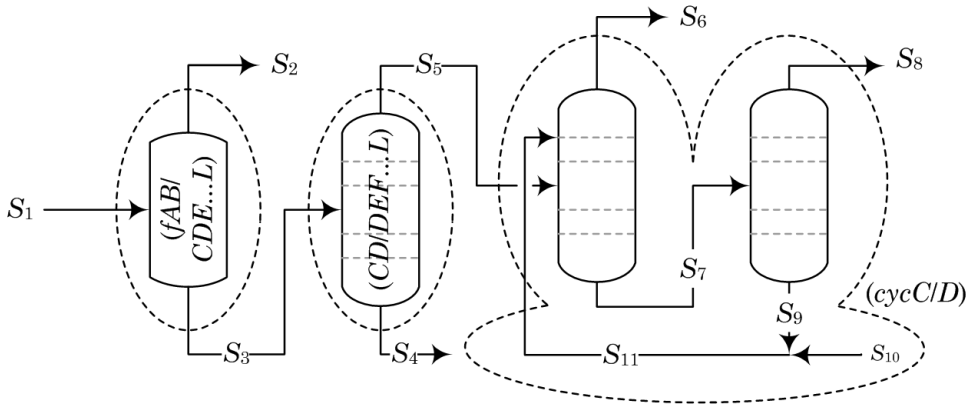

Figure 4.14 – Process flowsheet for the downstream separation using *OS* as entrainer.

Figure 4.15 depicts the process flowsheet if an ionic liquid (*IL*) is used as entrainer.

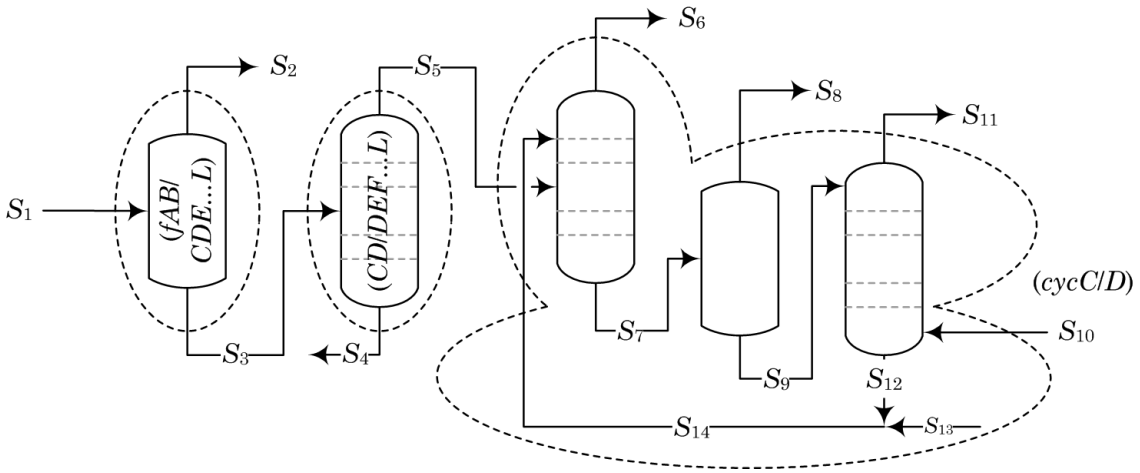

Figure 4.15 – Process flowsheet for the downstream separation using *IL* as entrainer.

Ranks 3 and 4 are selected to perform the mass balance as well as reverse simulation.

Rank 3 – $[EMIM]^+[BF_4]^-$

Mass balance

The mass balance results for the process flowsheet in Figure 4.15 using $[EMIM]^+[BF_4]^-$ are given in Table 4.17.

Table 4.17 – Mass balance results for the downstream separation (rank 3).

Stream	S_1	S_3	S_5	S_6	S_8	S_{10}	S_{11}
Phase	Liquid	Liquid	Liquid	Liquid	Vapor	Vapor	Vapor
T (*°C*)	30	28.88	78.59	78.32	110	25	82.90
P (*atm*)	1	1	1	1	0.1	1	0.1
F (*kmole*/*h*)	18085.5935	17809.0729	566.0283	434.1901	67.6339	2070.02	2134.3081
Mole fraction							
A	0.000003						
B	0.014076				0.028400		
C	0.024718	0.024747	0.770823	0.9999	0.971500		0.000122
D	0.952069	0.965981	0.229173	0.000008	0		0.030000
E	0.004827	0.004897		0	0		0
F	0.001007	0.001022	0.000002	0	0.000010		0
G	0.000086	0.000087		0	0.000001		0
H	0.000822	0.000835					
I	0.000043	0.000043	0.000001				
J	0.000008	0.000009					
K	0.000023	0.000024					
L	0.002320	0.002356					
Air						1.000000	0.9699
Solvent (IL)				0.000004	0.000080		0.000015

Reverse simulation

The design parameters for the distillation columns are back calculated based on the *DF* method described in Section 2.3.4 and given in Table 4.18.

Table 4.18 – Design parameters for the distillation columns.

Design parameter	*Distillation column*	*Extractive column*	*Stripping column*
Number of stage	32	30	8
Feed stage location	17	22	1, 4
Reflux ratio	3.2	0.52	
DF_{max}	0.35	0.48	

Rank 4 – Ethylene glycol (EG)

Mass balance

The mass balance results for the process flowsheet in Figure 4.14 using *EG* are given in Table 4.19.

Table 4.19 – Mass balance results for the downstream separation (rank 4).

Stream	S_1	S_3	S_5	S_6	S_8	S_{11}
Phase	Liquid	Liquid	Liquid	Liquid	Liquid	Liquid
T (°*C*)	30	28.88	78.59	78.32	42	75
P (*atm*)	1	1	1	1	0.1	1
F (*kmole*/*h*)	18085.5935	17809.0729	566.0283	432.6021	139.8310	613
Mole fraction						
A	0.000003					
B	0.014076					
C	0.024718	0.024747	0.770823	0.998481	0.031202	
D	0.952069	0.965981	0.229173	0.000910	0.924866	
E	0.004827	0.004897				
F	0.001007	0.001022	0.000002		0.000009	
G	0.000086	0.000087			0.000003	
H	0.000822	0.000835				
I	0.000043	0.000043	0.000001			
J	0.000008	0.000009				
K	0.000023	0.000024				
L	0.002320	0.002356				
Solvent (EG)				0.0006091	0.043920	1.000000

Reverse simulation

The design parameters for the distillation columns are given in Table 4.20.

Table 4.20 – Design parameters for the distillation columns.

Design parameters	*Distillation column*	*Extractive column*	*Recovery column*
Number of stage	32	30	15
Feed stage location	17	22	5
Reflux ratio	3.2	0.52	0.54
DF_{max}	0.35	0.48	0.59

4.2.5.7 Step 7 –Final Verification

The process flowsheets have been validated by rigorous simulation by means of the PROII® simulator (PROII[77]).

Table 4.21 gives the energy consumption for each process flowsheet obtained by rigorous simulation. Tables 4.22–4.23 provide the detailed mass balance for the process flowsheet ranks 3 and 4, respectively.

Table 4.21 – Energy consumption from rigorous simulation *vs*. predicted energy.

Rank	Solvent candidate	$x_{solvent}$	DF_i	Predicted energy, *Ex* (*MkJ/h/kmole*)	Energy demand (*MkJ/h/kmole*)
1	$[BMIM]^+[Cl]^-$	0.45	0.42	0.0260	0.02985
2	$[EMIM]^+[DMP]^-$	0.45	0.37	0.0296	0.03338
3	$[EMIM]^+[BF_4]^-$	0.45	0.37	0.0299	0.03340
4	EG	0.52	0.48	0.0317	0.039285

Table 4.22 – Mass balance results from rigorous simulation for the downstream separation (rank 3).

Stream	S_1	S_3	S_5	S_6	S_8	S_{10}	S_{11}
Phase	Liquid	Liquid	Liquid	Liquid	Vapor	Vapor	Vapor
T (*°C*)	30	28.88	78.59	78.32	110	25	82.90
P (*atm*)	1	1	1	1	0.1	1	0.1
F (*kmole*/*h*)	18085.5935	17809.0729	566.0283	434.1901	67.6339	2070.02	2134.3081
Mole fraction							
A	0.000003						
B	0.014076				0.028400		
C	0.024718	0.024747	0.770823	0.9999	0.971500		0.000122
D	0.952069	0.965981	0.229173	0.000008	0		0.030000
E	0.004827	0.004897		0	0		0
F	0.001007	0.001022	0.000002	0	0.000010		0
G	0.000086	0.000087		0	0.000001		0
H	0.000822	0.000835					
I	0.000043	0.000043	0.000001				
J	0.000008	0.000009					
K	0.000023	0.000024					
L	0.002320	0.002356					
Air						1.000000	0.9699
Solvent (IL)				0.000004	0.000080		0.000015

Table 4.23 – Mass balance results from rigorous simulation for the downstream separation (rank 4).

Stream	S_1	S_3	S_5	S_6	S_8	S_{11}
Phase	Liquid	Liquid	Liquid	Liquid	Liquid	Liquid
T (°*C*)	30	28.88	78.59	78.32	42	75
P (*atm*)	1	1	1	1	0.1	1
F (*kmole*/*h*)	18085.5935	17809.0729	566.0283	432.6021	139.8310	613
Mole fraction						
A	0.000003					
B	0.014076					
C	0.024718	0.024747	0.770823	0.998481	0.031202	
D	0.952069	0.965981	0.229173	0.000910	0.924866	
E	0.004827	0.004897				
F	0.001007	0.001022	0.000002		0.000009	
G	0.000086	0.000087			0.000003	
H	0.000822	0.000835				
I	0.000043	0.000043	0.000001			
J	0.000008	0.000009				
K	0.000023	0.000024				
L	0.002320	0.002356				
Solvent (EG)				0.0006091	0.043920	1.000000

4.2.6 Discussion

The verification (simulation) results confirm that the ranking of the alternatives obtained by means of the flowsheet property model to predict the energy consumption index is truly predictive (see Table 4.21). The *PGC* methodology provides results that match those obtained through rigorous simulation, and the mass balance results from the two sources match. The ability to define (estimate) the design parameters of the unit operations using the reverse approach also provides an efficient way to obtain the alternative designs. It should be noted that the comparison of process flowsheet structures using different types of process−groups is limited by the availability of the energy consumption index model.

4.3 Succinic Acid Production Process

To offset the inherent high cost of processing biological materials such as lignocellulosic biomass, the possibilities of producing co–products with higher market value should be taken into account when designing bioethanol production processes. Thus, the objective in this case was to identify specific chemical routes which, starting from the glucose and/or ethanol platform, enhance the economy of the bioethanol production process. Based on a market analysis, and also comparing the minimum number of required processing steps against the selling price, succinic acid (SA) was identified as a potential product to be produced from the glucose platform. The succinic acid production process has distinct advantages over the bioethanol production process. For example, in the bioethanol production process, 2 moles of CO_2 are formed per mole of glucose consumed. The succinic acid production process on the other hand, consumes CO_2 (theoretically 1 mole CO_2 per mole succinic acid produced). Therefore, the introduction of succinic acid as a commodity building–block has the potential to reduce the environmental impact. Furthermore, integrating the succinic acid and ethanol fermentations with their recovery would decrease the amount of carbon lost as waste CO_2 and a third chemical could also be produced through the esterification of succinic acid with ethanol to yield an organic acid ester, diethyl succinate. Therefore, three commercial products could be produced: succinic acid, ethanol, and diethyl succinate.

Process description

As the importance of succinic acid for use as a biodegradable polymer has increased, biological production by fermentation has been in focus as the alternative to petrochemical–based processes**.** Many different microorganisms have been screened and studied for succinic acid production. Among them, *Actinobacillus succinogenes* (Guettler *et al.*[34]; Song & Lee[85]), *Anaerobiospirillum succiniciproducens* (Lee *et al.*[58]; Lee *et al.*[59]; Song & Lee[85]), and, *Mannheimia succiniciproducens* (Lee *et al.*[60]; Song & Lee[85]; Song *et al.*[86]) have been found to produce much larger amounts of succinic acid than other microorganisms, while some by–products such as acetic acid, formic acid, lactic acid, maleic acid, pyruvic acid, fumaric acid, and ethanol are also formed. The accompanying generation of by–products potentially limits the economic advantages of its production by fermentation at an industrial scale, as the yield of succinic acid is reduced and the downstream processing becomes more complex and expensive.

The downstream processing typically accounts for over 50–80% of the total production cost in classical fermentation–based processes (Song *et al.*[86]). For an economical recovery process of succinic acid from the fermentation broth, various separation techniques such as precipitation, distillation, electrodialysis and liquid−liquid solvent−based extraction have been reported. Electrodialysis is a widely used separation process, in which ionized compounds are separated from non–ionized compounds by ion exchange membrane, and is used in wastewater treatment, pharmaceutical production and food processing.

Succinic acid normally exists in the form of ionized–succinate salt in a fermentation broth, while other chemicals, such as carbohydrates, proteins and amino acids are mostly non–ionized. Most specialty commodity applications of succinic acid require the free acid form rather than the salt form. Therefore, the succinic acid purification process composed of conventional electrodialysis followed by water–splitting electrodialysis membrane stacks, which removes most of the salt cation and produces a highly pure acid stream, was developed by Glassner *et al*[30]. In order to remove the residual cationic, anionic and amino acids, cation and anion exchange resins were integrated into the above process as the final purification step (Glassner *et al.*[30]). Although this process increased the concentration of succinic acid from 51.5 % to 79.6 % (*w*/*w*) and completely removed proteins and salts, the concentration of acetic acid increased from 13.2 % to 19.9 % (Song *et al.*[86]).

Another purification process employing precipitation of succinic salts was developed by Datta *et al.*[17]. Succinate in the fermentation broth is precipitated as calcium succinate by adding calcium hydroxide, which can neutralize the fermentation broth at the same time. Calcium succinate is recovered by filtration, and converted to succinic acid by adding sulphuric acid. Succinic acid is recovered by filtration, and further purified by acidic and basic ion exchangers. This process dramatically improved the purity of succinic acid from 44.5 % in the fermentation broth to 94.2 % (*w*/*w*) after the purification. Unlike the succinic acid recovery process based on the electrodialysis, it could not completely remove proteins mainly due to the saturation of the ion exchange sites with the succinate anion.

The above two processes are rather complex, which results in relatively high purification costs. In addition, these processes typically yield large amounts of solid and slurry wastes that need to be further treated and properly disposed of, especially calcium and sodium sulphates that are generated and precipitated by adding acids during the acidification step (Song *et al.*[86]). However, it is impossible to apply only one separation process for product recovery, concentration, acidification and purification of succinic acid to its required purity.

The reactive extraction of succinic acid with amine–based extractant, by using hydrophobic tertiary amines, has been considered as an effective and economical purification method in recent years because the process is operated at normal temperature and pressure (Kim *et al.*[55]; Huh *et al.*[46]). This process is based on reversible reaction between the extractant and the extracted carboxylic acid. The selective separation of a specific acid from the fermentation broth containing mixed salts can be achieved based on pK_a values of the acids and operating pH (Tamada *et al.*[89]; Yang *et al.*[99]; Tung & King[91]; Eyal & Canari[21]). The use of tri–n–octylamine as an extractant resulted in the recovery of succinic acid from the binary mixture of succinic acid and acetic acid with high selectivity and high extraction efficiency (Hong *et al.*[39]). More recently, the integrated succinic acid recovery process composed of reactive extraction, vacuum distillation and crystallization was developed by Huh *et al.*[47]. It allowed purification of succinic acid with a purity of 99.8 % (*w*/*w*) and a yield of 73.1 % (*w*/*w*) from the actual fermentation broth of *M. succiniciproducens*. Furthermore, no acetic acid was detected

after vacuum distillation. This process is much simpler and more cost–effective than those mentioned above.

In order to make the biological production of succinic acid by fermentation process more competitive compared to the petrochemical–based process, it is crucial to develop more efficient fermentative microorganisms and/or more efficient product recovery schemes. Therefore, this case study highlights the application of the *PGC* methodology with the objective to generate novel separation schemes for the downstream processing for succinic acid recovery from the fermentation broth.

4.3.1 PGC Methodology Application

4.3.1.1 Step 1 –Synthesis Problem Definition

Given the product stream, a multi–component mixture from a saccharification bioreactor, determine a physically feasible process flowsheet for the production of succinic acid from glucose. The mixture information requires the identities of the components coming out the saccharification bioreactor, their composition, *T* and/or *P* of the mixture (if available). The product specification is the minimum acceptable product purity, for example ≥ 99.5 % *wt*. The flowsheet specification is the energy consumption of the process, and the design objective (target) is to minimize this value. Table 4.24 lists the inlet stream feed flowrates to the succinic acid process facility (left hand column).

In the saccharification reactor, cellulose is converted to glucose, a process that can be catalyzed by enzymes. The available glucose in the slurry to be converted into ethanol and succinic acid is equal to 178 *kmole*/*h* (32110 *kg*/*h*). In order to know the amount of glucose that should be converted into succinic acid, a mass balance analysis has been performed based on a succinic acid production capacity of 1.605 *kmole*/*h* (190.34 kg_{SA}/*h*) and an annual load equal to 8406 *h*/*yr*. This succinic acid production capacity corresponds to 10% of the current worldwide succinic acid production according to the BREW Project[73]. Considering a yield equal to 0.775 (Song *et al*.[86]), the amount of glucose needed to produce this amount of succinic acid is equal to 1.3655 *kmole*/*h* (246 *kg*/*h*). From mass balance calculations, the amount of saccharified slurry containing this amount of glucose corresponds to 124.5394 *kmole*/*h* (2811.6 *kg*/*h*). The remaining slurry is then sent to the bioethanol production plant.

Table 4.24 – Components involved in the SA production process.

Inlet stream composition to SA process		Outlet stream components involve in the SA downstream separation	
Component	Flowrates (*kmole/h*)	Label	Component
Water	119.9728	*A*	Hydrogen
Acetic acid	0.1271	*B*	Oxygen
Furfural	8.2235E-03	*C*	Carbon dioxide
HMF	5.8968E-03	*D*	Ammonia
Glucose	1.3655	*E*	Water
Xylose	0.6894	*F*	Formic acid
Arabinose	0.0286	*G*	Acetic acid
Mannose	0.1159	*H*	Furfural
Galactose	7.0774E-03	*I*	Pyruvic acid
Cellulose	0.3067	*J*	HMF
Hemicellulose	0.2061	*K*	Succinic acid
Arabinan	8.5897E-03	*L*	Soluble sugars (SS)
Mannan	0.0327	*M*	Insoluble solids (IS)
Galactan	1.9980E-03		
Cellulase	0.2201		
Lignin	1.4427		

4.3.1.2 Step 2 –Synthesis Problem Analysis

As the objective is to produce succinic acid from glucose, a search is performed in the open literature and/or databases to investigate the chemical reactions yielding the desired product. The biochemical reactions taking place in the fermentor have been taken from Song *et al.*[86] and they are listed in Table 8.9 in the Appendix. As formic acid, pyruvic acid, carbon dioxide, hydrogen, ammonia, biomass, and oxygen are found to be either products and/or reactants in the reactions, the pure component and mixture property analysis for the downstream separation is therefore performed taking into account these components. As in the bioethanol process case study, the same assumptions have been made with respect to soluble sugars and insoluble solids. On the other hand, some of the compounds such as aldehydes (furfural and HMF) are assumed to be inert as they do not take part in the reactions. Based on these assumptions, the feasible process separation techniques for the downstream separation are identified by means of the thermodynamic insights based method (Jaksland[49]) for the mixture involving the compounds listed in Table 4.24 (right column).

From the ratios of pure component properties in Table 4.25, the first split was identified as the separation task between ammonia(*D*)/formic acid(*F*) and the corresponding separation techniques associated with these properties are *distillation* and *flash operation.* Based on physical property ratios, *liquid membrane*, *pervaporation*, and

crystallization separation techniques were found suitable to be used in the synthesis problem.

Table 4.25 – Pure component property ratios along with separation techniques.

Property	Split	Ratio	Separation technique (Jaksland[48,49])
T_b	Ammonia(*D*)/Formic acid(*F*)	1.56(>1.40)	*Distillation* *Flash operation*
T_m	SS(*L*)/HMF(*J*) Succinic Acid(*K*)/HMF(*J*)	1.38(>1.27) 1.50(>1.27)	*Crystallization*
R_g	Water(*G*)/Formic acid(*F*)	3.00(>1.03)	*Liquid membrane*
V_M	Acetic acid(*G*)/Formic acid(*F*) Water(*G*)/Formic acid(*F*)	1.52(>1.08) 2.10(>1.08)	*Liquid membrane* *Pervaporation*
VP	Ammonia(*D*)/Formic acid(*F*)	175.85(>15)	*Distillation* *Flash operation*

The mixture analysis revealed the existence of four binary azeotropes listed in Table 4.26. Therefore, *azeotropic distillation*, *extractive distillation*, and *liquid–liquid extraction* were also potential separation techniques to be considered.

Table 4.26 – Composition of azeotropes in the process at 1 *atm*.

Binary pair	$T(K)$	x_1	
Water(1)/Formic acid(2)	372.29	0.6343	Min. Boil.
Water(1)/Acetic acid(2)	371.97	0.8384	Min. Boil.
Water(1)/Furfural(2)	371.14	0.8940	Min. Boil.
Pyruvic Acid(1)/Furfural(2)	429.16	0.3403	Min. Boil.

After performing the first separation task, the resulting mixture is a multi–component mixture of organic acids, aldehydes, and water. The nature of this mixture is analyzed through its *DF* diagram as depicted in Figure 4.16.

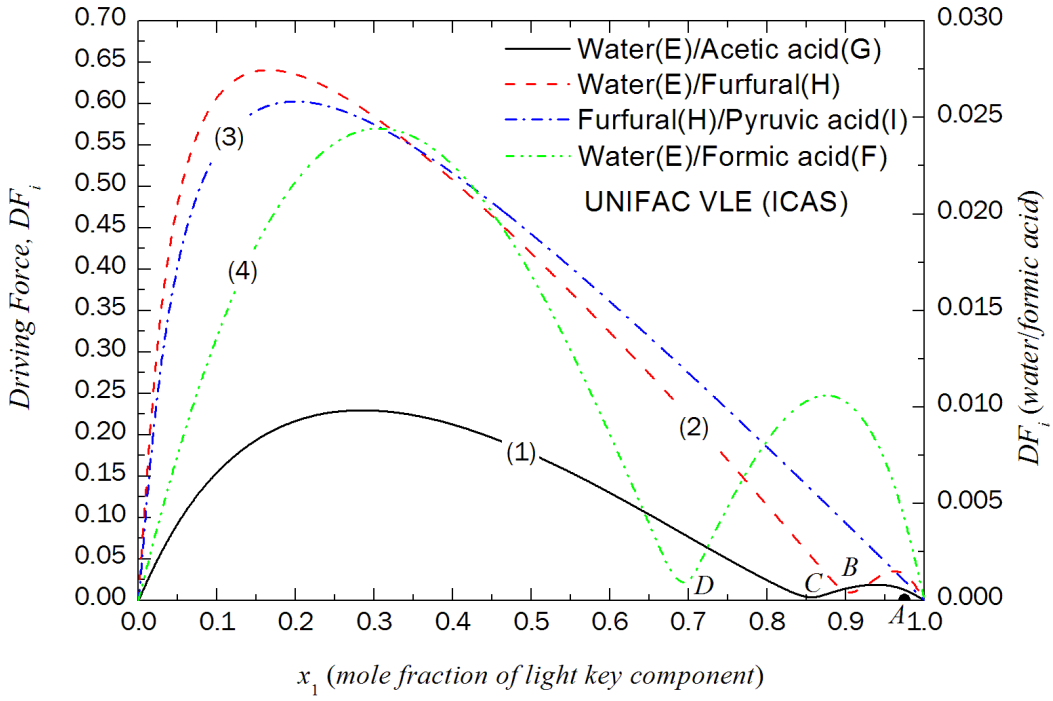

Figure 4.16 – *DF* diagrams for water/acetic acid, water/furfural, furfural/pyruvic acid and water/formic acid systems.

The black solid (1) line in Figure 4.16 represents the *DF* diagram for the binary pair water/acetic acid incorporating the remaining components as fixed components. Similarly, the red dashed (2), blue dash dotted (3), and green dash dotted (4) lines represent the *DF* diagrams for the binary pairs water/furfural, furfural/pyruvic acid, and water/formic acid, respectively. Despite the fact that the binary pair between water and furfural (red dash line) reaches the highest value of the *DF*, it is clear that it is not possible to separate beyond the azeotrope (point *B*). On the other hand, it can be observed that the azeotrope between the binary pair furfural/pyruvic acid disappears (blue dash dotted line) due to the effect of the other components in the mixture. Consequently, the split between the furfural and pyruvic acid is taken to be the following separation task and the corresponding separation technique is *distillation*.

4.3.1.3 Step 3 –Process–Group Selection

The objective is to match the *PG*s against the separation techniques. The corresponding *PG*s are retrieved from the *PG* database and matched with the separation techniques identified in step 2. First, a reaction task has been identified to produce SA. This reaction task is represented by the fermentation of glucose in a single fermentor to produce SA as the main product. There are two *PG*s representing a reaction task, a kinetic model based reactor and fixed conversion reactor. As the stoichiometry of the

reactions, together with the conversion value, are available (Song *et al.*[86]), a fixed conversion reactor *PG* is selected from the *PG* database (see Table 2.1).

The inlet stream of the fixed conversion reactor *PG* is the mixture in Table 4.24 (left hand column) together with the required reactants. The outlet stream is a mixture of non–reacted glucose, inerts (furfural, HMF, others soluble sugars, and insoluble solids), succinic acid (*K*), and the corresponding by–products resulting from side reactions. To remove the insoluble solids, a solid–liquid separation *PG* is integrated with the mixture leaving the fermentor. The same analysis for the downstream separation is performed as in the bioethanol process case study to select the *PG*s matching the separation techniques identified in the step 2. As the separation techniques identified in step 2 are *flash*, *distillation*, *pervaporation*, *liquid membrane*, *crystallization*, *liquid–liquid extraction*, and, *extractive distillation*, *PG*s representing these separation techniques are selected from the *PG* database (see Table 2.1). Before going further, *liquid–liquid extraction* is considered rather than *extractive distillation* and *azeotropic distillation* due to the highly dilute nature of the mixture and to be a separation technique that does not need energy as input. Table 4.27 provides the final selection of the *PG*s to be used in the generation of flowsheet structures.

Table 4.27 – Final selection of the *PG*'s in the synthesis problem.

Fixed conversion reactor	
13	(*rACDEGHJLM/pABCDFEGHIJKLM*)
Simple solid–liquid separation	
13	(*slABCDFEGHIJKL/M*)
Flash separation	
12	(*fABCD/FEGHIJKL*) (*ABCD/FEGHIJKL*)
11	(*fABCD/FEGHIJK*) (*fBCD/FEGHIJKL*) (*ABCD/FEGHIJK*) (*BCD/FEGHIJKL*)
10	(*fBCD/FEGHIJK*) (*fCD/FEGHIJKL*) (*BCD/FEGHIJK*) (*CD/FEGHIJKL*)
9	(*fCD/FEGHIJK*) (*fD/FEGHIJKL*) (*CD/FEGHIJK*) (*D/FEGHIJKL*)
8	(*fD/FEGHIJK*) (*D/FEGHIJK*) (*FEGH/IJKL*)
Distillation	
12	(*ABCD/FEGHIJKL*)
11	(*ABCD/FEGHIJK*) (*BCD/FEGHIJKL*)
10	(*BCD/FEGHIJK*) (*CD/FEGHIJKL*)
9	(*CD/FEGHIJK*) (*D/FEGHIJKL*)
8	(*D/FEGHIJK*) (*FEGH/IJKL*)
Pervaporation & liquid membrane	
8	(*pervE/FGIJHKL*) (*lmemE/FGIJHKL*)
Crystallization	
7	(*crsKL/JGIFH*)
6	(*crsKL/JGIF*) (*crsL/JGIFH*)
4	(*crsKL/JG*) (*crsL/JGI*) (*crsKL/JI*)
Liquid–liquid extraction	
8	(*lleFEGHIJKL/S/SK/FEGHIJL*)

4.3.1.4 Step 4 –Generation of Flowsheet Candidates

By combining the *PG*s listed in Table 4.27, 67 feasible design candidates have been generated. Out of these 67 design candidates, 18 were found to be best with respect to the minimum energy consumption (see Table 4.28).

4.3.1.5 Step 5 –Ranking/Selection of Flowsheet Candidates

Table 4.28 is providing the list of 18 generated flowsheet structures through the **SFILES** notation (d'Anterroches[15,16]). For the purpose of simplification of the **SFILES** strings, a backbone fragment has been used. The **SFILES** string fragment (iACDEGHIJLM)(backbone) corresponds to:

(iACDEGHIJLM)(rACDEGHIJLM/pABCDEFGHIJKLM)

Table 4.28 – Flowsheet structures of interest in the synthesis problem.

Rank	Alternative **SFILES** string	*Ex* (*MkJ/h/kmole*)
1	(iACDEGHIJLM)(backbone)(slABCDFEGHIJKL/M) **[**(gadJHIKLEGDF/BAC)**[**(fD/FEGKHIJL)**[**(pervLJKHIGF/E)[(oE)](crsKL/JGIFH)[(oKL)](oJGIFH)**]**(oD)**]**(oBAC)**]**(oM)	0.065095
2	(iACDEGHIJLM)(backbone)(slABCDFEGHIJKL/M) **[**(gadJHIKLEGDF/BAC)**[**(fD/FEGKHIJL)**[**(lmemLJKHIGF/E)[(oE)](crsKL/JGIFH)[(oKL)](oJGIFH)**]**(oD)**]**(oBAC)**]**(oM)	0.065095
3	(iACDEGHIJLM)(backbone)(slABCDFEGHIJKL/M) **[**(gadJHIKLEGDF/BAC)**[**(fD/FEGKHIJL)**[**(ladLJKHIGF/E)[(oE)](crsKL/JGIFH)[(oKL)](oJGIFH)**]**(oD)**]**(oBAC)**]**(oM)	0.065095
4	(iACDEGHIJLM)(backbone)(slABCDFEGHIJKL/M) **[**(gadJHIKLEGDF/BAC)**[**(D/FEGKHIJL)**[**(pervLJKHIGF/E)[(oE)](crsKL/JGIFH)[(oKL)](oJGIFH)**]**(oD)**]**(oBAC)**]**(oM)	0.065095
5	(iACDEGHIJLM)(backbone)(slABCDFEGHIJKL/M) **[**(gadJHIKLEGDF/BAC)**[**(D/FEGKHIJL)**[**(lmemLJKHIGF/E)[(oE)](crsKL/JGIFH)[(oKL)](oJGIFH)**]**(oD)**]**(oBAC)**]**(oM)	0.065095
6	(iACDEGHIJLM)(backbone)(slABCDFEGHIJKL/M) **[**(gadJHIKLEGDF/BAC)**[**(D/FEGKHIJL)**[**(ladLJKHIGF/E)[(oE)](crsKL/JGIFH)[(oKL)](oJGIFH)**]**(oD)**]**(oBAC)**]**(oM)	0.065095
7	(iACDEGHIJLM)(backbone)(slABCDFEGHIJKL/M) **[**(fABCD/FEGKHIJL)**[**(pervLJKHIGF/E)[(oE)](crsKL/JGIFH)[(oKL)](oJGIFH)**]**(oABCD)**]**(oM)	0.242613
8	(iACDEGHIJLM)(backbone)(slABCDFEGHIJKL/M) **[**(ABCD/FEGKHIJL)**[**(pervLJKHIGF/E)[(oE)](crsKL/JGIFH)[(oKL)](oJGIFH)**]**(oABCD)**]**(oM)	0.242613
9	(iACDEGHIJLM)(backbone)(slABCDFEGHIJKL/M) **[**(fABCD/FEGKHIJL)**[**(lmemLJKHIGF/E)[(oE)](crsKL/JGIFH)[(oKL)](oJGIFH)**]**(oABCD)**]**(oM)	0.242613
10	(iACDEGHIJLM)(backbone)(slABCDFEGHIJKL/M) **[**(ABCD/FEGKHIJL)**[**(lmemLJKHIGF/E)[(oE)](crsKL/JGIFH)[(oKL)](oJGIFH)**]**(oABCD)**]**(oM)	0.242613
11	(iACDEGHIJLM)(backbone)(slABCDFEGHIJKL/M) **[**(fABCD/FEGKHIJL)**[**(ladLJKHIGF/E)[(oE)](crsKL/JGIFH)[(oKL)](oJGIFH)**]**(oABCD)**]**(oM)	0.242613
12	(iACDEGHIJLM)(backbone)(slABCDFEGHIJKL/M) **[**(ABCD/FEGKHIJL)**[**(ladLJKHIGF/E)[(oE)](crsKL/JGIFH)[(oKL)](oJGIFH)**]**(oABCD)**]**(oM)	0.242613

Continued on next page

Rank	Alternative **SFILES** string	*Ex* (*MkJ/h/kmole*)
13	(iACDEGHIJLM)(backbone)(slABCDFEGHIJKL/M) **[**(fABCD/FEGKHIJL)**[**(lleFEGHIJKL/S/SK/FEGHIJKL)[(oFEGHIJL)](oSK)**]**(oABCD)**]**(oM)	0.242613
14	(iACDEGHIJLM)(backbone)(slABCDFEGHIJKL/M) **[**(ABCD/FEGKHIJL)**[**(lleFEGHIJKL/S/SK/FEGHIJKL)[(oFEGHIJL)](oSK)**]**(oABCD)**]**(oM)	0.242613
15	(iACDEGHIJLM)(backbone)(slABCDFEGHIJKL/M) **[**(fABCD/FEGKHIJL)**[**(FEGH/IJKL)[(oFEGH)](crsKL/JI)[(oKL)](oJI)**]**(oABCD)**]**(oM)	0.483227
16	(iACDEGHIJLM)(backbone)(slABCDFEGHIJKL/M) **[**(ABCD/FEGKHIJL)**[**(FEGH/IJKL)[(oFEGH)](crsKL/JI)[(oKL)](oJI)**]**(oABCD)**]**(oM)	0.483227
17	(iACDEGHIJLM)(backbone)(slABCDFEGHIJKL/M) **[**(pervLJKHIG/FCABDE)(crsKL/JGIFH)[(oKL)](oJGIFH)**]**(oFCABDE)(oM)	–
18	(iACDEGHIJLM)(backbone)(slABCDFEGHIJKL/M) **[**(lmemLJKHIG/FCABDE)(crsKL/JGIFH)[(oKL)](oJGIFH)**]**(oFCABDE)(oM)	–

It should be noted that the flowsheet structures 1–6, 7–14, and 15–16 have the same energy consumption index, respectively. This is explained by the fact that the energy index is only calculated for the ordinary distillation and flash separation process–groups, the other *PGs* do not contribute to the energy consumption. It should be noted also that the comparison of flowsheet structures using different types of process–groups as it is the case for the flowsheet structures 17 and 18, is limited by the availability of the energy consumption index property model.

The flowsheet structures 13 and 15 are selected for reverse simulation:

(iACDEGHIJLM)(backbone)(slABCDFEGHIJKL/M)
[(fABCD/FEGKHIJL)**[**(lleFEGHIJKL/S/SK/FEGHIJKL)[(oFEGHIJL)](oSK)**]**(oABCD)**]**(oM)

(iACDEGHIJLM)(backbone)(slABCDFEGHIJKL/M)
[(fABCD/FEGKHIJL)**[**(FEGH/IJKL)[(oFEGH)](crsKL/JI)[(oKL)](oJI)**]**(oABCD)**]**(oM)

4.3.1.6 Step 6 –Reverse Simulation

Figures 4.17–4.18 show the representation of the selected flowsheet structures by means of the corresponding process–groups. Figure 4.17 depicts the flowsheet structure that uses a liquid–liquid extraction solvent based separation process–group to recover succinic acid. Note that the solvent identity is not known at this time and therefore the type of unit operation to recover the solvent is also not known.

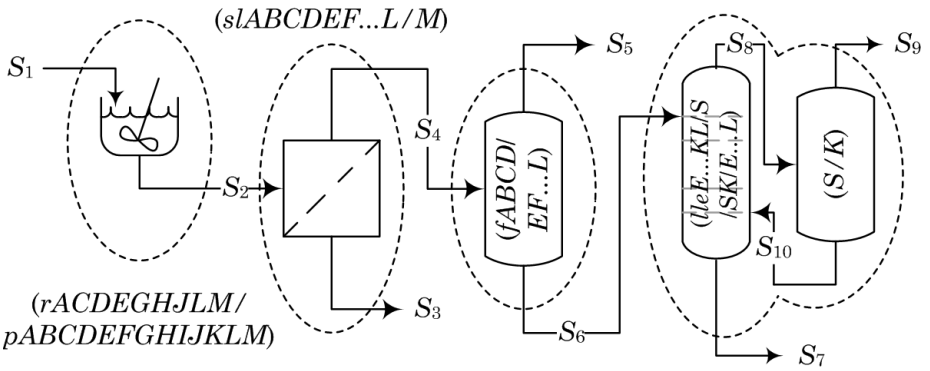

Figure 4.17 – Process flowsheet for the downstream separation in the SA production process (Rank 13).

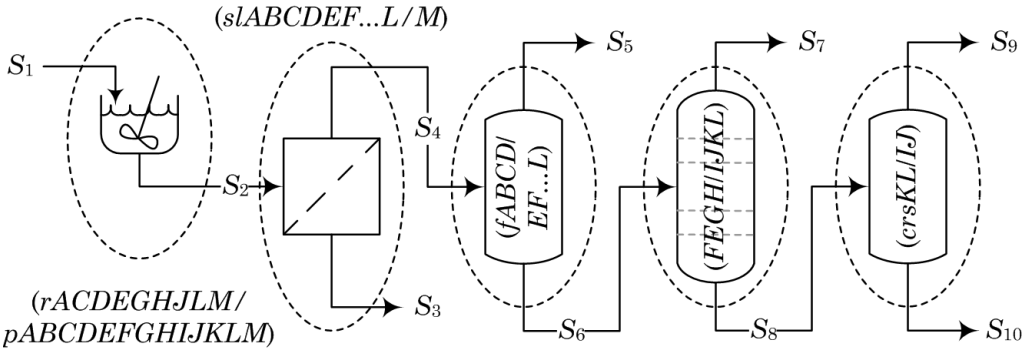

Figure 4.18 – Process flowsheet for the downstream separation in the SA production process (Rank 15).

Rank 13 – Liquid–liquid extraction

Mass balance

The mass balance results for the process flowsheet in Figure 4.17 are given in Table 4.29.

Table 4.29 – Mass balance results for the downstream separation.

Stream	S_1	S_2	S_3	S_4	S_5	S_6
Phase	Mixed	Mixed	Solid	Liquid	Vapor	Liquid
T (*°C*)	38.49	39.00	39.00	39.00	101.45	101.45
P (*atm*)	1.00	1.00	1.00	1.00	1.00	1.00
F (*kmole*/*h*)	127.8127	127.7664	2.4742	125.2922	83.8170	41.3877
Mole fraction						
A	0.012621	0.002397		0.002444	0.002699	
B		0.000100		0.000102	0.000131	
C	0.012620					
D	0.000400					
E	0.938630	0.952399		0.971206	0.995328	0.924264
F						0.000000
G	0.000994	0.001272		0.001297	0.000965	0.001972
H	0.000064	0.000064		0.000066	0.000075	0.000048
I		0.002397		0.002444	0.000760	0.005860
J	0.000046	0.000046		0.000047	0.000038	0.000065
K		0.012629		0.012878	0.000003	0.038979
L	0.017263	0.009331		0.009516		0.028806
M	0.017360	0.019365	1.000000			

Reverse simulation of the Liquid–liquid extraction PG

As in the previous case study, the solvent is not known up to this point and it is now found through the ProCAMD software (Harper & Gani[37]). The following two solvents have been identified as potential candidates: *n*–butyl acetate and *n*–decyl acetate. The verification of the creation of two liquid phases at room temperature is confirmed through the *LLE* ternary phase diagram calculation for both solvents by using ICAS (Gani, *et al.*[23]; Gani[26]). Figure 4.19 shows the ternary *LLE* phase diagrams.

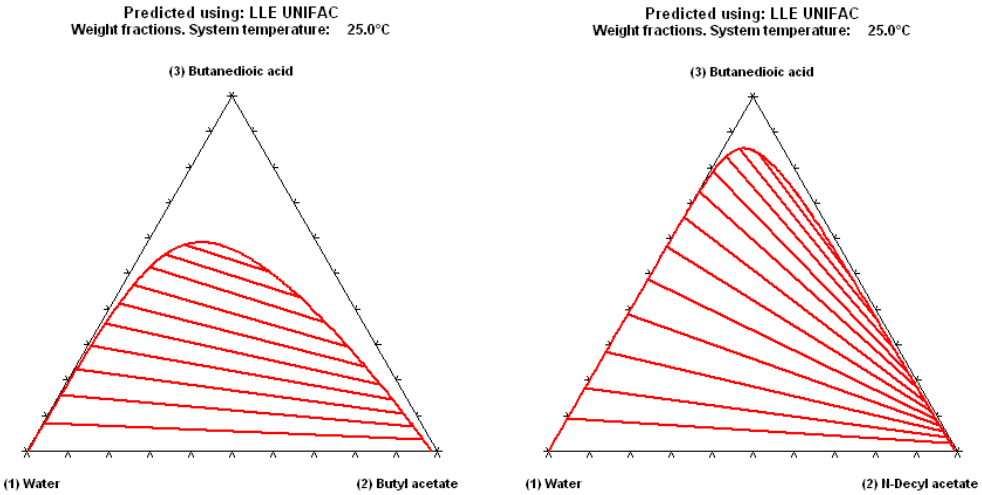

Figure 4.19 – LLE ternary phase diagrams for the system succinic acid/water/solvent.

Note that each solvent candidate represents a process flowsheet, meaning that there will be as many different process flowsheets as potential solvent candidates can be used to initialize the liquid–liquid based separation *PG* in the process flowsheet in Figure 4.17. Consequently, as shown in the bioethanol production process, the performance of each process flowsheet can be evaluated by means of the solvent performance. As there is no energy consumption in a liquid–liquid extraction based separation process, the solvent performance is assessed with respect to its *DF*.

Figure 4.20 depicts the *DF* diagram on a solvent free basis for both solvent candidates. In this case, *n*–decyl acetate is selected as the extractive agent since it is immiscible with water and can promote a higher *DF* than *n*–butyl acetate, as shown in Figure 4.20. Nevertheless, criteria such as price and/or toxicity must be taken into account when making the final selection.

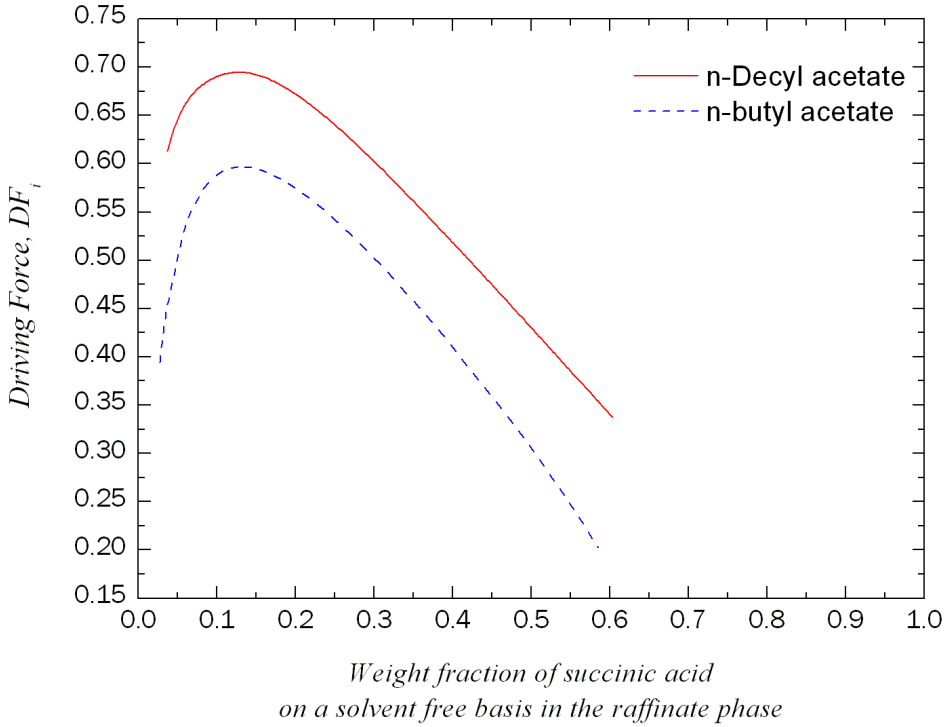

Figure 4.20 – *DF* diagram for the ternary system succinic acid/water/solvent on a solvent free basis.

From the *DF* diagram in Figure 4.20, a target *DF* of 0.7 is selected, which corresponds to a value of *fs* equal to 0.0374. From the mass balance equation (8.21) in Appendix, it is calculated that the solvent flowrate corresponds to 26.6 *kmole*/*h*. From the specifications of the liquid–liquid extraction solvent based separation *PG* (see Appendix), the recovery of the component to be extracted (succinic acid) is assumed to be equal to or greater than 99.5%, in addition the conditions of operation are room temperature (298.15 *K*) and 1 atm. The addition of solvent to the SA/water mixture causes the separation of water from the mixture obtaining a mixture of SA/solvent from which SA is obtained as precipitate. Afterwards, the recovery of SA from the mixture SA/solvent can be performed by filtration. This has been verified through the solid–liquid phase diagram for the system SA/*n*–decyl acetate, depicted in Figure 4.21.

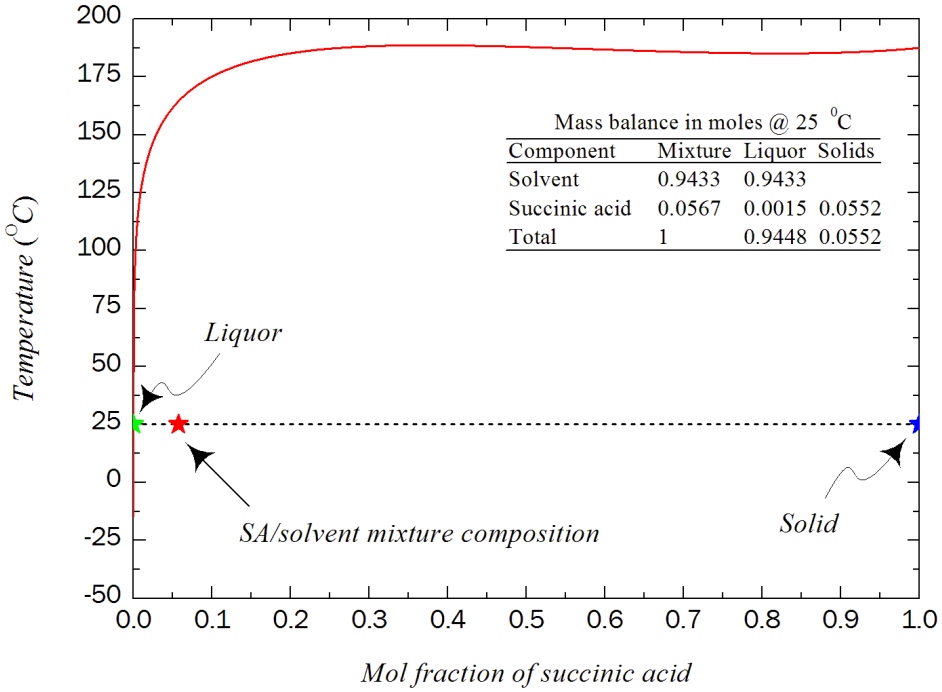

Figure 4.21 – Solid–liquid phase diagram for the binary system succinic acid/*n*–decyl acetate.

As shown on the diagram of Figure 4.21, at 25 °*C* the liquid phase (liquor) contains 0.158 % mole and the solid phase 100 % mole of SA. Once the solvent flowrate has been determined to reach the target *DF*, the remaining task is to determine the number of equilibrium stages for the liquid–liquid extraction solvent based separation *PG*. This is performed by means of the diagram *X* ($kg_{solute}/kg_{carrier}$) versus *Y* ($kg_{solute}/kg_{solvent}$). The *XY* diagram can be constructed based on experimental liquid–liquid equilibrium data or through a thermodynamic model. In this case the original UNIFAC *LLE* model with the corresponding parameters has been used. From Figure 4.22 it is clear that four equilibrium stages are required to achieve the target *DF* of 0.7. At this point, all the necessary information such as design parameters, conditions of operation, mass balance, are available to perform a rigorous simulation.

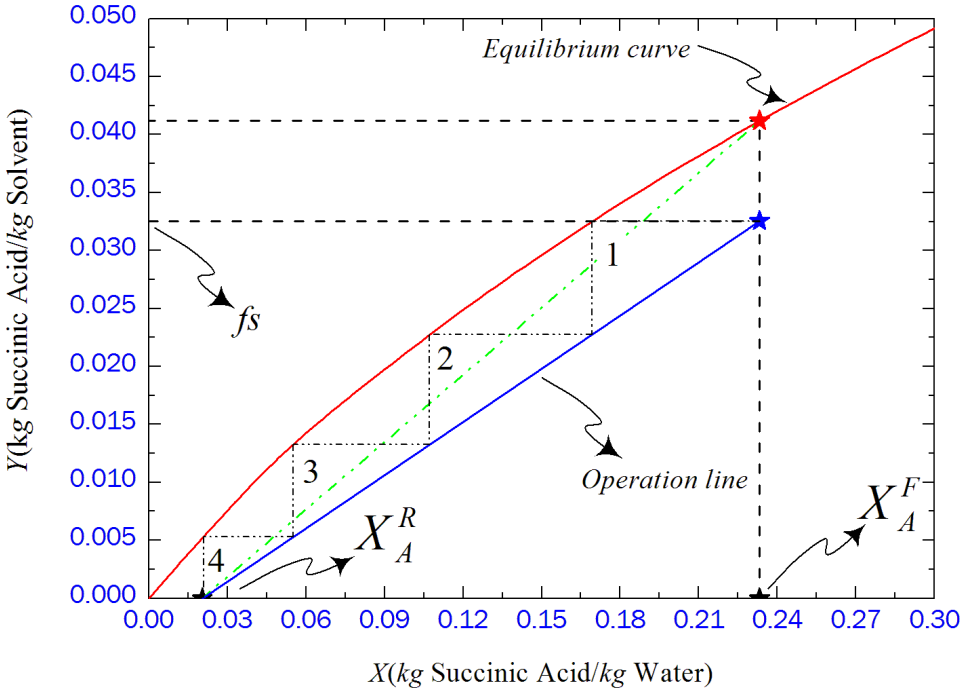

Figure 4.22 – Graphical determination of the number of equilibrium stages for the liquid–liquid extraction based separation *PG*.

Rank 15 – Distillation

Mass balance

The mass balance results for the process flowsheet in Figure 4.18 are given in Table 4.30.

Table 4.30 – Mass balance results for the downstream separation.

Stream	S_1	S_2	S_3	S_4	S_5	S_6	S_7
Phase	Mixed	Mixed	Solid	Liquid	Vapor	Liquid	Liquid
T (*°C*)	38.49	39.00	39.00	39.00	100	100	100
P (*atm*)	1.00	1.00	1.00	1.00	1.00	1.00	1.00
F (*kmole*/*h*)	127.8127	127.7664	2.4742	125.2922	83.8170	41.3877	36.3632
Mole fraction							
A	0.012621	0.002397		0.002444	0.002699		
B		0.000100		0.000102	0.000131		
C	0.012620						0
D	0.000400						
E	0.938630	0.952399		0.971206	0.995328	0.924264	0.998600
F						0.000000	
G	0.000994	0.001272		0.001297	0.000965	0.001972	0.000943
H	0.000064	0.000064		0.000066	0.000075	0.000048	0.000052
I		0.002397		0.002444	0.000760	0.005860	0.000375
J	0.000046	0.000046		0.000047	0.000038	0.000065	0.000041
K		0.012629		0.012878	0.000003	0.038979	
L	0.017263	0.009331		0.009516		0.028806	
M	0.017360	0.019365	1.000000				

Continued on next page

Stream	S_8	S_9	S_{10}
Phase	Liquid	Liquid	Solid
T ($°C$)	100.00	25	25
P (atm)	1.00	1.00	1.00
F ($kmole/h$)	5.0246	3.4112	1.6134
Mole fraction			
A			
B			
C			
D			
E	0.386400	0.569047	
F			
G	0.009487	0.013972	
H			
I	0.045600	0.067155	
J	0.000243	0.000359	
K	0.321100		1.000000
L	0.237299	0.349467	
M			

Reverse simulation of the distillation process–group

In order to provide an energy efficient distillation column as well as a near−optimum design, the design parameters for the distillation column are back−calculated based on the *DF* method described in section 2.3.4. Based on the output specification and on the maximum *DF* for the binary pair furfural/pyruvic acid (as shown in Figure 4.16), the results from the reverse simulation for the distillation column is given in Table 4.31

Table 4.31 − Design parameters for the distillation column.

Design parameter	*Value*
Number of stages	20
Feed stage location	9
Purity light key (furfural)	–
Recovery light key (furfural)	> 0.995
Purity heavy key (pyruvic acid)	–
Recovery heavy key (pyruvic acid)	> 0.995
Reflux ratio	0.10
DF_{max}	0.60

According to the *DF* diagram in Figure 4.16, the top product contains water and furfural with some traces of acetic acid, pyruvic acid. Besides of the heavier compounds which are soluble sugars, HMF, and succinic acid, the bottom product contains water, pyruvic acid, and traces of acetic acid, that need to be removed. In the case of HMF its vapor pressure at 368.1 *K* (94.95 °*C*) has been determined experimentally (Verevkin *et al.*[93]) to be equal to 40.04 *Pa* (0.000394 *atm*). Therefore, it is reasonable to assume a recovery for HMF in the bottom productof equal to or greater than 99.5%.

4.3.1.7 Step 7–Final Verification

The process flowsheets depicted in Figures 4.17–4.18 have been validated by rigorous simulation using the PROII® simulator (PROII[77]). Tables 4.32–4.33 provided the detailed mass balance for each design process flowsheet. The conditions of operation for the crystallization process have been verified trough the solid−liquid phase diagram. The input stream is the bottom stream from the distillation column whose temperature is equal to 130.24 °*C*. Therefore, in order to obtain a succinic acid recovery of more than 99.5 %, it is necessary to cool by as much as 25 °*C* as shown in Figure 4.23.

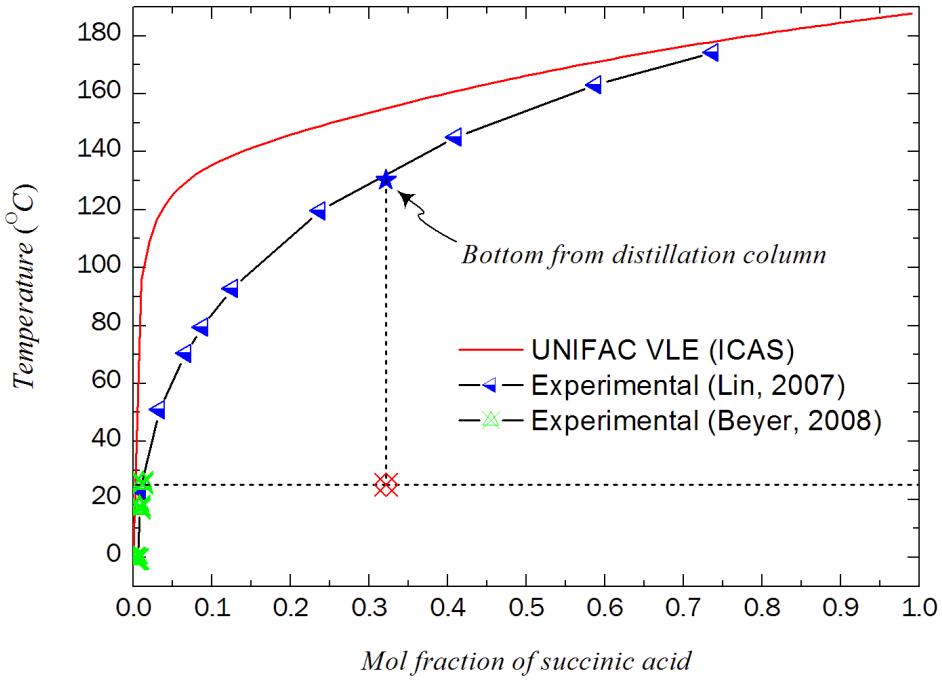

Figure 4.23 – Solid–liquid phase diagram for the binary system succinic acid/water(Lin *et al.*[65]; Beyer[9]).

Table 4.32 – Mass balance results from rigorous simulation (rank 13).

Stream	S_1	S_2	S_3	S_4	S_5	S_6
Phase	Mixed	Mixed	Solid	Liquid	Vapor	Liquid
T (*°C*)	38.49	39.00	39.00	39.00	101.45	101.45
P (*atm*)	1.00	1.00	1.00	1.00	1.00	1.00
F (*kmole*/*h*)	127.8127	127.7664	2.4742	125.2922	83.8170	41.3877
Mole fraction						
A	0.012621	0.002397		0.002444	0.002699	
B		0.000100		0.000102	0.000131	
C	0.012620					
D	0.000400					
E	0.938630	0.952399		0.971206	0.995328	0.924264
F						0.000000
G	0.000994	0.001272		0.001297	0.000965	0.001972
H	0.000064	0.000064		0.000066	0.000075	0.000048
I		0.002397		0.002444	0.000760	0.005860
J	0.000046	0.000046		0.000047	0.000038	0.000065
K		0.012629		0.012878	0.000003	0.038979
L	0.017263	0.009331		0.009516		0.028806
M	0.017360	0.019365	1.000000			

Table 4.33 – Mass balance results from rigorous simulation (rank 15).

Stream	S_1	S_2	S_3	S_4	S_5	S_6	S_7
Phase	Mixed	Mixed	Solid	Liquid	Vapor	Liquid	Liquid
T (*°C*)	38.49	39.00	39.00	39.00	101.45	101.45	99.92
P (*atm*)	1.00	1.00	1.00	1.00	1.00	1.00	1.00
F (*kmole*/*h*)	127.8127	127.7664	2.4742	125.2922	83.8170	41.3877	36.3632
Mole fraction							
A	0.012621	0.002397		0.002444	0.002699		
B		0.000100		0.000102	0.000131		
C	0.012620						0
D	0.000400						
E	0.938630	0.952399		0.971206	0.995328	0.924264	0.998600
F						0.000000	
G	0.000994	0.001272		0.001297	0.000965	0.001972	0.000943
H	0.000064	0.000064		0.000066	0.000075	0.000048	0.000052
I		0.002397		0.002444	0.000760	0.005860	0.000375
J	0.000046	0.000046		0.000047	0.000038	0.000065	0.000041
K		0.012629		0.012878	0.000003	0.038979	
L	0.017263	0.009331		0.009516		0.028806	
M	0.017360	0.019365	1.000000				

Continued on next page

Stream	S_8	S_9	S_{10}
Phase	Liquid	Liquid	Solid
T ($°C$)	130.24	25	25
P (atm)	1.00	1.00	1.00
F ($kmole/h$)	5.0246	3.4112	1.6134
Mole fraction			
A			
B			
C			
D			
E	0.386400	0.569047	
F			
G	0.009487	0.013972	
H			
I	0.045600	0.067155	
J	0.000243	0.000359	
K	0.321100		1.000000
L	0.237299	0.349467	
M			

4.3.2 Discussion

It has been demonstrated through the succinic acid production process, how the *PGC* methodology is able to generate completely new process flowsheets. The generation of a novel process flowsheet relies on the availability of process–groups representing novel process unit operations. For instance, other interesting potential options using liquid–liquid based separation process–groups involve ionic liquids as extractant agents. Nevertheless, this option relies on either the possibility of finding ionic liquids matching the solubility target, or through a CAMD technique to design those candidates matching the target. In the same way, the crystallization process–group can be initialized with ionic liquids to be used in the generation of flowsheet structures. Therefore, the application range of the process–groups to be used in the generation of flowsheet structures can be extended as long as the components involved in the separation task fulfill the property dependence requirements of the corresponding process–group.

4.4 Diethyl Succinate Production Process

Biobased chemical production is a growing multibillion dollar industry converting renewable resources into valuable products. A $15 billion market could be based on succinate for producing bulk chemicals such as 1,4–butanediol (a precursor to "stronger–than–steel" plastics), ethylenediamine disuccinate (a biodegradable chelator), adipic acid (nylon precursor), and diethyl succinate (a green solvent for replacement of methylene chloride, solvent for cleaning metal or for paint stripping) (Zeikus *et al.*[100]).

Some of the methylene chloride usages are listed below:

- Methylene chloride is predominantly used as a solvent in paint strippers and removers; as a process solvent in the manufacture of pharmaceuticals, and film coatings; as a metal cleaning and finishing solvent in electronics manufacturing; and as an agent in urethane foam blowing.
- Methylene chloride is also used as a propellant in aerosols for products such as paints, automotive products, and insect sprays.
- It is used as an extraction solvent for spice oleoresins, hops, and for the removal of caffeine from coffee. However, due to concern over residual solvent, most decaffeinators no longer use methylene chloride.
- Methylene chloride is also approved for use as a postharvest fumigant for grains and strawberries and as a degreening agent for citrus fruit.

Therefore, diethyl succinate (DES) has the enormous potential to be used as a suitable replacement for methylene chloride applications. Recently, Gani *et al.*[27] addressed the design problem of a replacement solvent for methylene chloride in a reactive system. Methylene chloride properties were used as benchmark by Gani *et al.*[27]. The replacement solvent should match the performance and properties of methylene chloride but should have more favourable environmental, health, and safety properties. Based on these guidelines, Gani *et al.*[27] specified the following solvent target properties: $180 < T_m(K) < 260$, $260 < T_b(K) < 410$, $17 < SP(MP^{1/2}) < 25$, $0.5 < logK_{OW} < 4$. The potential solvent candidate should be partially miscible with water and be neutral with respect to reaction chemicals. The following solvents matching the constraints above were identified by Gani *et al.*[27]: ethyl acetate, isopropyl acetate, ethyl propionate, toluene, and methylcyclopentane. Table 4.34 lists the target physical properties of methylene chloride and the ones for DES.

Table 4.34 – Physical properties of DCM and DES.

Property	DCM	DES
$T_b(K)$	**312.75**	489.65
$T_m(K)$	**178.25**	252.35
$SP(MP^{1/2})$	**20.37**	19.4185
$logK_{OW}$		1.26

From Table 4.34 it can be cocluded that DES could also be considered as a potential candidate for replacement of methylene chloride for the reactive system studied by Gani *et al.*[27]. In addition to the potential applications of diethyl succinate mentioned above, succinate esters are excellent fuel oxygenates. For instance, incorporation of diethyl succinate in diesel results in a reduction in particulate emissions depending on the grade of the fuel. The diethyl succinate is fully miscible with diesel and requires no co–solvents or additional additives.

Process description

A conventional process for diethyl succinate production involves a stirred batch or continuous reactor with sulfuric acid as a homogeneous catalyst. Because the extent of reaction is thermodynamically limited, intermediate product removal and multiple reaction stages are required to achieve complete succinic acid conversion. Many of the difficulties when using homogeneous catalysts can be eliminated through the use of heterogeneous catalysts such as ion exchange resins or supported clays. The heterogeneous catalyst allows easy mechanical separation of the catalyst from the reaction media by decantation or filtration, reduces or eliminates corrosion problems, and facilitates continuous process operation (Kolah *et al.*[56]).

Another option is the use of reactors coupled with a membrane–based separation, such as pervaporation, to enhance the conversion of reactants for thermodynamically or kinetically limited reactions via selective removal of one or more species from the reaction mixture. Benedict *et al.*[8] proposed a reaction pervaporation–system to carry out esterification of lactic acid and succinic acid with ethanol to produce ethyl lactate and diethyl succinate. The efficiency of the reaction pervaporation–system is tested by attainment of near total utilization of the stoichiometrically limiting reactant within a reasonable time by stripping water, a reaction product. Protocols for recovery of ethyl lactate and diethyl succinate from pervaporation retentate are discussed by the authors Benedict *et al*[8].

4.4.1 PGC Methodology Application

4.4.1.1 Step 1 –Synthesis Problem Definition

Given the raw materials, determine a physically feasible process flowsheet for the production of diethyl succinate (DES). Diethyl succinate is produced by an esterification reaction between ethanol and succinic acid, producing water as a by–product. The product specification is the minimum acceptable product purity, for example ≥ 99.5 % *wt*. The flowsheet specification is the energy consumption of the process, and the design objective (target) is to minimize this value.

4.4.1.2 Step 2 –Synthesis Problem Analysis

As the objective is to produce diethyl succinate, a search is performed in the open literature and/or databases to investigate the chemical reactions yielding the desired product. The chemical reactions below taking place in the reactor have been taken from Kolah *et al.*[56] and they described the pathways involved in the esterification of succinic acid with ethanol. The reaction information also contains the kinetic parameters. As diethyl succinate is produced from succinic acid via the intermediate formation of monoethyl succinate, this component has to be taken into account for the pure component/mixture analysis.

$$\mathrm{SA} + \mathrm{EtOH} \underset{k_1/K_{eq_{x,1}}}{\overset{k_1}{\rightleftharpoons}} \mathrm{MES} + \mathrm{W} \tag{4.1}$$

$$\mathrm{MES} + \mathrm{EtOH} \underset{k_2/K_{eq_{x,2}}}{\overset{k_2}{\rightleftharpoons}} \mathrm{DES} + \mathrm{W} \tag{4.2}$$

According to the reaction analysis the components involved in the synthesis problem are listed in Table 4.35.

Table 4.35 – Compounds involved in the synthesis problem.

Label	Compound
A	Ethanol
B	Water
C	Diethyl succinate (DES)
D	Monoethyl succinate (MES)
E	Succinic acid (SA)

Table 4.36 shows the ratios of pure component properties involved in the synthesis problem.

Table 4.36 – Pure component property ratios along with the separation techniques.

Property	Split	Ratio	Separation technique (Jaksland[48,49])
T_m	Water/SA DES/SA	1.69(>1.27) 1.83(>1.27)	*Crystallization*
R_g	Ethanol/Water	3.67(>1.03)	*Liquid membrane*
V_M	Ethanol/Water SA/Ethanol MES/Water MES/EtOH	3.24(>1.08) 1.66(>1.08) 7.52(>1.08) 2.32(>1.08)	*Liquid membrane* *Pervaporation*
SP	Water/Ethanol Water/SA MES/Water	1.83(>1.28) 1.63(>1.28) 2.23(>1.28)	*Liquid membrane* *Pervaporation*
VP	Water/DES EtOH/DES	388(>15) 970(>15)	*Distillation,* *Flash operation*

From the analysis of the mixture, *flash/evaporation*, *distillation*, *liquid membrane*, and *pervaporation*, have been identified to be feasible separation techniques to perform the separation of water and ethanol from the other components in the synthesis problem. *Crystallization* has been identified to be a feasible separation technique to perform the separation of succinic acid from DES and MES.

The mixture analysis reveals the existence of two binary azeotropes listed in Table 4.37. Therefore, *azeotropic distillation*, *extractive distillation*, and *liquid–liquid extraction* might also be potential separation techniques to be considered in the synthesis problem.

Table 4.37 – Composition of the azeotropes in the process at 1 *atm*.

Binary pair	$T(K)$	x_1	
Water(1)/Ethanol(2)	352.50	0.1372	Min. Boil.
Water(1)/DES(2)	371.65	0.9478	Min. Boil.

4.4.1.3 Step 3–Process–Group Selection

From the synthesis problem analysis, the stoichiometry of the reaction together with the kinetic parameters is known. The reactor is represented with a kinetic model based reactor process–group. The inlet stream of the process–group is a mixture of ethanol, succinic acid, and catalyst; and the outlet stream is a mixture of non–reacted ethanol and succinic acid, as well as methyl succinate, diethyl succinate, and water together with the catalyst.

The same analysis for the downstream separation is performed as in the previous case studies to select the *PG*s matching the separation techniques identified in step 2. As the separation techniques identified in step 2 are *flash*, *distillation*, *pervaporation*, *liquid membrane*, *crystallization*, *PG*s representing these separation techniques are selected from the *PG* database (see Table 2.1). Table 4.38 lists the final selection of the *PG*s to be used in the generation of flowsheet structures

Table 4.38 – Final selection of the *PG*'s in the synthesis problem.

Kinetic model based reactor
5 (*rAEpABCDE*)
Flash separation
5 (*fAB/CDE*)
4 (*fA/CDE*), (*fAB/CD*)
3 (*fB/CD*) (*fA/CD*)
2 (*fB/C*)
Distillation
5 (*AB/CDE*)
4 (*A/CDE*) (*AB/CD*)
3 (*B/CD*) (*A/CD*)
2 (*B/C*)
Pervaporation & liquid membrane
5 (*pervCDEA/B*) (*lmemCDEA/B*)
4 (*pervCDE/A*) (*lmemCDE/A*) (*pervCDA/B*) (*lmemCDA/B*)
3 (*pervCD/E*) (*lmemCD/E*) (*pervCD/B*) (*lmemCD/B*) (*pervCD/A*) (*lmemCD/A*)
2 (*pervC/D*) (*lmemC/D*) (*pervC/B*) (*lmemC/B*) (*pervC/E*) (*lmemC/E*)
Crystallization
5 (*crsE/DBCA*)
4 (*crsE/DCA*), (*crsA/DBC/A*)
3 (*crsED/C*) (*crsDC/A*)
2 (*crsE/C*)

4.4.1.4 Step 4 –Generation of Flowsheet Candidates

Given the SA and ethanol raw materials to be converted into DES and by–products, using 5 separation techniques and a reactor process–group represented by 37 process–groups, these structures are ranked using the minimum energy consumption criterion, 40 feasible flowsheet structures are generated.

4.4.1.5 Step 5 –Ranking/Selection of Flowsheet Candidates

Table 4.39 provides the list of 40 generated easible flowsheet structures using the **SFILES** notation (d'Anterroches[15,16]).

Table 4.39 – Flowsheet structures of interest in the synthesis problem.

Rank	Alternative **SFILES** string	*Ex* (*MkJ/h/kmole*)
1	(iAE)(rAE/pABCDE)(fAB/CDE)**[**(crsE/DC)[(oE)](oDC)**]**(oAB)	0.090842
2	(iAE)(rAE/pABCDE)(fAB/CDE)**[**(lmemE/DC)[(oE)](oDC)**]**(oAB)	0.090842
3	(iAE)(rAE/pABCDE)(fAB/CDE)**[**(pervE/DC)[(oE)](oDC)**]**(oAB)	0.090842
4	(iAE)(rAE/pABCDE)(AB/CDE)**[**(crsE/DC)[(oE)](oDC)**]**(oAB)	0.090842
5	(iAE)(rAE/pABCDE)(AB/CDE)**[**(lmemE/DC)[(oE)](oDC)**]**(oAB)	0.090842
6	(iAE)(rAE/pABCDE)(AB/CDE)**[**(pervE/DC)[(oE)](oDC)**]**(oAB)	0.090842
7	(iAE)(rAE/pABCDE)(pervCDEA/B)**[**(fA/CDE)**[**(crsE/DC)[(oE)](lmemC/D)[(oC)](oD)**]**(oA)**]**(oB)	0.050955
8	(iAE)(rAE/pABCDE)(pervCDEA/B)**[**(fA/CDE)**[**(crsE/DC)[(oE)](pervC/D)[(oC)](oD)**]**(oA)**]**(oB)	0.050955
9	(iAE)(rAE/pABCDE)(pervCDEA/B)**[**(fA/CDE)**[**(lmemCD/E)[(oE)](lmemC/D)[(oC)](oD)**]**(oA)**]**(oB)	0.050955
10	(iAE)(rAE/pABCDE)(pervCDEA/B)**[**(fA/CDE)**[**(lmemCD/E)[(oE)](pervC/D)[(oC)](oD)**]**(oA)**]**(oB)	0.050955
11	(iAE)(rAE/pABCDE)(pervCDEA/B)**[**(fA/CDE)**[**(pervCD/E)[(oE)](lmemC/D)[(oC)](oD)**]**(oA)**]**(oB)	0.050955
12	(iAE)(rAE/pABCDE)(pervCDEA/B)**[**(fA/CDE)**[**(pervCD/E)[(oE)](pervC/D)[(oC)](oD)**]**(oA)**]**(oB)	0.050955
13	(iAE)(rAE/pABCDE)(pervCDEA/B)**[**(lmemCDE/A)**[**(crsE/DC)[(oE)](lmemC/D)[(oC)](oD)**]**(oA)**]**(oB)	–
14	(iAE)(rAE/pABCDE)(pervCDEA/B)**[**(lmemCDE/A)**[**(crsE/DC)[(oE)](pervC/D)[(oC)](oD)**]**(oA)**]**(oB)	–
15	(iAE)(rAE/pABCDE)(pervCDEA/B)**[**(lmemCDE/A)**[**(lmemCD/E)[(oE)](lmemC/D)[(oC)](oD)**]**(oA)**]**(oB)	–
16	(iAE)(rAE/pABCDE)(pervCDEA/B)**[**(lmemCDE/A)**[**(lmemCD/E)[(oE)](pervC/D)[(oC)](oD)**]**(oA)**]**(oB)	–
17	(iAE)(rAE/pABCDE)(pervCDEA/B)**[**(lmemCDE/A)**[**(pervCD/E)[(oE)](lmemC/D)[(oC)](oD)**]**(oA)**]**(oB)	–
18	(iAE)(rAE/pABCDE)(pervCDEA/B)**[**(lmemCDE/A)**[**(pervCD/E)[(oE)](pervC/D)[(oC)](oD)**]**(oA)**]**(oB)	–
19	(iAE)(rAE/pABCDE)(pervCDEA/B)**[**(pervCDE/A)**[**(crsE/DC)[(oE)](lmemC/D)[(oC)](oD)**]**(oA)**]**(oB)	–
20	(iAE)(rAE/pABCDE)(pervCDEA/B)**[**(pervCDE/A)**[**(crsE/DC)[(oE)](pervC/D)[(oC)](oD)**]**(oA)**]**(oB)	–

Continued on the next page

Rank	Alternative **SFILES** string	*Ex* (*MkJ/h/kmole*)
21	(iAE)(rAE/pABCDE)(pervCDEA/B)**[**(pervCDE/A)**[**(lmemCD/E)[(oE)](lmemC/D)[(oC)](oD)**]**(oA)**]**(oB)	–
22	(iAE)(rAE/pABCDE)(pervCDEA/B)**[**(pervCDE/A)**[**(lmemCD/E)[(oE)](pervC/D)[(oC)](oD)**]**(oA)**]**(oB)	–
23	(iAE)(rAE/pABCDE)(pervCDEA/B)**[**(pervCDE/A)**[**(pervCD/E)[(oE)](lmemC/D)[(oC)](oD)**]**(oA)**]**(oB)	–
24	(iAE)(rAE/pABCDE)(pervCDEA/B)**[**(pervCDE/A)**[**(pervCD/E)[(oE)](pervC/D)[(oC)](oD)**]**(oA)**]**(oB)	–
25	(iAE)(rAE/pABCDE)(pervCDEA/B)**[**(crsE/DCA)**[**(A/CD)[(oA)](lmemC/D)[(oC)](oD)**]**(oE)**]**(oB)	0.064713
26	(iAE)(rAE/pABCDE)(pervCDEA/B)**[**(crsE/DCA)**[**(A/CD)[(oA)](pervC/D)[(oC)](oD)**]**(oE)**]**(oB)	0.064713
27	(iAE)(rAE/pABCDE)(pervCDEA/B)**[**(crsE/DCA)**[**(fA/CD)[(oA)](lmemC/D)[(oC)](oD)**]**(oE)**]**(oB)	0.064713
28	(iAE)(rAE/pABCDE)(pervCDEA/B)**[**(crsE/DCA)**[**(fA/CD)[(oA)](pervC/D)[(oC)](oD)**]**(oE)**]**(oB)	0.064713
29	(iAE)(rAE/pABCDE)(pervCDEA/B)**[**(crsE/DCA)**[**(lmemCD/A)[(oA)](lmemC/D)[(oC)](oD)**]**(oE)**]**(oB)	–
30	(iAE)(rAE/pABCDE)(pervCDEA/B)**[**(crsE/DCA)**[**(lmemCD/A)[(oA)](pervC/D)[(oC)](oD)**]**(oE)**]**(oB)	–
31	(iAE)(rAE/pABCDE)(pervCDEA/B)**[**(crsE/DCA)**[**(pervCD/A)[(oA)](pervC/D)[(oC)](oD)**]**(oE)**]**(oB)	–
32	(iAE)(rAE/pABCDE)(pervCDEA/B)**[**(crsE/DCA)**[**(pervCD/A)[(oA)](pervC/D)[(oC)](oD)**]**(oE)**]**(oB)	–
33	(iAE)(rAE/pABCDE)(pervCDEA/B)**[**(crsE/DCA)**[**(crsDC/A)[(oA)](pervC/D)[(oC)](oD)**]**(oE)**]**(oB)	–
34	(iAE)(rAE/pABCDE)(pervCDEA/B)**[**(crsE/DCA)**[**(crsDC/A)[(oA)](pervC/D)[(oC)](oD)**]**(oE)**]**(oB)	–
35	(iAE)(rAE/pABCDE)(pervCDEA/B)**[**(A/CDE)**[**(crsE/DC)[(oE)](lmemC/D)[(oC)](oD)**]**(oA)**]**(oB)	0.050955
36	(iAE)(rAE/pABCDE)(pervCDEA/B)**[**(A/CDE)**[**(crsE/DC)[(oE)](pervC/D)[(oC)](oD)**]**(oA)**]**(oB)	0.050955
37	(iAE)(rAE/pABCDE)(pervCDEA/B)**[**(A/CDE)**[**(lmemCD/E)[(oE)](lmemC/D)[(oC)](oD)**]**(oA)**]**(oB)	0.050955
38	(iAE)(rAE/pABCDE)(pervCDEA/B)**[**(A/CDE)**[**(lmemCD/E)[(oE)](pervC/D)[(oC)](oD)**]**(oA)**]**(oB)	0.050955
39	(iAE)(rAE/pABCDE)(pervCDEA/B)**[**(A/CDE)**[**(pervCD/E)[(oE)](lmemC/D)[(oC)](oD)**]**(oA)**]**(oB)	0.050955
40	(iAE)(rAE/pABCDE)(pervCDEA/B)**[**(A/CDE)**[**(pervCD/E)[(oE)](pervC/D)[(oC)](oD)**]**(oA)**]**(oB)	0.050955

It should be noted that the flowsheet structures 1–6, 7–12, 25–28, and 35–40 have the same energy consumption index, respectively. This is explained by the fact that the energy index is only calculated for the ordinary distillation and flash separation process–groups, while the other *PGs* do not contribute to the energy consumption. It should be noted also that the comparison of flowsheet structures using different types of process–groups as it is the case for the flowsheet structures 13–24 and 29–34, is limited by the availability of the energy consumption index property models. The flowsheet structure 35 is selected for reverse simulation.

(iAE)(rAE/pABCDE)(pervCDEA/B)**[**(A/CDE)**[**(crsE/DC)[(oE)](lmemC/D)[(oC)](oD)**]**(oA)**]**(oB)

Figure 4.24 depicts the representation of the selected flowsheet structure by means of the corresponding process–groups.

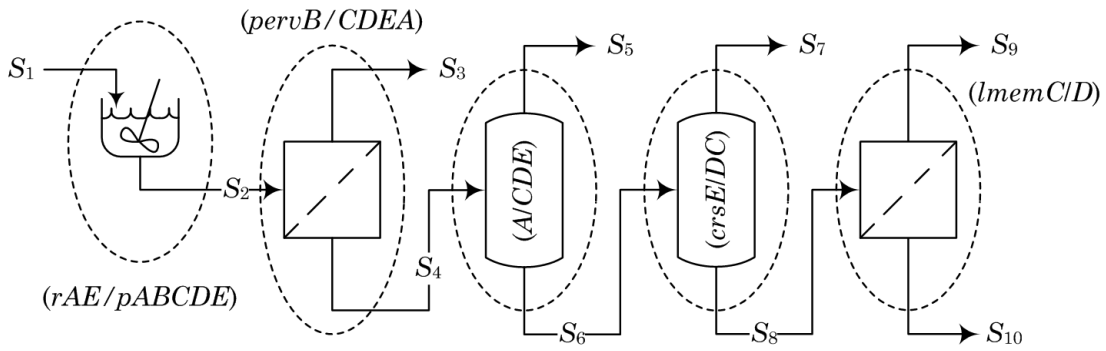

Figure 4.24 – Process flowsheet for the DES production process (Rank 35).

4.4.1.6 Step 6 –Reverse Simulation

Since the flowsheet structure of the diethyl succinate production is now available (Figure 4.24), the next steps are the resolution of the mass balance between the process–groups and the reverse simulation, *i.e.* the determination of the design parameters of the unit operations. In this case study, the reverse simulation procedure of the kinetic based reactor process–group is highlighted. The mass balance is performed through each process–group in the process flowsheet structure. Operating conditions such as, pressure and temperature of the output streams are given by the process–group specifications. In the case of the kinetic based reactor process–group, the mass balance calculations rely on the availability of the attainable region diagram. In the following sections, the analysis by means of the attainable region concept for the set of esterification reactions (eqs. 4.1–4.2) is presented following the procedure outlined in chapter 2, section 2.3.4. The mass balance for the process flowsheet structure in Figure 4.24 is presented followed by the reverse simulation of the kinetic based reactor process–group.

Attainable Region Analysis

The initial characteristics of the reaction network given by eqs. 4.1–4.2 are provided in Table 4.40.

Table 4.40 – Parameters for resin–catalyzed succinic acid esterification with ethanol.

Parameter	Value	Units
k_1^0	5.3E07	$kg_{soln}/kg_{cat}s$
k_2^0	8.0E07	$kg_{soln}/kg_{cat}s$
$E_{A,1}$	66000	$kJ/kmole$
$E_{A,2}$	70000	$kJ/kmole$
$K_{eq_x,1}$	5.3	
$K_{eq_x,2}$	1.2	

The rate of formation of each species in the reaction mixture has been taken from Kolah *et al.*[56]. In this particular example the fundamental processes are reaction and mixing. As mentioned in Chapter 2, there are two limits on mixing in a reactor: a plug flow reactor (PFR) in which a slug of fluid does not undergo any axial mixing along the reactor length, and a continuously stirred tank reactor (CSTR), in which each volume element undergoes complete mixing.

The mass balance equations for the PFR are:

$$\frac{dC_{SA}}{d\tau} = -w_{cat}k_1\eta_1\left(\frac{MW_{soln}}{\rho_{soln}}\right)\left(C_{SA}C_{EtOH} - \frac{C_{MES}C_W}{K_{eq_x,1}}\right) \tag{4.3}$$

$$\frac{dC_{MES}}{d\tau} = -w_{cat}k_2\eta_2\left(\frac{MW_{soln}}{\rho_{soln}}\right)\left(C_{MES}C_{EtOH} - \frac{C_{DES}C_W}{K_{eq_x,2}}\right) - w_{cat}k_1\eta_1\left(\frac{MW_{soln}}{\rho_{soln}}\right)\left(\frac{C_{MES}C_W}{K_{eq_x,1}} - C_{SA}C_{EtOH}\right) \tag{4.4}$$

$$\frac{dC_{DES}}{d\tau} = -w_{cat}k_2\eta_2\left(\frac{MW_{soln}}{\rho_{soln}}\right)\left(\frac{C_{DES}C_W}{K_{eq_x,2}} - C_{MES}C_{EtOH}\right) \tag{4.5}$$

$$\frac{dC_{\mathrm{EtOH}}}{d\tau} = -w_{\mathrm{cat}} k_1 \eta_1 \left(\frac{MW_{\mathrm{soln}}}{\rho_{\mathrm{soln}}} \right) \left(C_{\mathrm{SA}} C_{\mathrm{EtOH}} - \frac{C_{\mathrm{MES}} C_{\mathrm{W}}}{K_{\mathrm{eq}_x,1}} \right) - w_{\mathrm{cat}} k_2 \eta_2 \left(\frac{MW_{\mathrm{soln}}}{\rho_{\mathrm{soln}}} \right) \left(C_{\mathrm{MES}} C_{\mathrm{EtOH}} - \frac{C_{\mathrm{DES}} C_{\mathrm{W}}}{K_{\mathrm{eq}_x,2}} \right) \tag{4.6}$$

$$\frac{dC_{\mathrm{W}}}{d\tau} = -w_{\mathrm{cat}} k_1 \eta_1 \left(\frac{MW_{\mathrm{soln}}}{\rho_{\mathrm{soln}}} \right) \left(\frac{C_{\mathrm{MES}} C_{\mathrm{W}}}{K_{\mathrm{eq}_x,1}} - C_{\mathrm{SA}} C_{\mathrm{EtOH}} \right) - w_{\mathrm{cat}} k_2 \eta_2 \left(\frac{MW_{\mathrm{soln}}}{\rho_{\mathrm{soln}}} \right) \left(\frac{C_{\mathrm{DES}} C_{\mathrm{W}}}{K_{\mathrm{eq}_x,2}} - C_{\mathrm{MES}} C_{\mathrm{EtOH}} \right) \tag{4.7}$$

The mass balance equations for the CSTR are:

$$\frac{C^0_{\mathrm{SA}} - C_{\mathrm{SA}}}{\tau} = -w_{\mathrm{cat}} k_1 \eta_1 \left(\frac{MW_{\mathrm{soln}}}{\rho_{\mathrm{soln}}} \right) \left(C_{\mathrm{SA}} C_{\mathrm{EtOH}} - \frac{C_{\mathrm{MES}} C_{\mathrm{W}}}{K_{\mathrm{eq}_x,1}} \right) \tag{4.8}$$

$$\frac{C^0_{\mathrm{MES}} - C_{\mathrm{MES}}}{\tau} = -w_{\mathrm{cat}} k_2 \eta_2 \left(\frac{MW_{\mathrm{soln}}}{\rho_{\mathrm{soln}}} \right) \left(C_{\mathrm{MES}} C_{\mathrm{EtOH}} - \frac{C_{\mathrm{DES}} C_{\mathrm{W}}}{K_{\mathrm{eq}_x,2}} \right) - w_{\mathrm{cat}} k_1 \eta_1 \left(\frac{MW_{\mathrm{soln}}}{\rho_{\mathrm{soln}}} \right) \left(\frac{C_{\mathrm{MES}} C_{\mathrm{W}}}{K_{\mathrm{eq}_x,1}} - C_{\mathrm{SA}} C_{\mathrm{EtOH}} \right) \tag{4.9}$$

$$\frac{C^0_{\mathrm{DES}} - C_{\mathrm{DES}}}{\tau} = w_{\mathrm{cat}} k_2 \eta_2 \left(\frac{MW_{\mathrm{soln}}}{\rho_{\mathrm{soln}}} \right) \left(\frac{C_{\mathrm{DES}} C_{\mathrm{W}}}{K_{\mathrm{eq}_x,2}} - C_{\mathrm{MES}} C_{\mathrm{EtOH}} \right) \tag{4.10}$$

$$\frac{C^0_{\mathrm{EtOH}} - C_{\mathrm{EtOH}}}{\tau} = -w_{\mathrm{cat}} k_1 \eta_1 \left(\frac{MW_{\mathrm{soln}}}{\rho_{\mathrm{soln}}} \right) \left(C_{\mathrm{SA}} C_{\mathrm{EtOH}} - \frac{C_{\mathrm{MES}} C_{\mathrm{W}}}{K_{\mathrm{eq}_x,1}} \right) - w_{\mathrm{cat}} k_2 \eta_2 \left(\frac{MW_{\mathrm{soln}}}{\rho_{\mathrm{soln}}} \right) \left(C_{\mathrm{MES}} C_{\mathrm{EtOH}} - \frac{C_{\mathrm{DES}} C_{\mathrm{W}}}{K_{\mathrm{eq}_x,2}} \right) \tag{4.11}$$

$$\frac{C_{\mathrm{W}}^{0}-C_{\mathrm{W}}}{\tau}=-w_{\mathrm{cat}}k_{1}\eta_{1}\left(\frac{MW_{\mathrm{soln}}}{\rho_{\mathrm{soln}}}\right)\left(\frac{C_{\mathrm{MES}}C_{\mathrm{W}}}{K_{\mathrm{eq}_{x},1}}-C_{\mathrm{SA}}C_{\mathrm{EtOH}}\right)- w_{\mathrm{cat}}k_{2}\eta_{2}\left(\frac{MW_{\mathrm{soln}}}{\rho_{\mathrm{soln}}}\right)\left(\frac{C_{\mathrm{DES}}C_{\mathrm{W}}}{K_{\mathrm{eq}_{x},2}}-C_{\mathrm{MES}}C_{\mathrm{EtOH}}\right) \tag{4.12}$$

C_{SA} and C_{DES} are selected as state variables. Firstly, C_{DES} is a state variable because it is this value that we wish to optimize. C_{SA} is a state variable due to it is the limiting reactant in this case, and τ is the independent variable (time). The following step is then the construction of the *AR*.

Constructing the Attainable Region

Step 1: Draw the PFR trajectory from the feed point. The trajectory of the reaction in the C_{SA}–C_{DES} space diagram of the PFR can be drawn by means of the following relation and it is depicted in Figure 4.25:

$$\frac{dC_{\mathrm{DES}}}{dC_{\mathrm{SA}}}=\frac{k_{2}\eta_{2}\left(\frac{C_{\mathrm{DES}}C_{\mathrm{W}}}{K_{\mathrm{eq}_{x},2}}-C_{\mathrm{MES}}C_{\mathrm{EtOH}}\right)}{k_{1}\eta_{1}\left(C_{\mathrm{SA}}C_{\mathrm{EtOH}}-\frac{C_{\mathrm{MES}}C_{\mathrm{W}}}{K_{\mathrm{eq}_{x},1}}\right)} \tag{4.13}$$

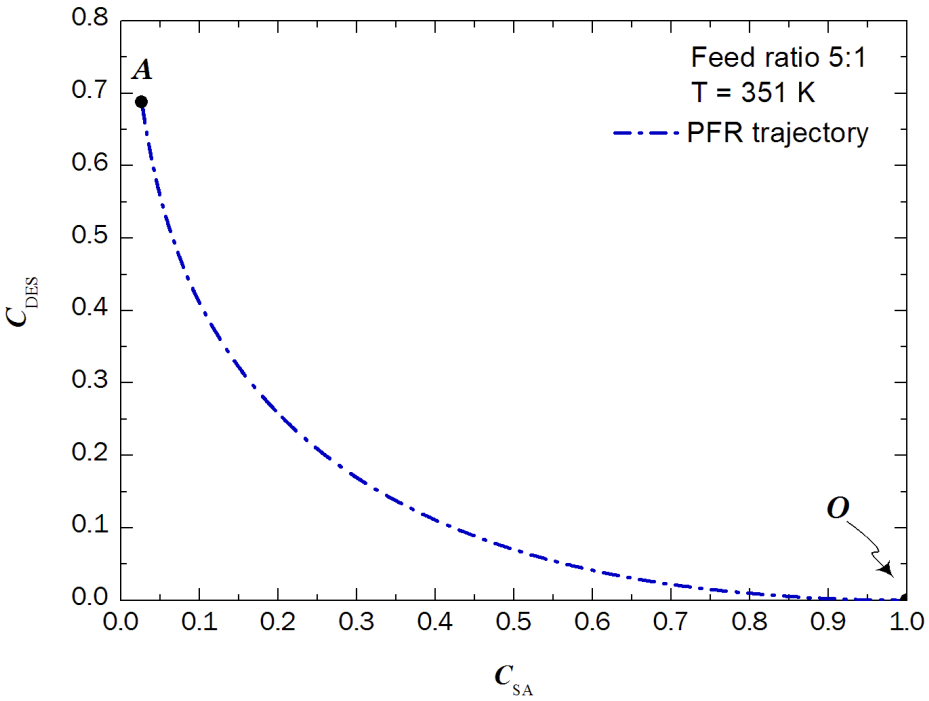

Figure 4.25 – PFR trajectory in the C_{SA}–C_{DES} space diagram where point *O* represents the feed point.

Where $\boldsymbol{C}_{SA} = C_{SA}/C_{SA}^{0}$ and $\boldsymbol{C}_{DES} = C_{DES}/C_{SA}^{0}$

Step 2: Finding the convex hull of the curve. This is done graphically by means of the segment ***OA***. Form Figure 4.26, it can be seen that a point on the segment ***OA*** represents a PFR with by–pass.

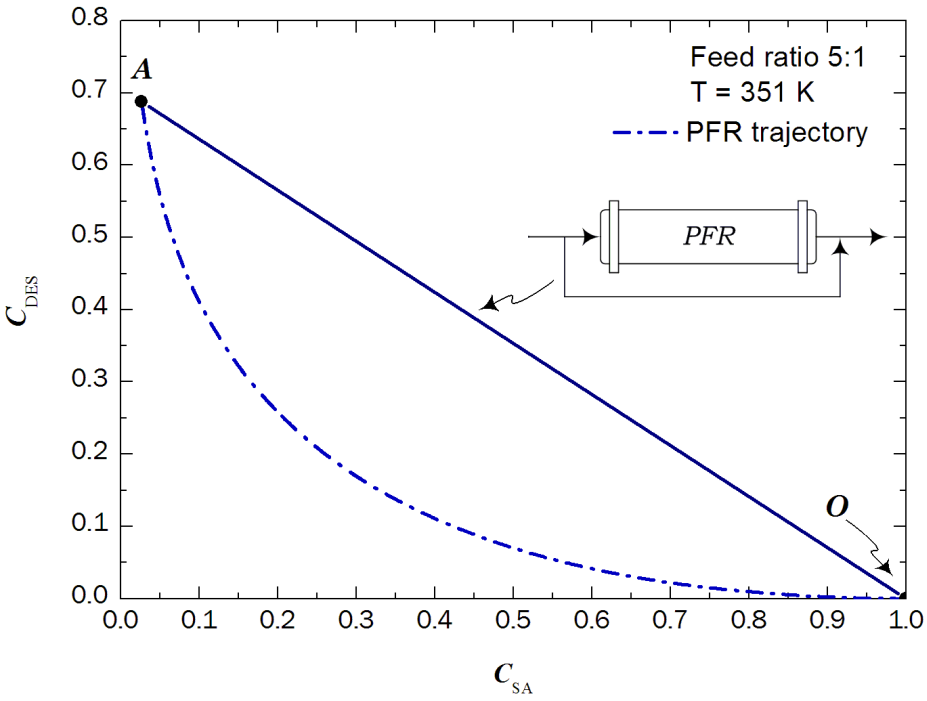

Figure 4.26 – Determination of *AR* candidate (extension through mixing solid line).

Step 3: Draw the CSTR trajectory from the feed point. The trajectory of the reaction in the C_{SA}–C_{DES} space diagram of the CSTR can be drawn by means of the following relation and it is depicted in Figure 4.27.

$$C_{DES}^{0} - C_{DES} = \frac{k_2\eta_2\left(\frac{C_{DES}C_{W}}{K_{eq_x,2}} - C_{MES}C_{EtOH}\right)}{k_1\eta_1\left(C_{SA}C_{EtOH} - \frac{C_{MES}C_{W}}{K_{eq_x,1}}\right)}\left(C_{SA}^{0} - C_{SA}\right) \qquad (4.14)$$

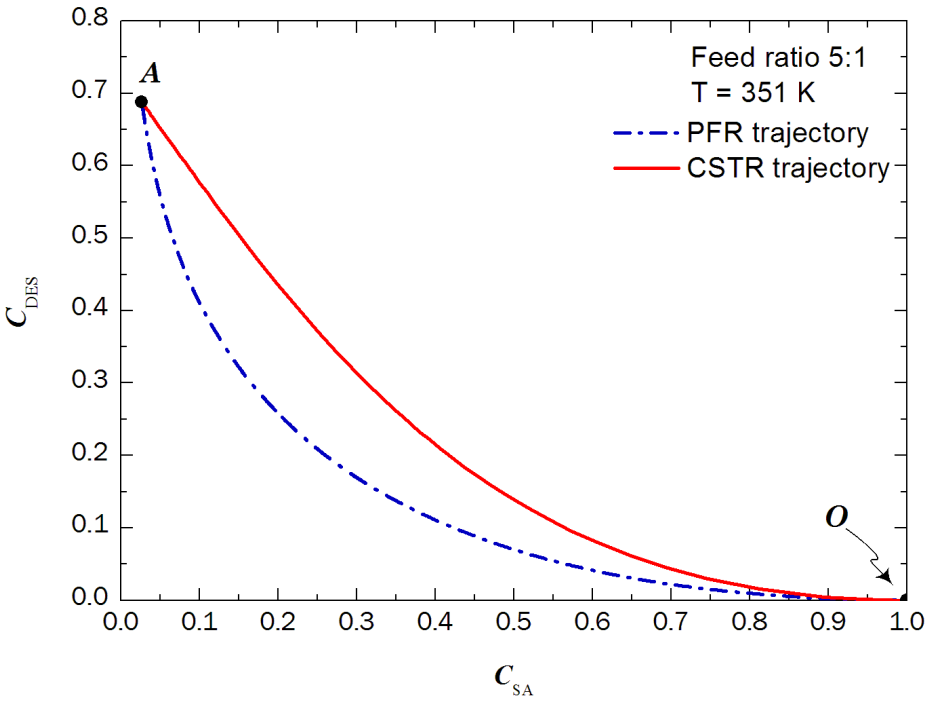

Figure 4.27 – PFR and CSTR trajectories in the C_{SA}–C_{DES} space diagram where point *O* represents the feed point.

Figure 4.27 shows the PFR and CSTR trajectories starting at the same feed point (***O***) and ending both at the equilibrium point (***A***). For a given conversion value, the CSTR gives a better selectivity than the PFR until the point (***A***) is reached. The equilibrium point ***A*** corresponds to maximum conversion of SA (the abscissa axis does directly represent conversion). As the CSTR region is not convex, the full correction of the convexity is obtained by building the convex hull. We proceed as before, adding a convex hull at the right of the CSTR trajectory, starting at the feed point. This is done by drawing the tangent ***OA*** as depicted in Figure 4.28.

Step 4: Finding the convex hull of the curve. This is done graphically by means of the segment ***OA***. Form Figure 4.28, it can be seen that a point on the segment ***OA*** represents a CSTR with by–pass. The new augmented region is convex. No other mixed reactors can be found above the boundary that could give a higher amount of DES.

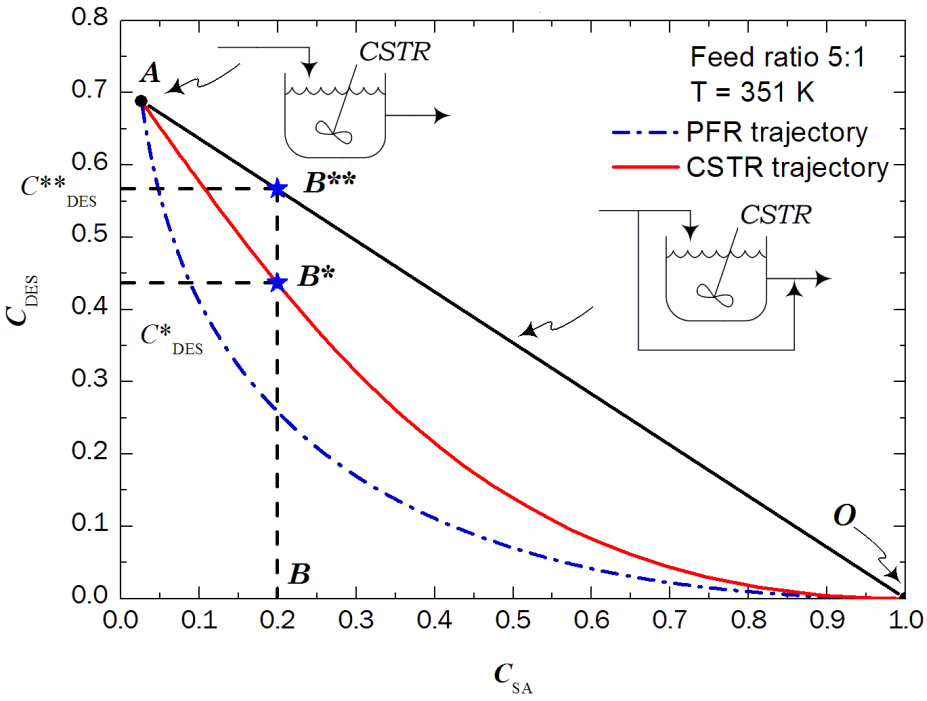

Figure 4.28 – Determination of *AR* candidate (extension through mixing solid line).

Interpretation of the boundary: After obtaining the *AR* candidate, the synthesis of the reaction network is straightforward. Figure 4.28 shows the possible configurations. The effluent concentration at point (***A***) is achieved in a CSTR. If the desired effluent is to the right of point (***A***) on the boundary, a CSTR operating at point (***A***) with feed by–pass is used to reach the point.

Finding the optimum: The final step is to determine the optimum for the specified objective function. Let us considere that we would like to stop the reaction at a 80 % conversion of SA (point ***B***). From Figure 4.28 it can be seen that the maximum concentration of DES at a 80 % conversion of SA by using a single CSTR (point ***B****) corresponds to 0.43 $kmole/m^3$. If, for example, one operated the CSTR with feed by–pass point (***B*****) the maximum concentration of DES at a 80 % conversion of SA corresponds to 0.567 $kmole/m^3$. The reactor configuration that gives this outlet concentration is a CSTR with feed by–pass depicted in Figure 4.29.

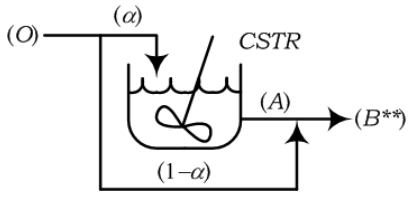

Figure 4.29 – Reactor configuration with feed by–pass.

By means of a mass balance, the feed mixing fraction α to attain the outlet concentration at point (***B******) is determined. From the *AR* analysis CSTR design parameters such as residence time and volume are available.

Mass balance

The mass balance is now performed through the process−groups in the flowsheet structure. Through the Lever Arm Rule it is found that the feed mixing fraction α to reach the desired concentration is equal to 0.176. The mass balance for the reactor process−group is provided in Table 4.41.

Table 4.41 – Mass balance for the reactor process−group.

	Feed point (***O***)	Equilibrium point (***A***)	Operating point (***B******)
C_{SA} $kmole/m^3$	1	0.0268	0.197
C_{ETOH} $kmole/m^3$	5	3.34	3.63
C_{MES} $kmole/m^3$	0	0.285	0.235
C_{DES} $kmole/m^3$	0	0.688	0.567
C_{W} $kmole/m^3$	0	1.66	1.368

In the case of the pervaporation process−group, it is assumed that the membrane exhibits very high selectivity for permeation of water. Therefore the recovery of water on the permeate side is assumed to be equal to or greater than 99.5 %. For the rest of the process−groups in Figure 4.24 the mass balance specifications are defined.

Reverse simulation of the reactor process−group

The inlet temperature of the CSTR reactor is 351 *K*, the temperature at which the *AR* analysis has been performed. From the *AR* analysis, the residence time (τ) to reach the outlet concentration at the operating point (***B******) is directly available and corresponds to τ = 780 *min*. From the reaction stoichiometry the molar flowrate is constant in the reactor. The actual flowrate in the outlet of the reactor is equal to 0.4 m^3/h in a liquid state at T = 351 *K* and P = 1 *atm*. This implies that a reactor with a volume equal to 5.1 m^3 is needed.

Reverse simulation of the distillation process−group

In order to provide an energy efficient distillation column as well as near optimum design, the design parameters for the distillation column are back calculated based on the *DF* method described in section 2.3.4.

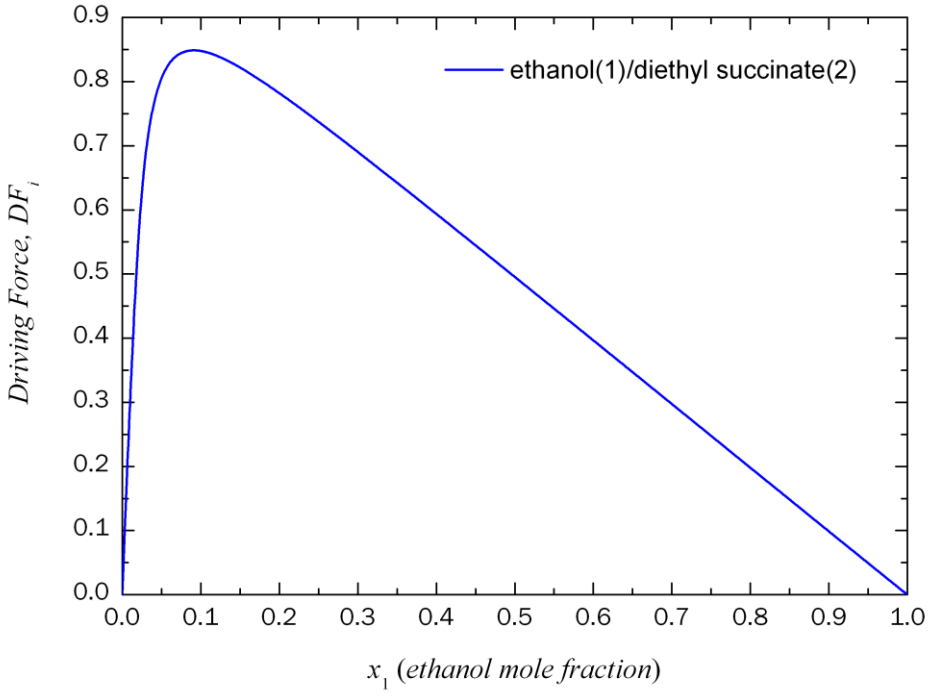

Figure 4.30 – *DF* diagram for binary pair ethanol/diethyl succinate.

Based on the output specification and on the maximum *DF* for the binary pair DES/ETOH as shown in Figure 4.30, the reverse simulation results for the distillation column are given in Table 4.42.

Table 4.42 – Reverse simulation results for the distillation column.

Design parameter	*Value*
Number of stages	10
Feed stage location	9
Purity light key (ethanol)	> 0.995
Recovery light key (ethanol)	> 0.995
Purity heavy key (DES)	–
Recovery heavy key (DES)	> 0.995
Reflux ratio	0.54
DF_{max}	0.85

4.4.1.7 Step 7 –Final Verification

The final verification has been performed by using the PROII (PROII[77]) simulator. With respect to the distillation column, it was not possible to obtain pure ethanol by using only one distillation column. A three–step distillation was needed, where the first step is performed at atmospheric pressure and the next two steps are performed under vacuum. In the first step, ethanol, (the more volatile component) is exclusively recovered as distillate. In the second step, the remaining ethanol and a small portion of diethyl succinate are obtained as distillate. The distillate from the third step is exclusively diethyl succinate. Therefore, the crystallization and liquid membrane based separation units were not necessary.

4.4.2 Discussion

By first solving the mass balance based on the process–group specifications, and then calculating the design parameters of the unit operations through the reverse simulation methods, the process flowsheet design can be performed independently for the unit operations of each process–group. As long as the design of the unit operations satisfies the specifications of the process–groups, the mass balance is satisfied and does not need to be performed again with the design of each unit operation. In particular, the results of this case study show that the reverse simulation of the reactor process–group based on the *AR* analysis provides the ideal reactor configuration together with all the necessary design parameters, such as, temperature, residence time, and sizing of the reactor unit.

5 Conclusions

5.1 Achievements

In this thesis, a framework for process synthesis/design and analysis has been developed. The framework has been presented together with a set of computer–aided methods and tools which support in the systematic search for the solution of the integrated synthesis/design problem. The framework for process synthesis/design and analysis is composed of five main stages. *i) The definition of a base case design* –where a pre–analysis of the product qualities and its characteristics define the process needs. *ii) Modelling and simulation* –which implies the generation of data related to the production steps of each process operation. *iii) Analysis of important issues* –based on the generated data, the objective is to establish the process points (targets) where improvements can be made. *iv) Process synthesis and design* –once the targets have been defined the objective is to generate design candidates that match these targets. The focus in this stage is to improve the performance of a process flowsheet in terms of its energy consumption. For the synthesis and design of more efficient processes in terms of energy consumption this achieved by applying the process–group contribution (*PGC*) methodology *v) Performance evaluation and selection* –finally the most promising design candidates are identified based on suitable performance criteria. The performance criteria chosen depend on the final goal of the design problem to be solved. The main achievements/advantages of the developed framework are analyzed below.

- The framework is a step–by–step procedure, which allows a systematic analysis of the process/product needs and consequently an easier application. The user of the framework is guided from the collecting data (stage 1) to the generation of flowsheet candidates matching the targets (stage 4) and ending with the final verification (stage 5).

- Systematic model–based methods and tools (ProPred, ProCAMD, ProCAFD, PDS, TML, databases) support the framework at every stage which can help to reduce time and man–power resources. For instance, if the objective is the replacement of a solvent due to environmental concerns, the ProCAMD tool is used to design molecules in such a way that the environmental impact is minimized in the process. If the objective is to design more efficient separation processes in terms of energy consumption, then the PDS tool is used for the design of the unit operations based on the *DF* approach.

- The framework together with the models, methods and tools is generic and can be applied to a large range of problems, either to improve an existing process flowsheet (known as retrofit problem) or to design a new process flowsheet.

Emphasis is given on the *PGC* methodology in stage 4 within this framework, which is used to generate and test feasible design flowsheet candidates based on principles of the group−contribution approach used in chemical property estimation. Where the three fundamental pillars of the *PGC* methodology are the process−groups (building blocks), connectivity rules to join the process−groups and flowsheet property models to evaluate the performance of the flowsheet structures. With respect to the *PGC* methodology, some aspects deserve the following concluding remarks:

- The process−group database has been extended with groups (mainly for solvent−based separations), thereby, extending the application range of the *PGC* methodology.

- Based on the *DF* theory, it is clear that any process−group contribution method calculating the energy consumption (as flowsheet property) is component independent if it is based on the *DF* as input (known) variable, in the sense that different component binary pairs may have the same *DF*.

- As the *DF* can be computed for any type of two−phases system as long as the composition data of the two co−existing phases are available, the application range of the flowsheet property model has been extended to predict the energy consumption for solvent−based separation processes. In particular for those solvent−based separation processes using organic solvents, ionic liquids, and hyperbranched polymers as entrainers.

- For each type of solvent, a set of parameters a_k has been developed; thereby the corresponding solvent−based separation process−group can be initialized with three different solvents depending on the problem specifications.

- Based on the *DF* theory, modelling/design of separation processes based on vapor−liquid, liquid−liquid or solid−liquid driving forces can also be handled by the flowsheet property model together with the corresponding set of parameters a_k.

- The combination of the process−groups to form flowsheet structures does not depend on the resolution of the mass and energy balances as the connectivity rules and specifications are *a priori* defined from the built−in mass/energy balances of the process−groups. This means that during the generation of flowsheet structures, no detailed simulation is performed, and only a mass balance is needed at the end of the generation step before going further to the reverse simulation step.

- Finally, as the reverse simulation methods supporting the methodology are based on the *AR* and *DF* concepts, this guarantees a near optimal (if it is not the optimal) performance design with respect to selectivity for reactor units and with respect to energy consumption for separation schemes. Reverse simulation procedures for liquid−liquid extraction solvent−based separation and solvent−based azeotropic separation (using ionic liquids as well as hyperbranched polymers) process−groups, respectively, have been developed.

5.2 Remaining Challenges and Future Work

The developed framework significantly narrows down the search space from many possible process flowsheets to just few so that the most promising design flowsheet candidates can be further investigated in detail. However, *a posteriori* analysis of the most promising flowsheet design candidates can include issues related to heat/mass integration and/or environmental impact, or life cycle assessment. Nevertheless, flowsheet property models that can handle these "flowsheet properties" (for instance, environmental impact) need to be developed.

An issue that has not been dealt within this thesis, and which is highly relevant for bioprocesses is how one deals with batch processes. It is well known that batch processes are most likely to be found in the bioprocesses field, for example used by bio–based pharmaceutical industries. It would be obvious to extend the framework, (particularly the process–group concept) to also incorporate batch operations. The *PG*–concept could be extended to generate a set of the most promising batch sequences and then being further discriminated, based on scheduling considerations.

Another issue is with respect to the difficulty to compare different types of flowsheet structures having a diversity of process unit operations as in a bioprocess. This opens the possibility to a challenging problem of the extension of the current flowsheet property model. The flowsheet property model should be able to predict the performance of the entire process flowsheet involving different types of process–groups as well as units with different mode of operation (continuous and batch process).

Finally, the issue of controllability analysis should be considered within the framework. In this respect the *DF* and *AR* concepts come up as suitable tools to provide a framework for the simultaneous solution of design and control problems in an integrated manner. The operation and control of a separation process is the easiest when operated at maximum *DF*. With respect to *AR*, the same principle can be applied in operating a reactor. The *AR* and *DF* concepts can be extended to the determination of the optimal design–control structure and perhaps even the design of the controllers, based on the analysis of the derivatives of the *AR* and *DF* with respect to the candidate control variables (sensitivity analysis).

6 References

[1] Alvarado–Morales, M., Terra, J., Gernaey, K. V., Woodley, J. M., & Gani, R. (2009). Biorefining: Computer aided tools for sustainable design and analysis of bioethanol production. *Chemical Engineering Research and Design*, *87*(9), 1171–1183.

[2] Angira, R., & Babu, B. V. (2006). Optimization of process synthesis and design problems: A modified differential evolution approach. *Chemical Engineering Science*, *61*(14), 4070–4721.

[3] Azapagic, A., (2002). Sustainable Development Progress Metrics IChemE Sustainable Development Working Group. (IChemE Rugby, UK).

[4] Barnicki, S. D., & Fair, J. R. (1990). Separation Systems Synthesis: A Knowledge–Based Approach. 1. Liquid Mixture Separations. *Industrial & Engineering Chemistry Research, 29* (3), 421–432.

[5] Barnicki, S. D., & Fair, J. R. (1992). Separation Systems Synthesis: A Knowledge–Based Approach. 2. Gas/Vapor Mixtures. *Industrial & Engineering Chemistry Research, 31* (7), 1679–1694.

[6] Bek–Pedersen, E. (2002). Synthesis and Design of Distillation based Separation Schemes. PhD. Thesis, CAPEC, Department of Chemical Engineering, Technical University of Denmark.

[7] Bek–Pedersen, E., & Gani, R. (2004). Design and synthesis of distillation systems using a driving–force–based approach. *Chemical Engineering and Processing*, *43*(*), 251–262.

[8] Benedict, D. J., Parulekar, S. J., & Tsai, S–P. (2006). Pervaporation–assisted esterification of lactic and succinic acids with downstream ester recovery. *Journal of Membrane Science*, *281*, 435–445.

[9] Beyer, K. D., Friesen, K., Bothe, J. R., & Palet, B. (2008). Phase Diagrams and Water Activities of Aqueous Dicarboxylic Acid Systems of Atmospheric Importance. *AIChE Journal, 112*(46), 11704–11713.

[10] Biegler, L. T., Grossmann, I. E., & Westerberg, A. W. (1997).Systematic Methods of Chemical Process Design. Prentice Hall PTR, One Lake Street, Upper Saddle River, New Jersey 07458.

[11] Carvalho, A., Matos, H., & Gani, R. (2008). Design of sustainable chemical processes: systematic retrofit analysis and generation & evaluation of alternatives. *Process Safety and Environmental Protection*, *86*(5), 328–346.

[12] Chen, Y., & Fan, L. T. (1993). Synthesis of complex separation schemes with stream splitting. *Chemical Engineering Science, 48*(7), 1251–1264.

[13] Constantinou, L., & Gani, R. (1994). New group contribution method for estimating properties of pure compounds. *AIChE Journal, 40*(10), 1697–1710.

[14] Daichendt, M. M., & Grossmann, I. E. (1997). Integration of Hierarchical Decomposition and Mathematical Programming for the Synthesis of Process Flowsheets. *Computers and Chemical Engineering*, *22*(1–2), 147–175.

[15] d'Anterroches, L. & Gani, R. (2005). Group contribution based process flowsheet synthesis, design and modelling. *Fluid Phase Equilibria*, *228–229*(), 141–146.

[16] d'Anterroches, L. (2005). Process Flow Sheet Generation & Design through a Group Contribution Approach. PhD. Thesis, CAPEC, Department of Chemical Engineering, Technical University of Denmark.

[17] Datta, R., Glassner, D. A., Jain, M. K., & Vick Roy, J. R. (1992). Fermentation and purification process of succinic acid. US Patent 5,143,834.

[18] Douglas, J. M. (1985). A hierarchical decision procedure for process synthesis. *AIChE Journal*, *31*(3), 353–362.

[19] Douglas, J. M. (1988). Conceptual Design of Chemical Processes. McGraw–Hill, New York.

[20] Douglas, J. M. (1992). Process synthesis for waste minimization. *Industrial & Engineering Chemistry Research*, *31*(1), 238–243.

[21] Eyal, A. M., & Canari, R. (1995). pH Dependence of Carboxylic Acid Extraction by Amine–Based Extractants: Effects of pK_a, Amine Basicity, and Dilute Properties. *Industrial & Engineering Chemistry Research*, *34*(5), 1789–1798.

[22] Gani, R., & O'Connell, J. P. (1989). A Knowledge based system for the selection of thermodynamic models. *Computers and Chemical Engineering*, *13*(4/5), 397–404.

[23] Gani, R., Hytoft, G., Jaksland, C., & Jensen, A. K. (1997) Integrated Computer Aided System for Integrated Design of Chemical Processes. *Computers and Chemical Engineering*, *21*(10), 1135–1146.

[24] Gani, R., Nielsen, B., & Fredenslund, A. (1991). A Group Contribution Approach to Computer Aided Molecular Design. *AIChE Journal*, *37*(9), 1318–1332.

[25] Gani, R., & Bek–Pedersen, E. (2000). Simple New Algorithm for Distillation Column Design. *AIChE Journal*, *46*(6), 1271–1274.

[26] Gani, R. (2002). ICAS Documentation. CAPEC, Department of Chemical Engineering, Technical University of Denmark.

[27] Gani, R., Arenas Gómez, P., Folić, M., Jiménez–Gonzáles, C., & Constable, D. J. C. (2008). Solvents in organic síntesis: Replacement and multi–step reaction systems. *Computers and Chemical Engineering*, *32*(10), 2420–2444.

[28] Gao, Y., Kipling, K., Glassey, J., Willis, M., Montague, G., Zhou, Y., & Titcher–Hooker, H. J. (2010). Application of agent–based system for bioprocess description and process improvement. *Biotechnology Progress*, *26*(3), 706–716.

[29] Glasser, D., & Hildebrandt, D. (1997). Reactors and Process Synthesis. *Computers and Chemical Engineering*, *21*(SS), S775–S783.

[30] Glassner, D. A., & Datta, R. (1992). Process for the production and purification of succinic acid. US Patent 5,143,834.

[31] Grossmann, I. E. (1985). Mixed–integer programming approach for the synthesis of integrated process flowsheets. *Computers and Chemical Engineering*, *9*(5), 463–482.

[32] Grossmann, I. E., & Daichendt, M. M. (1996). New trends in optimisation–based approaches for process synthesis. *Computers and Chemical Engineering*, *20*(6–7), 665–683.

[33] Grossmann, I. E. (2002). Review of nonlinear mixed–integer and disjunctive programming techniques. *Optimization and Engineering*, *3*, 227–252.

[34] Guettler, M. V., Rumler, D., & Jain, M. K. (1999). *Actinobacillus succinogenes* sp. nov., a novel succinic–acid–producing strain from the bovine rumen. *International Journal of Systematic Bacteriology*, *49*(1), 207–216.

[35] Hamelinck, C. N., van Hooijdonk, G., & Faaij, A. P. C., (2005). Ethanol from lignocellulosic biomass: techno–economic performance in short–, middle– and long–term. *Biomass and Energy*, *28*(4), 384–410.

[36] Harper, P. M. (2000). A Multi–Step and Multi–Level Framework for Computer Aided Molecular Design. PhD. Thesis, CAPEC, Department of Chemical Engineering, Technical University of Denmark.

[37] Harper, P. M., & Gani, R. (2000). A multi–step and multi–level approach for computer aided molecular design. *Computers and Chemical Engineering*, *241*(2–7), 677–683.

[38] Hildebrandt, D., & Glasser, D. (1990). The Attainable Region and Optimal Reactor Structures. *Chemical Engineering Science*, *45*(8), 2161–2168.

[39] Hong, Y. K., Hong, W. H., & Chang H. N. (2000). Selective extraction of succinic acid from binary mixture of succinic acid and acetic acid. *Biotechnology Letters*, *22*(), 871–874.

[40] Horn, F. (1964). Attainable and Non–Attainable Regions in Chemical Reaction Technique. In: *Proceedings of the Third European Symposium on Chemical Reaction Engineering*. 293–303.

[41] Hostrup, M. (2001). Integrated Approach to Computer Aided Process Synthesis. PhD. Thesis, CAPEC, Department of Chemical Engineering, Technical University of Denmark.

[42] http://ilthermo.boulder.nist.gov/ILThermo/mainmenu.uix

[43] http://www.icis.com

[44] http://www.mbi.org

[45] http://www.solvent–innovation.de

[46] Huh, Y, S., Hong, Y. K., Hong, W. H., & Chang, H. N. (2004). Selective extraction of acetic acid from the fermentation broth produced by *Mannheimia succiniciproducens*. *Biotechnology Letters*, *26*(), 1581-1584.

[47] Huh, Y, S., Jun, Y. –S., Hong, Y. K., Song, H., Lee, S. Y., & Hong, W. H. (2006). Effective purification of succinic acid from fermentation broth produced by. *Mannheimia succiniciproducens*. *Process Biochemistry*, *41*(6), 1461–1465.

[48] Jaksland, C. A., Gani, R., & Lien, K. M. (1995). Separation process design and synthesis based on thermodynamic insights. *Chemical Engineering Science*, *50*(3), 511–530.

[49] Jaksland, C. A. (1996). Separation Process Design and Synthesis Based on Thermodynamic Insights. PhD. Thesis, CAPEC, Department of Chemical Engineering, Technical University of Denmark.

[50] Joback, K. G., & Reid, R. C. (1987). Estimation of pure component properties from group–contributions. *Chemical Engineering Communications*, *57*(1), 233–243.

[51] Johns, W. R. (2001) Process Synthesis: Poised for a wider role. *Chemical Engineering Progress*, April, 59–65.

[52] Jork, C., Seiler, M., Beste, Y.A., & Arlt, W. (2004). Influence of ionic liquids on the phase behavior of aqueous azeotropic system. *Journal of Chemical & Engineering Data, 49*(4), 852–857.

[53] Kamm. B., Gruber, P. R., & Kamm, M. (2006). Biorefineries–Industrial Processes and Products. Status Quo and Future Directions. Vol. 2. WILEY−VCH Verlag GmbH & Co. KGaA, Weinheim.

[54] Karuppiah, R., Peschel, A., Grossmann, I. E., Martín, M., Martinson, W., & Zullo, L. (2008). Energy Optimization for the Design of Corn−Based Ethanol Plants. *AIChE Journal*, *54*(6), 1499−1525.

[55] Kim, A. S., Hong, Y. K., & Hong, W. H. (2004). Effect of salts on the extraction characteristics of succinic acid by predispersed solvent extraction. *Biotechnology and Bioprocess Engineering*, *9*(3), 207−211.

[56] Kolah, A. P., Asthana, N. S., Vu, D. T., Lira, C. T., & Miller D. J. (2008). Reaction Kinetics for the Heterogeneously Catalyzed Esterification of Succinic Acid with Ethanol. *Industrial & Engineering Chemistry Research*, *47*(15), 5313−5317.

[57] Kravanja, Z., & Glavič, P. (1997). Cost targeting for HEN through simultaneous optimization approach: a unified pinch technology and mathematical programming design of large HEN. *Computers and Chemical Engineering*, *21*(8), 833–853.

[58] Lee, P. C., Lee, W. G., Kwon, S., Lee, S. Y., & Chang, H. N. (1999). Succinic acid production by *Anaerobiospirillum succiniciproducens*: effects of the H_2/CO_2 supply and glucose concentration. *Enzyme Microbial Technology*, *24*(8/9), 549–554.

[59] Lee, P. C., Lee, W. G., Lee, S. Y., & Chang, H. N. (2001). Succinic acid production with reduced by−product formation in the fermentation of *Anaerobiospirillum succiniciproducens* using glycerol as a carbon source. *Biotechnology and Bioengineering*, *72*(1), 41−48.

[60] Lee, P. C., Lee, S. Y., Hong, H. S., & Chang, H. N. (2002). Isolation and characterization of a new succinic acid-producing bacterium, *Mannheimia succiniciproducens* from bovine rumen. *Applied Microbiology and Biotechnology*, *58*(5), 663−668.

[61] Li, C., Zhang, X., Zhang, S., & Suzuki, K. (2009). Environmentally conscious design of chemical processes and products: Multi−optimization method. *Chemical Engineering Research & Design*, *87*(2), 233−243.

[62] Li, X., & Kraslawski, A. (2004). Conceptual process synthesis: past and current trends. *Chemical Engineering and Processing*, *43*(5), 589−600.

[63] Lienqueo, M. E., Leser, E. W., & Asenjo, J. A. (1996). An Expert System for the Selection and Synthesis of Multistep Protein Separation Processes. *Computers and Chemical Engineering*, *20*(SA), S189–S194.

[64] Lin, B., & Miller, D. C. (2004). Tabu search algorithm for chemical process optimization. *Computers and Chemical Engineering*, *28*(11), 2287−2306.

[65] Lin, H.M., Tien, H. Y., Hone, Y. T., & Lee, M. J. (2007). Solubility of selected dibasic carboxylic acids in water, in ionic liquid of [Bmim][BF4], and in aqueous [Bmim][BF4] solutions. *Fluid Phase Equilibria*, *253*(2), 130−136.

[66] Linninger, A. A. (2002). Metallurgical process design–a tribute to Douglas's conceptual design approach. *Industrial & Engineering Chemistry Research*, *41*(16), 3797–3805.

[67] Leser, E. W., & Asenjo, J. A. (1992). Rational design of purification processes for recombinant proteins. *Journal of Chromatography Biomedical Applications*, *584*(1), 43−57.

[68] Marrero, J., & Gani, R. (2001). Group−contribution based estimation of pure component properties. *Fluid Phase Equilibria*, *183–208*(1–2), 183–208.

[69] Martin, R., Rincon, G., & Blanco, B. (2006). Process Synthesis: A Holistic Approach. *Rev. Fac. Ing. UCV. 21*(1), 49−55.

[70] Nath, R., & Motard, R. L. (1978). Evolutionary synthesis of separation processes. In: Proceedings of the 85th National Meeting of AIChE, Philadelphia.

[71] Nishida, N., Stephanopoulos, G., & Westerberg, A. W. (1981). A Review of Process Synthesis. *AIChE Journal*, *27*(3), 321–351.

[72] Oja, V., & Suuberg, E. M. (1999). Vapor Pressures and Enthalpies of Sublimation of D−Glucose, D−Xylose, Cellobiose, and Levoglucosan. *Journal of Chemical & Engineering Data*, *44*(1), 26–29.

[73] Patel, M. K. (2006). Medium and Long−term Opportunities and Risks of the Biotechnological Production of Bulk Chemicals from Renewable Resources, The Potential of the White Biotechnology. The BREW Project, Utrecht University, Netherlands.

[74] Peters, M. S., Timmerhaus, K.D., West, R. E. (2003). Plant Design and Economics for Chemical Engineers. 5th Ed., McGraw−Hill, Boston.

[75] Petrides D. P. (1994). BioPro Designer: An Advanced Computing Environment for Modeling and Design of Integrated Biochemical Processes. *Computers and Chemical Engineering*, *18*(SS), S621–S625.

[76] Powers, G. J. (1972). Heuristic synthesis in process development. *Chemical Engineering Progress*, *68*(8), 88.

[77] PROII User's Guide (2006). Simulation science Inc., Brea, USA.

[78] Raeesi, B., Reza Pishvaie, M., & Rashtchian, D. (2008). Optimization of a process synthesis superstructure using an ant colony algorithm. *Chemical Engineering Technology*, *31*(3), 452–462.

[79] Rigopoulos, S. & Linke, P. (2002). Systematic development of optimal activated sludge process designs. *Computers and Chemical Engineering*, *26*(*), 585–597.

[80] Satyanarayana, K., & Gani, R., (2007). ICAS Documentation, Internal Report PEC07–32, CAPEC, Department of Chemical and Biochemical Engineering, Technical University of Denmark.

[81] Seader, J. D., & Westerberg, A. W. (1977). A combined heuristic and evolutionary strategy for synthesis of simple separation sequences. *AIChE Journal*, *23*(6), 951–954.

[82] Seiler, M., Jork, C., Kavarnou, A., Arlt, W., & Hirsch, R. (2004). Separation of azeotropic mixtures using hyperbranched polymers or ionic liquids. *AIChE Journal*, *50*(10), 2439–2454.

[83] Siirola, J. J., & Rudd, D. F. (1971). Computer aided synthesis of chemical process designs. *Industrial & Engineering Chemistry Fundamentals*, *10*(3), 353–362.

[84] Smith, R., & Linnhoff, B. (1988). The design of separators in the context of overall processes. *Trans. IChemE. ChERD*, *66*, 195.

[85] Song, H., & Lee, S. Y. (2006). Production of succinic acid by bacterial fermentation. *Enzyme and Microbial Technology*, *39*(3), 352–361.

[86] Song, H., Huh, Y. S., Lee, S. Y., Hong, W. H., & Hong, Y. K. (2007). Recovery of succinic acid produced by fermentation of a metabolically engineered *Mannheimia succiniciproducens* strain. *Journal of Biotechnology*, *132*(4): 445−452.

[87] Steffens, M. A., Fraga, E. S., & Bogle, I. D. L. (2000). Synthesis of Bioprocesses Using Physical Properties Data. *Biotechnology and Bioengineering*, *68*(2), 218–230.

[88] Sunder, M. S., & Prasad, D. H. L. (2003). Phase Equilibria of Water + Furfural and Dichloromethane + *n*–Hexane. *Journal of Chemical & Engineering Data*, *48*(2), 221–223.

[89] Tamada, J. A., Kertes, A. S., & King, C. J. (1990). Extraction of Carboxylic Acids with Amine Extractants. 1. Equilibria and Law of Mass Action Modeling. *Industrial & Engineering Chemistry Research*, *29*(7), 1319–1326.

[90] Thompson, R., & King, C. (1972). Systematic Synthesis of Separation Systems. *AIChE Journal*, *18*(), 941–.

[91] Tung, L. A., & King, C. J. (1994). Sorption and Extraction of Lactic and Succinic Acids at pH>pK_{a1}. 2. Regeneration and Process Considerations. *Industrial & Engineering Chemistry Research*, *33*(12), 3224–3229.

[92] van de Vusse, J. G. (1964). Plug–flow reactor versus tank reactor. *Chemical Engineering Science*, *19*(12), 994–996.

[93] Verevkin, S. P., Emel'yanenko, V. N., Stepurko, E. N., Ralys, R. V., & Zaitsau, D. H. (2009). Biomass–Derived Platform Chemicals: Thermodynamic Studies on the Conversion of 5–Hydroxymethylfurfural into Bulk Intermediates. *Industrial & Engineering Chemistry Research*, *48*(22), 10087–10093.

[94] Wang, J–F., Li, C–X., Wang, Z–H., Li, Z–J., & Jiang, Y–B. (2007). Vapor pressure measurement for water, methanol, ethanol, and their binary mixtures in the presence of an ionic liquid 1–ethyl–3-methylimidazolium dimethylphosphate. *Fluid Phase Equilibrium*, *255*(2), 186–192.

[95] Westerberg, A. W. (1989). Synthesis in Engineering Design. *Computers and Chemical Engineering*, *13*(4–5), 365–376.

[96] Willke, Th., & Vorlop, K. –D. (2004). Industrial bioconversion of renewable resources as an alternative to conventional chemistry. *Applied Microbiology and Biotechnology*, *66*(2), 131–121.

[97] Wilson G. M., & Jasperson, L. V., (1996). Critical Constants, Tc, Pc, estimation based on zero, first and second order methods. *AIChE spring meeting*, New Orleans, LA.

[98] Wooley, R., Ruth, M., Sheehan, J., Ibsen, K., Majdeski, H., & Galvez, A. (1999). Lignocellulosic Biomass to Ethanol Process Design and Economics Utilizing Co–Current Dilute Acid Prehydrolysis and Enzymatic Hydrolysis–Current and Futuristic Scenarios. National Renewable Energy Laboratory (NREL)/TP–580–26157, Golden Colorado USA.

[99] Yang, S. T., White, S. A., & Hsu, S. T. (1991).Extraction of Carboxylic Acids with Ternary and Quaternary Amines: Effect of pH. *Industrial & Engineering Chemistry Research*, *30*(6), 1335–1342.

[100] Zeikus, J. G., Jain, M. K., & Elankovan, P. (1999). Biotechnology of succinic acid production and markets for derived industrial products. *Applied Microbiology and Biotechnology*, *51*(5): 545–552.

[101] Zhang, L., Han, J., Deng, D., & Ji, J. (2007). Selection of ionic liquids as entrainers for separation of water and 2–propanol. *Fluid Phase Equilibria*, *255*, 179–185.

[102] Zhou, Y. H., & Titchener–Hooker, N. J. (1999). Visualizing Integrated Bioprocess Designs Through "Windows of Operation". *Biotechnology and Bioengineering*, *65*(5), 550–557.

7 Nomenclature

$[BMIM]^+[BF_4]^-$	1–butyl–3–methylimidazolium tetrafluoroborate
$[BMIM]^+[Cl]^-$	1–butyl–3–methylimidazolium chloride
C_i	concentration of component *i* ($kmole/m^3$)
DES	diethyl succinate
$E_{A,i}$	energy of activation for reaction *i* (*kJ*/*kmole*)
$[EMIM]^+[BF_4]^-$	1–ethyl–3–methylimidazolium tetrafluoroborate
$[EMIM]^+[DMP]^-$	1–ethyl–3-methylimidazolium dimethylphosphate
$[EMIM]^+[EtSO_4]^-$	1–ethyl–3–methylimidazolium ethylsulfate
EG	ethylene glycol
EtOH	ethanol
Ex	Energy consumption index (*MkJ*/*kmole*/*h*)
F	flowrate (*kg*/*h*, *kmole*/*h*)
f_s	solubility (kgi/kg_S, $kmolei/kmole_S$)
HMF	5–(hydroxymethyl) furfural
IL	ionic liquid
k_i	rate constant for catalyzed reaction *i* ($kg_{soln}/kg_{cat}s$)
k_i^0	pre–exponential factor for catalyzed reaction *i* ($kg_{soln}/kg_{cat}s$)
$K_{eq,i}$	mole fraction based reaction *i* equilibrium constant
MES	monoethyl succinate
MW_{soln}	reaction solution molecular weight (*kg*/*kmole*)
P	pressure (*atm*)
R	gas constant (*kJ*/*kmoleK*)
Rg	radius of gyration (*nm*)
RR	reflux ratio
RR_{min}	minimum reflux ratio
S	solvent flowrate (*kg*/*h*, *kmole*/*h*)
SA	succinic acid
SSCF	simultaneous saccharification and co–fermentation
SP	solobility parameter $(kJ/m^3)^{0.5}$
T	temperature (°*C*, *K*)
Tb	normal boiling point (°*C*, *K*)
Tm	normal melting point (°*C*, *K*)
Vm	molar volume ($m^3/kmol$)
VP	normal vapor pressure (*atm*, *Pa*)
W	water
WDV	Van der Waals volume ($m^3/kmol$)
w_{cat}	catalyst concentration (kg_{cat}/kg_{soln})

X_i^F	mass ratio of solute *i* to component *j* in the feed
X_A^R	mass ratio of solute *i* to component *j* in the raffinate
x_j	mole fraction of component *i*

Greek letters

η_i	intraparticle effectiveness factor for reaction *i*
ρ_{soln}	reaction solution density (kg/m^3)
τ	residence time (s)
δ	dipole moment $E^{-30}(Cm)$

8 Appendices

8.1 Data for Case Studies

8.1.1 Pure Component Property Data

Table 8.1 – Required properties for the simulation of the base case design.

Liquid/gases	Conventional solids
Critical temperature	Heat of formation
Critical pressure	Heat capacity
Vapor pressure	Density
I.G: heat of formation	
I.G. heat capacity	
Heat of vaporization	
Density	

Table 8.2 – List of compounds involved in the synthesis problems.

PROII Library	User–defined
Ethanol	Glucose
Water	Xylose
Acetic acid	Arabinose
Lactic acid	Mannose
Succinic acid	Galactose
Glycerol	Cellobiose
Furfural	Xylitol
Ethylene glycol	HMF
Sulfuric acid	Cellulose
Ammonia	Mannan
Ammonium acetate	Galactan
Ammonium sulphate	Arabinan
Calcium hydroxide	Hemicellulose
Calcium sulfate	Lignin
Carbon dioxide	*Z. mobilis*
Oxygen	Cellulase
	Biomass
	IL

8.1.2 Prices and Miscellaneous

Table 8.3 – Raw material and utility prices.

Raw material	Cost	Units	Year
Feedstock	0.0300	*USD/kg*	2007[53]
Diesel	1.2000	*USD/kg*	1999[98]
Sulfuric acid	0.0850	*USD/kg*	2006[43]
Calcium hydroxide	0.0740	*USD/kg*	2006[43]
Ammonia	0.7450	*USD/kg*	2008[43]
Nutrients (CSL)	0.1654	*USD/kg*	1999[98]
Water	0.0003	*USD/kg*	2002[72]
Utility	**Cost**	**Units**	**Year**
LP steam	0.0075	*USD/kg*	2002[74]
HP steam	0.0094	*USD/kg*	2002[74]
Cooling water	0.0002	*USD/kg*	2002[74]
Electricity	0.1300	*USD/kWh*	2002[74]

8.1.3 List of Reactions

8.1.3.1 Bioethanol Production Process

Taken from Wooley *et al.*[98].

Table 8.4 – Reactions taking place in the pre–treatment reactor.

Reaction	Conversion	Modeled
$C_6H_{10}O_5 + H_2O \rightarrow C_6H_{12}O_6$	Cellulose	0.065
$C_6H_{10}O_5 + 1/2\ H_2O \rightarrow 1/2\ C_{12}H_{22}O_{11}$	Cellulose	0.007
$C_5H_8O_4 + H_2O \rightarrow C_5H_{10}O_5$	Hemicellulose	0.750
$C_5H_8O_4 \rightarrow C_4H_3OCHO + 2H_2O$	Hemicellulose	0.100
$C_6H_{10}O_5 + H_2O \rightarrow C_6H_{12}O_6$	Mannan	0.750
$C_6H_{10}O_5 \rightarrow C_6H_6O_3 + 2H_2O$	Mannan	0.150
$C_6H_{10}O_5 + H_2O \rightarrow C_6H_{12}O_6$	Galactan	0.750
$C_6H_{10}O_5 \rightarrow C_6H_6O_3 + 2H_2O$	Galactan	0.150
$C_5H_8O_4 + H_2O \rightarrow C_5H_{10}O_5$	Arabinan	0.750
$C_5H_8O_4 \rightarrow C_4H_3OCHO + 2H_2O$	Arabinan	0.100
$C_2H_4O_2 \rightarrow CH_3COOH$	Acetate	1.000

Table 8.5 – Reactions taking place in the ion exchange and overliming processes.

Reaction	Conversion	Modeled
$H_2SO_4 + 2NH_3 \rightarrow (NH_4)_2SO_4$	Sulfuric acid	1.000
$CH_3COOH + NH_3 \rightarrow CH_3COONH_4$	Acetic acid	1.000
$H_2SO_4 + Ca(OH)_2 \rightarrow CaSO_4 2H_2O$	Calcium hydroxide	1.000

Table 8.6 – Production SSCF saccharification reactions.

Reaction	Conversion	Modeled
$C_6H_{10}O_5 + 1/2\ H_2O \rightarrow 1/2\ C_{12}H_{22}O_{11}$	Cellulose	0.012
$C_6H_{10}O_5 + H_2O \rightarrow C_6H_{12}O_6$	Cellulose	0.800
$C_{12}H_{22}O_{11} + H_2O \rightarrow 2C_6H_{12}O_6$	Cellobiose	1.000

Table 8.7 – Production SSCF fermentation reactions.

Reaction	Conversion	Modeled
$C_6H_{12}O_6 \rightarrow 2CH_3CH_2OH + 2CO_2$	Glucose	0.920
$C_6H_{12}O_6 + 1.2NH_3 \rightarrow 6C_{1.8}O_{0.5}N_{0.2} + 2.4H_2O + 0.3O_2$	Glucose	0.027
$C_6H_{12}O_6 + 2H_2O \rightarrow 2C_3H_8O_3 + O_2$	Glucose	0.002
$C_6H_{12}O_6 + 2CO_2 \rightarrow 2HOOCCH_2CH_2COOH + O_2$	Glucose	0.008
$C_6H_{12}O_6 \rightarrow 3CH_3COOH$	Glucose	0.022
$C_6H_{12}O_6 \rightarrow 2CH_3CHOHCOOH$	Glucose	0.013
$3C_5H_{10}O_5 \rightarrow 5CH_3CH_2OH + 5CO_2$	Xylose	0.850
$C_5H_{10}O_5 + NH_3 \rightarrow 5C_{1.8}O_{0.5}N_{0.2} + 2H_2O + 0.25O_2$	Xylose	0.029
$3C_5H_{10}O_5 + 5H_2O \rightarrow 5C_3H_8O_3 + 2.5O_2$	Xylose	0.002
$C_5H_{10}O_5 + H_2O \rightarrow C_5H_{12}O_5 + 0.5O_2$	Xylose	0.006
$3C_5H_{10}O_5 + 5CO_2 \rightarrow 5HOOCCH_2CH_2COOH + 2.5O_2$	Xylose	0.009
$2C_5H_{10}O_5 \rightarrow 5CH_3COOH$	Xylose	0.024
$3C_5H_{10}O_5 \rightarrow 5CH_3CHOHCOOH$	Xylose	0.014

Table 8.8 – Production SSCF contamination loss reaction.

Reaction	Conversion	Modeled
$C_6H_{12}O_6 \rightarrow 2CH_3CHOHCOOH$	Glucose	1.000
$3C_5H_{10}O_5 \rightarrow 5CH_3CHOHCOOH$	Xylose	1.000
$3C_5H_{10}O_5 \rightarrow 5CH_3CHOHCOOH$	Arabinose	1.000
$C_6H_{12}O_6 \rightarrow 2CH_3CHOHCOOH$	Galactose	1.000
$C_6H_{12}O_6 \rightarrow 2CH_3CHOHCOOH$	Mannose	1.000

8.1.3.2 Succinic Acid Production Process

Taken from Song *et al.*[86].

Table 8.9 – Production fermentation reactions in the succinic acid process.

Reaction	Conversion	Modeled
$C_6H_{12}O_6 + 2CO_2 + 2H_2 \rightarrow 2HOOC\ CH_2\ _2 COOH + 2H_2O$	Glucose	0.59
$C_6H_{12}O_6 \rightarrow 3CH_3COOH$	Glucose	0.02
$C_6H_{12}O_6 + 6H_2O \rightarrow 6HCOOH + 6H_2$	Glucose	
$C_6H_{12}O_6 \rightarrow 2CH_3\ CO\ COOH + 2H_2$	Glucose	0.28
$C_6H_{12}O_6 + 1.2NH_3 \rightarrow 6CH_{1.8}O_{0.5}N_2 + 2.4H_2O + 0.3O_2$	Glucose	0.11

8.1.3.3 Diethyl Succinate Production Process

Mole Fraction based Kinetic Model

The kinetic model was taken from Kolah *et al.*[57]. The rate of formation of each species in the reaction mixture is described by eqs. 8.1–8.6 below:

$$\frac{dx_{SA}}{dt} = -w_{cat} k_1 \eta_1 \left(x_{SA} x_{EtOH} - \frac{x_{MES} x_W}{K_{eq_x,1}} \right) \tag{8.1}$$

$$\frac{dx_{MES}}{dt} = -w_{cat} k_2 \eta_2 \left(x_{MES} x_{EtOH} - \frac{x_{DES} x_W}{K_{eq_x,2}} \right) - w_{cat} k_1 \eta_1 \left(\frac{x_{MES} x_W}{K_{eq_x,1}} - x_{SA} x_{EtOH} \right) \tag{8.2}$$

$$\frac{dx_{DES}}{dt} = -w_{cat} k_2 \eta_2 \left(\frac{x_{DES} x_W}{K_{eq_x,2}} - x_{MES} x_{EtOH} \right) \tag{8.3}$$

$$\frac{dx_{EtOH}}{dt} = -w_{cat} k_1 \eta_1 \left(x_{SA} x_{EtOH} - \frac{x_{MES} x_W}{K_{eq_x,1}} \right) - w_{cat} k_2 \eta_2 \left(x_{MES} x_{EtOH} - \frac{x_{DES} x_W}{K_{eq_x,2}} \right) \tag{8.4}$$

$$\frac{dx_W}{dt} = -w_{cat} k_1 \eta_1 \left(\frac{x_{MES} x_W}{K_{eq_x,1}} - x_{SA} x_{EtOH} \right) - w_{cat} k_2 \eta_2 \left(\frac{x_{DES} x_W}{K_{eq_x,2}} - x_{MES} x_{EtOH} \right) \tag{8.5}$$

$$k_i = k_i^0 \exp\left(\frac{-E_{A,i}}{RT}\right) \tag{8.6}$$

Substituting

$$x_i = \frac{MW_{soln}}{\rho_{soln}} C_i \tag{8.7}$$

for each species into eqs. 8.1–8.5, gives:

$$\frac{dC_{SA}}{dt} = -w_{cat} k_1 \eta_1 \left(\frac{MW_{soln}}{\rho_{soln}}\right)\left(C_{SA}C_{EtOH} - \frac{C_{MES}C_W}{K_{eq_x,1}}\right) \tag{8.8}$$

$$\begin{aligned}\frac{dC_{MES}}{dt} = &-w_{cat} k_2 \eta_2 \left(\frac{MW_{soln}}{\rho_{soln}}\right)\left(C_{MES}C_{EtOH} - \frac{C_{DES}C_W}{K_{eq_x,2}}\right) - \\ &w_{cat} k_1 \eta_1 \left(\frac{MW_{soln}}{\rho_{soln}}\right)\left(\frac{C_{MES}C_W}{K_{eq_x,1}} - C_{SA}C_{EtOH}\right)\end{aligned} \tag{8.9}$$

$$\frac{dC_{DES}}{dt} = -w_{cat} k_2 \eta_2 \left(\frac{MW_{soln}}{\rho_{soln}}\right)\left(\frac{C_{DES}C_W}{K_{eq_x,2}} - C_{MES}C_{EtOH}\right) \tag{8.10}$$

$$\begin{aligned}\frac{dC_{EtOH}}{dt} = &-w_{cat} k_1 \eta_1 \left(\frac{MW_{soln}}{\rho_{soln}}\right)\left(C_{SA}C_{EtOH} - \frac{C_{MES}C_W}{K_{eq_x,1}}\right) - \\ &w_{cat} k_2 \eta_2 \left(\frac{MW_{soln}}{\rho_{soln}}\right)\left(C_{MES}C_{EtOH} - \frac{C_{DES}C_W}{K_{eq_x,2}}\right)\end{aligned} \tag{8.11}$$

$$\frac{dC_{\mathrm{W}}}{dt} = -w_{\mathrm{cat}} k_1 \eta_1 \left(\frac{MW_{\mathrm{soln}}}{\rho_{\mathrm{soln}}} \right) \left(\frac{C_{\mathrm{MES}} C_{\mathrm{W}}}{K_{\mathrm{eq}_x,1}} - C_{\mathrm{SA}} C_{\mathrm{EtOH}} \right) - w_{\mathrm{cat}} k_2 \eta_2 \left(\frac{MW_{\mathrm{soln}}}{\rho_{\mathrm{soln}}} \right) \left(\frac{C_{\mathrm{DES}} C_{\mathrm{W}}}{K_{\mathrm{eq}_x,2}} - C_{\mathrm{MES}} C_{\mathrm{EtOH}} \right) \tag{8.12}$$

8.2 Pre–calculated Values Based on Driving Force Approach to Design Simple Distillation Columns

Taken from Bek–Pedersen[6].

Table 8.10 – Pre–calculated values of the reflux ratio, minimum reflux ratio, number of stages, product purities, and driving force for ideal distillation.

$F_{Di\|Max}$	$X_{LK,\,Dist}$	$X_{LK,\,Bot}$	RR_{min}	$RR_{min}C$	N_{ideal}
0.045	0.995	0.005	9.89	14.83	96
	0.98	0.02	9.56	14.36	71
	0.95	0.05	8.90	13.35	54
	0.90	0.10	8.22	12.33	41
0.065	0.995	0.005	7.33	11.00	67
	0.98	0.02	7.10	10.65	50
	0.95	0.05	6.64	9.96	38
	0.90	0.10	6.64	8.58	29
0.101	0.995	0.005	4.50	6.74	44
	0.98	0.02	4.35	6.52	33
	0.95	0.05	4.05	6.08	25
	0.90	0.10	3.56	5.33	19
0.146	0.995	0.005	2.92	4.41	31
	0.98	0.02	2.84	4.26	23
	0.95	0.05	2.63	3.95	18
	0.90	0.10	2.29	3.44	14
0.172	0.995	0.005	2.35	3.53	27
	0.98	0.02	2.26	3.40	20
	0.95	0.05	2.09	3.13	15
	0.90	0.10	1.80	2.70	12
0.195	0.995	0.005	2.06	3.09	24
	0.98	0.02	1.89	2.97	18
	0.95	0.05	1.82	2.74	14
	0.90	0.10	1.57	2.35	11
0.225	0.995	0.005	1.73	2.60	21
	0.98	0.02	1.67	2.50	16
	0.95	0.05	1.53	2.30	12
	0.90	0.10	1.37	1.97	9
0.268	0.995	0.005	1.37	2.06	18
	0.98	0.02	1.31	1.97	13
	0.95	0.05	1.20	1.80	10
	0.90	0.10	1.02	1.52	8

Continued on the next page

$F_{Di}\|_{Max}$	$X_{LK,\,Dist}$	$X_{LK,\,Bot}$	RR_{min}	$RR_{min}C$	N_{ideal}
0.382	0.995	0.005	0.82	1.23	13
	0.98	0.02	0.78	1.17	10
	0.95	0.05	0.70	1.05	8
	0.90	0.10	0.57	0.86	6
0.478	0.995	0.005	0.54	0.81	10
	0.98	0.02	0.51	0.76	8
	0.95	0.05	0.44	0.67	6
	0.90	0.10	0.34	0.51	5

8.3 New Set of Process–Groups

In this section, a detailed description of the new set of process–group is presented. An overview of each process–group is given together with its main characteristics such as *property dependence* (the physical/chemical/structural property associated with the separation technique represented by the corresponding process–group is given); *initialization procedure* (how the process–group is set up to be used in a synthesis problem); *connectivity rules* (the connectivity rules and specifications inherent to the process-group are described); *reverse simulation* (the procedure to obtain the design parameters of the process–group is described); and the E_x *flowsheet property model*. In particular, with respect to the E_x property model, the procedure to obtain the E_x model parameters is described and highlighted by means of the solvent based azeotropic separation process–group. Then, the predictive nature of the property model is tested by means of an application example.

8.3.1 Solvent Based Azeotropic Separation Process–Group

The solvent based azeotropic separation process–group is representing the separation of an azeotropic mixture by means of extractive distillation. In general, two typical configurations to separate two components *A* and *B* forming an azeotrope using a solvent *S*, depending on the nature of the azeotrope, are possible. If the feed is a minimum–boiling azeotrope, a solvent, with a lower volatility than the key components of the feed mixture, is added to a tray above the feed stage and a few trays below the top of the column so that (1) the solvent is present in the downwards flowing liquid phase to the bottom of the column, and (2) little solvent is stripped and lost to the overhead vapor. If the feed is a maximum–boiling azeotrope, the solvent enters the column with the feed. The bottoms of the extractive distillation column are processed further to recover the solvent for recycle and complete the separation. For the recovery of the solvent a variety of process unit operations are feasible depending on the type of solvent. The solvent recovery in extractive distillation by using organic solvents as entrainer is mostly carried out using another distillation column. Unlike this conventional process, the recovery of non–volatile entrainers (such as ionic liquids or hyperbranched polymers) can be carried out by means of a stripping column, appropriate thin–film evaporators, dryers, or even crystallizers when applicable. An overview of this process group is available in Table 8.11.

Table 8.11 – Solvent based azeotropic separation PG overview.

Name	Solvent based azeotropic separation
Specific properties	Solvent free driving force Relative volatility Azeotrope Heat of vaporization Boiling point Solubility parameter
Unit operations	distillation column flash separation, stripping column thin–film evaporators, dryer, crystallizer
Representation example	(*cycA*/*B*)
Reverse simulation	Partially available

8.3.1.1 Property Dependence

The solvent based azeotropic separation *PG* can be used within a synthesis problem if the following property dependence is satisfied.

1. The mixture to be separated is a binary mixture.
2. The mixture is an azeotropic mixture.
3. The solvent free maximum driving force between the key components is within the range of the solvent based azeotropic separation *PG*.
4. The relative volatility of the key components must be within the range of the relative volatility of the process–group.

8.3.1.2 Initialization Procedure

When initializing the solvent based azeotropic separation *PG* with an azeotropic mixture, two options are possible. Either the binary mixture and the corresponding solvent are known and they match the property dependence, or the binary mixture matches the property dependence but no corresponding solvent is known. For the first scenario, the solvent based azeotropic separation *PG* is initialized with the binary mixture and the solvent. For the second scenario, as no solvent is known, the following procedure is applied to find a matching solvent. Firstly, a database search is performed to look for a potential solvent candidate. If no solvent is found, a CAMD problem is formulated with the targets being either the solvent free driving force or solvent fraction, but not both. If more than one potential solvent candidate is found criteria such as toxicity can be applied to keep the one with the lowest environmental impact.

8.3.1.3 Connectivity Rules and Specifications

The solvent based azeotropic separation *PG* has one inlet and two outlets process−groups when it is initialized with organic solvents. When non−volatile solvents are used, the *PG* has one inlet and three outlets process−groups. Therefore, the uptake of the solvent as well as the stripping medium are not considered to be inlets of the *PG*. The composition of the outlets is the one with the highest purity between 99.5% purity or above of the azeotrope.

8.3.1.4 Reverse Simulation

The reverse simulation of the solvent based azeotropic separation process−group is based on the *DF* approach presented in section 2.3.4.

8.3.1.5 Regression of the Energy Index (E_x) Model Parameters

In this section the procedure to obtain the energy index model parameters of the solvent based azeotropic separation *PG* is described. Then, the procedure is illustrated considering the use of ionic liquids (*IL*), organic solvents (*OS*) and hyperbranched polymers (*HyPol*). Then, the predictive nature of the flowsheet property model is tested by some application examples.

Procedure to obtain the E_x model parameters

1. Define the separation task related to the process−group.
2. Construct the solvent free *DF* diagram for different solvent fractions, either from experimental data or *VLE* calculations.
3. Perform a set of simulation tasks for different solvent fractions to generate *pseudo* experimental data with respect to energy consumption.
4. For each solvent fraction used in step 3, obtain df_{ij}^{k} from the solvent free *DF* diagram.
5. From Eq. (2.1) obtain the a_k parameters through the minimization of the energy consumption of the process as shown in the objective function given by Eq. (8.13).

$$Fobj = min \sum_{j=1}^{NP} \left(E_j^{exp} - E_j^{cal} \right)^2 \qquad (8.13)$$

Values for E_j^{exp} are generated through simulation and $E_j^{cal} = a_k / df_{ij}^{k}$. As a_k as df_{ij}^{k} are function of the solvent fraction.

Example to obtain the E_x model parameters

1. Define the separation task.

The separation task reads as follows: a preconcentrated saturated liquid feed (200 *kmole*/*h*) consisting of 70 mol % ethanol and 30 mol % water, is to be separated using extractive distillation in such a way that the ethanol purity of the distillate (140 *kmole*/*h*) amounts to 99.8 mol % and a minimum energy is used. Ionic liquid (*IL*) is used as entrainer. For the recovery of the *IL*, from an energetic viewpoint, one of the most promising regeneration schemes is the one which makes use of a flash drum and an atmospheric striping column. The flash drum allows the preconcentration of the *IL*, and then the remaining water fractions are separated from the *IL* using an adiabatic stripping column without reboiler and condenser. Dry air is used as the stripping medium. Subsequently the regenerated entrainer is recycled to the main column. Some of the conditions of operation have been taken from Seiler *et al.*[82].

2. Construct the solvent free *DF* diagram.

The ionic liquid $[EMIM]^+[BF_4]^-$ was used as entrainer in the extractive distillation process to break the azeotrope ethanol/water. The *VLE* for the system ethanol/water/*IL* was modeled by the common nonrandom two liquids (NRTL) model, due to the simplicity of this approach, and the *IL* was treated like a nondissociating component. The assumption of an ideal vapor phase was made. Once *VLE* data were generated by means of the NRTL model, the solvent free *DF* diagram is computed by the following set of equations:

$$FD_i = \left| y_i^{'} - x_i^{'} \right| \tag{8.14}$$

$$y_i^{'} = \frac{y_i}{1 - \sum_j^S y_j} \tag{8.15}$$

$$x_i^{'} = \frac{x_i}{1 - \sum_j^S x_j} \tag{8.16}$$

In equations 8.15 and 8.16 the summation is made for all the solvents present in the mixture. Figure 8.1 depicts the solvent free *DF* diagram for the ethanol/water/$[EMIM]^+[BF_4]^-$ system.

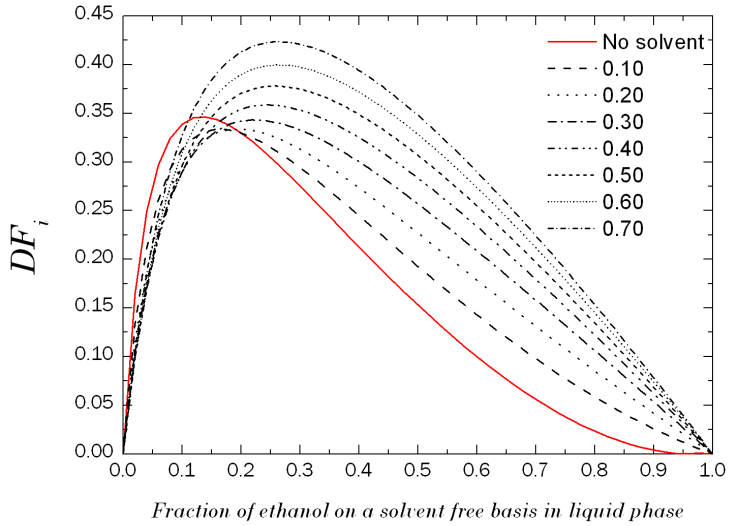

Figure 8.1 – Solvent free DF diagram for ethanol/water mixture separation with ionic liquid ($[EMIM]^+[BF4]^-$).

3. Perform a set of simulation tasks.

PROII® (PROII[77]) was used to perform the set of simulations to generate *pseudo* experimental data with respect to the energy consumption of the process. Table 8.12 summarizes the separation task and gives an overview of the fixed separation parameters and the process variables used in the simulation task.

Table 8.12 – Separation task for extractive distillation using ionic liquids.

Fixed Parameters		Process Variables
Extractive column		***Extractive column***
Operating Pressure (*Pa*)	1.013×10^5	Reflux ratio
Theoretical Stages	28	Entrainer fraction
Feed		
Flow rate (*kmole*/*h*)	200	
$x_{ethanol}$	0.7	
x_{water}	0.3	
Condition	Boiling liquid	
Feed stage	22	
Entrainer stage	3	
$T_{entrainer}$ (*K*)	348.15	
Distillate		
Flowrate (*kmole*/*h*)	140	
$x_{ethanol}$	0.998	
$x_{entrainer}$	<0.0001	
Entrainer recovery		***Entrainer recovery***
Flash drum		
Operating Pressure (*Pa*)	10^4	
Operating Temperature (*K*)	383.15	
Stripping column		
Theoretical Stages	8	
Operating Pressure (*Pa*)	1.013×10^5	
Feed stage	1	
Air flow/entrainer flow ($kg_{air}/kg_{entrainer}$)	0.7	Air flow
Air Temperature (*K*)	293.15	

4. For each solvent fraction obtain df_{ij}^{k} from the *DF* diagram.

For each entrainer (solvent) fraction used in the set of simulation tasks obtain df_{ij}^{k} from the solvent free *DF* diagram in Figure 8.1.

5. Obtain the a_k model parameters.

Obtain the a_k parameters by solving the equation 8.13 through fitting regression. Table 8.13 provides the parameters for each solvent fraction.

Table 8.13 – Model parameter results.

Ionic Liquids		
x_S	df_{ij}^k	a_k
0.28	0.3409	0.02150426
0.30	0.3433	0.01483252
0.33	0.3483	0.01355022
0.375	0.3542	0.01249599
0.40	0.3583	0.01197764
0.45	0.3682	0.01102273
0.50	0.3785	0.01070385
0.60	0.3996	0.01090200
0.70	0.4239	0.01181313

The same procedure has been applied to obtain the parameters when using organic solvents and hyperbranched polymers as entrainers. Table 8.14 provides the parameters for each type of solvent.

Table 8.14 – Model parameter results.

Organic solvents			Hyperbranched polymers		
x_S	df_{ij}^k	a_k	x_S	df_{ij}^k	a_k
0.279204	0.41837	0.0180	0.035	0.36	0.0234
0.29883	0.42339	0.0170	0.070	0.38	0.02014
0.332557	0.43182	0.0170			
0.374181	0.44189	0.0160			
0.399162	0.44811	0.0160			
0.449136	0.45997	0.0160			
0.472813	0.46529	0.0150			
0.499127	0.47096	0.0150			
0.522938	0.47568	0.0150			

Testing the model parameters

In this section, the application of the flowsheet property model along with the parameters is illustrated considering the following systems:

1. 2–Propanol/Water/$[EMIM]^+[BF_4]^-$
2. 2–Propanol/Water/$[BMIM]^+[BF_4]^-$

1. Construct the solvent free *DF* diagram for each system.

Parameters for the NRTL model were retrieved from Zhang *et al.*[101]. Tables 8.15 and 8.16 give the NRTL model binary interaction parameters for each system and Figures 8.2 and 8.3 depict their corresponding solvent free *DF* diagram.

Table 8.15 – NRTL parameters.

Component *i*	Water	2–Propanol	2–Propanol
Component *j*	$[EMIM]^+[BF_4]^-$	Water	$[EMIM]^+[BF_4]^-$
A_{ij} (*K*)	1174.8	9.3204	1231.4
A_{ji} (*K*)	-646.57	830.02	-92.591
α_{ij}	0.3	0.3	0.3

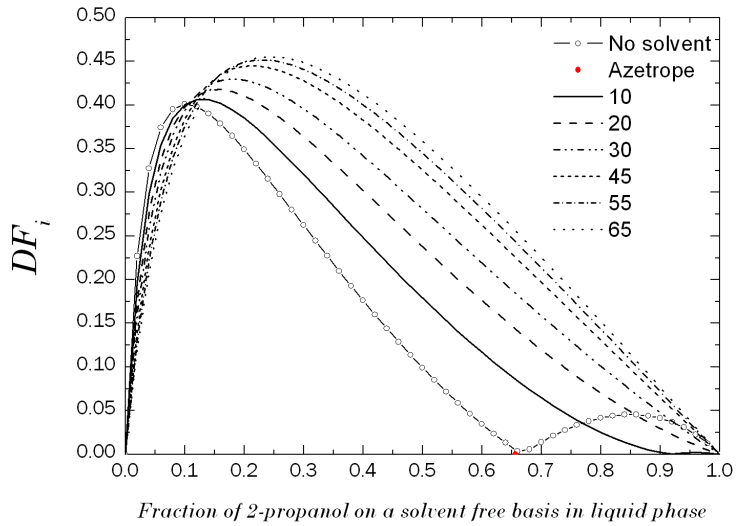

Figure 8.2 – Solvent free DF diagram for 2–propanol/water mixture separation with ionic liquid ($[EMIM]^+[BF4]^-$).

Table 8.16 – NRTL parameters.

Component *i*	Water	2–Propanol	2–Propanol
Component *j*	$[BMIM]^+[BF_4]^-$	Water	$[BMIM]^+[BF_4]^-$
A_{ij} (*K*)	1125.138	9.3204	1262.689
A_{ji} (*K*)	-546.692	830.02	-304.222
α_{ij}	0.3	0.3	0.3

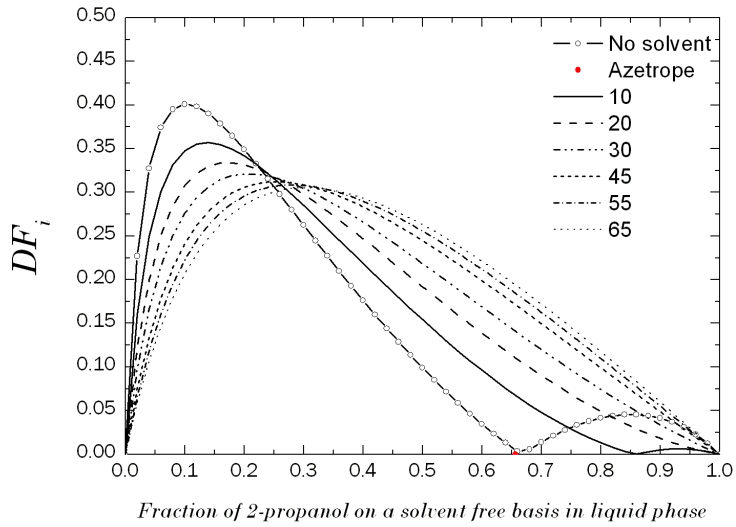

Figure 8.3 – Solvent free DF diagram for 2–propanol/water mixture separation with ionic liquid ($[BMIM]^+[BF4]^-$)

2. Set the solvent free *DF* target.

Let us select a solvent free *DF* target equal to 0.43. From Figure 8.2, it can be seen that the *DF* target can be attained with an $[EMIM]^+[BF_4]^-$ fraction of 0.30. From Figure 8.3, it can be seen that it is not possible to reach the target of 0.43. However, reducing the target driving force to 0.30, the fraction of $[BMIM]^+[BF_4]^-$ needed to attain this target is 0.45. From Table 8.13 the corresponding a_k parameters for each solvent fraction are retrieved, and then through the flowsheet property model, the energy consumption can be determined. The following step to be performed is the reverse simulation to determine the mass balance and the design parameters of the process–group. After reverse simulation, all necessary information is available to perform rigorous simulation. This is done by means of the PROII® (PROII[77]) simulator and the results are shown in Table 8.17.

Table 8.17 – Results from the flowsheet property model vs. rigorous simulation.

x_S	df_{ij}^k	a_k	***Predict energy, Ex (MkJ/h/kmole)***	***Energy demand, (MkJ/h/kmole)***
0.30	0.43	0.01483252	0.034494	0.035085
0.45	0.30	0.01102273	0.036742	0.041878

8.3.2 LLE Based Separation Process–Group

Considering the simplest liquid–liquid extraction process which involves only ternary systems, the liquid–liquid extraction solvent based separation process group is defined as follows.

The feed consists of two miscible components, the carrier *C*, and the solute *A*. Solvent, *S*, is a pure compound. Components *C* and *S* are at most only partially soluble in each other. Solute *A* is soluble in *C* and completely or partially soluble in *S*. During the extraction process, mass transfer of *A* from the feed to the solvent occurs, with less transfer of *C* to the solvent or *S* to the feed. However, complete or nearly complete transfer of component *A* to the solvent is seldom achieved in just one stage. Therefore a number of stages are necessary in one or two sections of countercurrent cascades to achieve the desired compositions.

Let us consider the case when the solvent *S* is totally immiscible with the component *C* of the mixture. Therefore the content of compound *C* in the raffinate is constant. By doing this consideration, the recovery of the component in the extract phase, solute *A*, is assumed equal to or greater than 99.5%. Due to the fact that the solvent *S* and compound *C* are not miscible at all, the recovery of the component *C* in the raffinate phase is assumed equal to or greater than 99.5% as depicted in Figure 8.4.

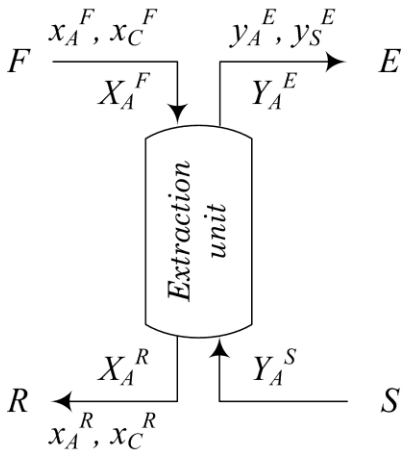

Figure 8.4 – Schematic representation of simple liquid–liquid extraction process.

Performing a mass balance of the compound to be extracted, in this case the solute, *A*, we have:

$$x_C^F F\, X_A^F + S Y_A^S = S Y_A^E + x_C^F F\, X_A^R \tag{8.17}$$

Rearranging the eq. 8.17, we obtain:

$$x_C^F F \;\; X_A^F - X_A^R \;\; = S \;\; Y_A^E - Y_A^S \tag{8.18}$$

$$\frac{x_C^F F}{S} = \frac{Y_A^E - Y_A^S}{X_A^F - X_A^R} \tag{8.19}$$

$Y_A^S = 0$, bacuse the solvent *S* is a pure component.

$$S = \frac{x_C^F F \;\; X_A^F - X_A^R}{Y_A^E} \tag{8.20}$$

We can define fs as the solubility in *kg A/kg S*. Therefore, $fs = Y_A^E$, and the eq. 8.20 can be written as:

$$fs = \frac{x_C^F F \;\; X_A^F - X_A^R}{S} \tag{8.21}$$

In eq. 8.21, two variables are unknown, the solubility *fs* and the solvent flowrate *S*. The other variables such as F, x_C^F, X_A^F, and X_A^R are specified based on the problem definition. Therefore, in order to solve eq. 8.21, either the solubility *fs* is specified or the solvent flowrate *S*, but not both. The overview of this process group is available in Table 8.18.

Table 8.18 – LLE based separation *PG* overview.

Name	*LLE* based separation
Specific properties	Solvent free driving force Solubility parameter Azeotrope
Unit operations	liquid–liquid extraction column mixer–settlers
Representation example	(*lleAB*/*S*/*SB*/*A*)
Reverse simulation	Available

8.3.2.1 Property Dependence

The *LLE* solvent based separation *PG* can be used with a mixture of *NC* components and the solvent within a synthesis problem if the following property dependence is satisfied.

1. The solubility parameter ratio between solute and solvent is greater than 1.1 and the solubility parameter ratio between carrier (co–solute) and solvent is lower than 1.1.

8.3.2.2 Initialization Procedure

When initializing the *LLE* solvent based separation *PG* two scenarios are possible. Either the mixture and the corresponding solvent are known, and the solvent is matching the target property dependence, or the mixture and the corresponding value of the target property are known, but no corresponding solvent is known.

For the first scenario, the liquid–liquid extraction solvent based separation is initialized with the mixture and the corresponding solvent. In this way the solvent flowrate *S* is calculated.

For the second scenario, as no solvent is known, the following procedure is applied.

- First a database search in the most common solvent database is performed to seek for a potential solvent candidate.

- If no solvent is found, a CAMD problem formulation is setup with the targets being to match the solubility fs or the solvent flowrate *S*. If more than one solvent is found, the WAR algorithm can be applied to keep the solvent with the lowest environmental impact.

8.3.2.3 Connectivity Rules and Specifications

The *LLE* solvent based separation *PG* has two inlet and two outlets process–groups. The recovery of the component to be extracted (solute) is assumed to be equal to or greater than 99.5%. The conditions of operation are assumed to be at room temperature (298.15 *K*) and 1 *atm*.

8.3.2.4 Reverse Simulation

Once the solvent has been identified, the solvent flowrate is calculated through the eq. 8.21 for a given target solubility, and then the number of equilibrium stages can

be determined easily by using the diagram *X* (*kg A*/*kg C*) versus *Y* (*kg A*/*kg S*) as is illustrated in chapter 4, section 4.3.1.6. The procedure to perform reverse simulation is outlined below.

1. Construct the solvent free *DF* diagram.
2. At the maximum solvent free *DF*, determine the solubility *fs*.
3. Through the eq. 8.21, determine the solvent flowrate *S*.
4. Construct the diagram *X* (*kg A*/*kg C*) versus *Y* (*kg A*/*kg S*).
5. Locate the operation line.
6. Determine the number of equilibrium stages.

8.3.2.5 Regression of Energy Index (E_x) Model Parameters

As a liquid–liquid solvent–based extraction process does not involve energy consumption, the maximum solvent free driving force df_{ij}^{k} is used as performance criteria. In this case as the solvent free driving force df_{ij}^{k} increases, it means that less amount of solvent is required to perform the separation task.

8.3.3 Crystallization Separation Process–Group

The crystallization process–group represents a crystallizer. The overview of this process–group is given in Table 8.19.

Table 8.19 – Crystallization separation *PG* overview.

Name	Crystallization process–group
Specific properties	Melting point Heat of fusion @ melting point
Unit operations	Crystallizer
Representation example	(*crsABC*/*S*)
Reverse simulation	Available

8.3.3.1 Property Dependence

The crystallization separation process–group can be used with a mixture of *NC* components if the following property dependence is satisfied.

1. The binary ratio for the melting point between the key components must be greater than 1.20.

8.3.3.2 Connectivity Rules and Specifications

The crystallization separation process–group consists of one inlet process–group and two outlet process–groups. The components to be crystallized are those components having a higher melting point than the key components. The recovery of the crystallized components is assumed to be equal to or greater than 99.5 %.

8.3.3.3 Reverse Simulation

The reverse simulation of the crystallization separation process–group is based on the *DF* concept presented in section 2.3.4, chapter 2.

8.3.4 Pervaporation Separation Process–Group

The pervaporation separation process–group represents a liquid–vapor separation. The overview of this process–group is given in Table 8.20.

Table 8.20 – Pervaporation separation *PG* overview.

Name	Pervaporation process–group
Specific properties	Molar volume Solubility parameter Partial pressure
Unit operations	Pervaporation unit
Representation example	(*pervABC*/*DE*)
Reverse simulation	Partially available

8.3.4.1 Property Dependence

The pervaporation separation process–group can be used with a mixture of *NC* components if the following property dependence is satisfied.

1. The binary ratio for the molar volume between the key components must be greater than 3.20.
2. The binary ratio for the solubility parameter between the key components must be greater than 1.90.

8.3.4.2 Connectivity Rules and Specifications

The pervaporation separation process−group consists of one inlet process−group and two outlet process−groups, the permeate side and the retentate side. The recovery of the components at the permeate side is assumed to be equal to or greater than 99.5 %.